MICROWAVE

THIRD EDITION

ENGINEERING

David M. Pozar

USEFUL RESULTS

Maxwell's equations:

$$\nabla \times \bar{E} = -j\omega\mu\bar{H} - \bar{M} \qquad \nabla \cdot \bar{D} = \rho$$

$$\nabla \times \bar{H} = j\omega\epsilon\bar{E} + \bar{J} \qquad \nabla \cdot \bar{B} = 0$$

Surface resistance and skin depth:

$$R_s = \sqrt{\frac{\omega\mu}{2\sigma}} \qquad \delta_s = \sqrt{\frac{2}{\omega\mu\sigma}}$$

Input impedance of terminated lossless transmission lines:

$$Z_{in} = Z_0 \frac{Z_L + jZ_0 \tan \beta\ell}{Z_0 + jZ_L \tan \beta\ell} \qquad \text{(arbitrary load)}$$

$$Z_{in} = jZ_0 \tan \beta\ell \qquad \text{(short-circuited line)}$$

$$Z_{in} = -jZ_0 \cot \beta\ell \qquad \text{(open-circuited line)}$$

Relations between load impedance and reflection coefficient:

$$\Gamma = \frac{Z_L - Z_0}{Z_L + Z_0} \qquad Z_L = Z_0 \frac{1+\Gamma}{1-\Gamma}$$

Definitions of return loss, insertion loss and SWR:

$$RL = -20 \log |\Gamma|, \quad IL = -20 \log |T|, \quad \text{SWR} = \frac{1+|\Gamma|}{1-|\Gamma|}$$

Conversion between dB and nepers:

$$1 \text{ neper} = 8.686 \text{ dB}$$

Elements of the ferrite permeability tensor:

$$\mu = \mu_0 \left(1 + \frac{\omega_0 \omega_m}{\omega_0^2 - \omega^2}\right) \qquad \omega_0 = \mu_0 \gamma H_0$$

$$\omega_m = \mu_0 \gamma M_s$$

$$\kappa = \mu_0 \frac{\omega \omega_m}{\omega_0^2 - \omega^2} \qquad \text{(or 2.8 MHz/Oersted)}$$

Conversion between some values of reflection coefficient, SWR, and return loss:

$\lvert\Gamma\rvert$	0.024	0.032	0.048	0.050	0.056	0.10	0.178	0.200	0.316	0.33
SWR	1.05	1.07	1.10	1.11	1.12	1.22	1.43	1.50	1.92	2.00
RL (dB)	32.3	30.0	26.4	26.0	25.0	20.0	15.0	14.0	10.0	9.6

The *ABCD* Parameters of Some Useful Two-Port Circuits.

Circuit	*ABCD* Parameters	
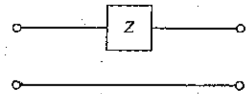	$A = 1$ $C = 0$	$B = Z$ $D = 1$
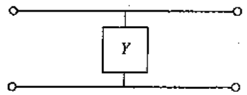	$A = 1$ $C = Y$	$B = 0$ $D = 1$
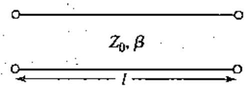	$A = \cos \beta l$ $C = jY_0 \sin \beta l$	$B = jZ_0 \sin \beta l$ $D = \cos \beta l$
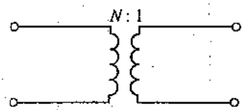	$A = N$ $C = 0$	$B = 0$ $D = \frac{1}{N}$
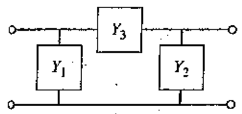	$A = 1 + \frac{Y_2}{Y_3}$ $C = Y_1 + Y_2 + \frac{Y_1 Y_2}{Y_3}$	$B = \frac{1}{Y_3}$ $D = 1 + \frac{Y_1}{Y_3}$
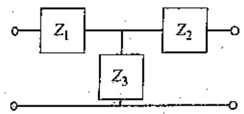	$A = 1 + \frac{Z_1}{Z_3}$ $C = \frac{1}{Z_3}$	$B = Z_1 + Z_2 + \frac{Z_1 Z_2}{Z_3}$ $D = 1 + \frac{Z_2}{Z_3}$

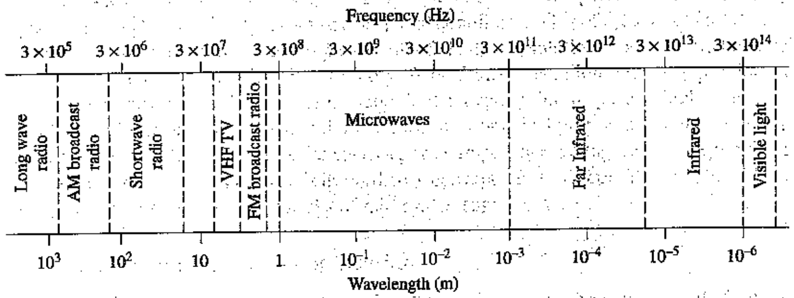

Typical Frequencies	
AM broadcast band	535–1605 kHz
Short wave radio band	3–30 MHz
FM broadcast band	88–108 MHz
VHF TV (2–4)	54–72 MHz
VHF TV (5–6)	76–88 MHz
UHF TV (7–13)	174–216 MHz
UHF TV (14–83)	470–890 MHz
US cellular telephone	824–849 MHz
	869–894 MHz
European GSM cellular	880–915 MHz
	925–960 MHz
GPS	1575.42 MHz
	1227.60 MHz
Microwave ovens	2.45 GHz
US DBS	11.7–12.5 GHz
US ISM bands	902–928 MHz
	2.400–2.484 GHz
	5.725–5.850 GHz
US UWB radio	3.1–10.6 GHz

Approximate Band Designations	
Medium frequency	300 kHz to 3 MHz
High frequency (HF)	3 MHz to 30 MHz
Very high frequency (VHF)	30 MHz to 300 MHz
Ultra high frequency (UHF)	300 MHz to 3 GHz
L band	1–2 GHz
S band	2–4 GHz
C band	4–8 GHz
X band	8–12 GHz
Ku band	12–18 GHz
K band	18–26 GHz
Ka band	26–40 GHz
U band	40–60 GHz
V band	50-75 GHz
E band	60-90 GHz
W band	75-110 GHz
F band	90-140 GHz

FIGURE 1.1 The electromagnetic spectrum.

since Maxwell's equations involve vector differential or integral operations on vector field quantities, and these fields are functions of spatial coordinates. One of the goals of this book, however, is to try to reduce the complexity of a field theory solution to a result that can be expressed in terms of simpler circuit theory. A field theory solution generally provides a complete description of the electromagnetic field at every point in space, which is usually much more information than we really need for most practical purposes. We are typically more interested in terminal quantities such as power, impedance, voltage, and current, which can often be expressed in terms of circuit theory concepts. It is this complexity that adds to the challenge, as well as the rewards, of microwave engineering.

Applications of Microwave Engineering

Just as the high frequencies and short wavelengths of microwave energy make for difficulties in analysis and design of microwave components and systems, these same factors provide unique opportunities for the application of microwave systems. This is because of the following considerations:

- Antenna gain is proportional to the electrical size of the antenna. At higher frequencies, more antenna gain is therefore possible for a given physical antenna size, which has important consequences for implementing miniaturized microwave systems.
- More bandwidth (information-carrying capacity) can be realized at higher frequencies. A 1% bandwidth at 600 MHz is 6 MHz (the bandwidth of a single television channel), and at 60 GHz a 1% bandwidth is 600 MHz (100 television channels). Bandwidth is critically important because available frequency bands in the electromagnetic spectrum are being rapidly depleted.
- Microwave signals travel by line of sight and are not bent by the ionosphere as are lower frequency signals. Satellite and terrestrial communication links with very high capacities are thus possible, with frequency reuse at minimally distant locations.
- The effective reflection area (radar cross section) of a radar target is usually proportional to the target's electrical size. This fact, coupled with the frequency characteristics of antenna gain, generally makes microwave frequencies preferred for radar systems.
- Various molecular, atomic, and nuclear resonances occur at microwave frequencies, creating a variety of unique applications in the areas of basic science, remote sensing, medical diagnostics and treatment, and heating methods.

The majority of applications of today's microwave technology are to communications systems, radar systems, environmental remote sensing, and medical systems. As the frequency allocations listed in Figure 1.1 show, RF and microwave communications systems are pervasive, especially today when wireless connectivity promises to provide voice and data access to "everyone, anywhere, at any time."

Probably the most ubiquitous use of microwave technology is in cellular telephone systems, which were first proposed in the 1970s. By 1997 there were more than 200 million cellular subscribers worldwide, and the number of subscribers and the capabilities of this service continue to grow. Satellite systems have been developed to provide cellular (voice), video, and data connections worldwide. Large satellite telephony systems, such as Iridium and Globalstar, unfortunately suffered from both technical drawbacks and weak business models, and have failed with losses of several billion dollars each. But smaller satellite systems, such as the Global Positioning Satellite (GPS) system and the Direct Broadcast Satellite (DBS) system, have been extremely successful. Wireless Local Area Networks (WLANs) provide high-speed networking between computers over short distances, and the demand for this capability is growing very fast. The newest wireless communications technology is Ultra Wide Band (UWB) radio, where the broadcast signal occupies a very wide frequency band but with a very low power level to avoid interference with other systems.

Radar systems find application in military, commercial, and scientific systems. Radar is used for detecting and locating air, ground, and seagoing targets, as well as for missile guidance and fire control. In the commercial sector, radar technology is used for air traffic control, motion detectors (door openers and security alarms), vehicle collision avoidance, and distance measurement. Scientific applications of radar include weather prediction, remote sensing of the atmosphere, the oceans, and the ground, and medical diagnostics and therapy. Microwave radiometry, which is the passive sensing of microwave energy emitted from an object, is used for remote sensing of the atmosphere and the earth, as well as medical diagnostics and imaging for security applications.

A Short History of Microwave Engineering

The field of microwave engineering is often considered a fairly mature discipline because the fundamental concepts of electromagnetics were developed over 100 years ago, and probably because radar, being the first major application of microwave technology, was intensively developed as far back as World War II. But even though microwave engineering had its beginnings in the last century, significant developments in high-frequency solid-state devices, microwave integrated circuits, and the ever-widening applications of modern microsystems have kept the field active and vibrant.

The foundations of modern electromagnetic theory were formulated in 1873 by James Clerk Maxwell [1], who hypothesized, solely from mathematical considerations, electromagnetic wave propagation and the notion that light was a form of electromagnetic energy. Maxwell's formulation was cast in its modern form by Oliver Heaviside, during the period from 1885 to 1887. Heaviside was a reclusive genius whose efforts removed many of the mathematical complexities of Maxwell's theory, introduced vector notation, and provided a foundation for practical applications of guided waves and transmission lines. Heinrich Hertz, a German professor of physics and a gifted experimentalist who also understood the theory published by Maxwell, carried out a set of experiments during the period 1887–1891 that completely validated Maxwell's theory of electromagnetic waves. Figure 1.2 shows a photograph of the original equipment used by Hertz in his experiments.

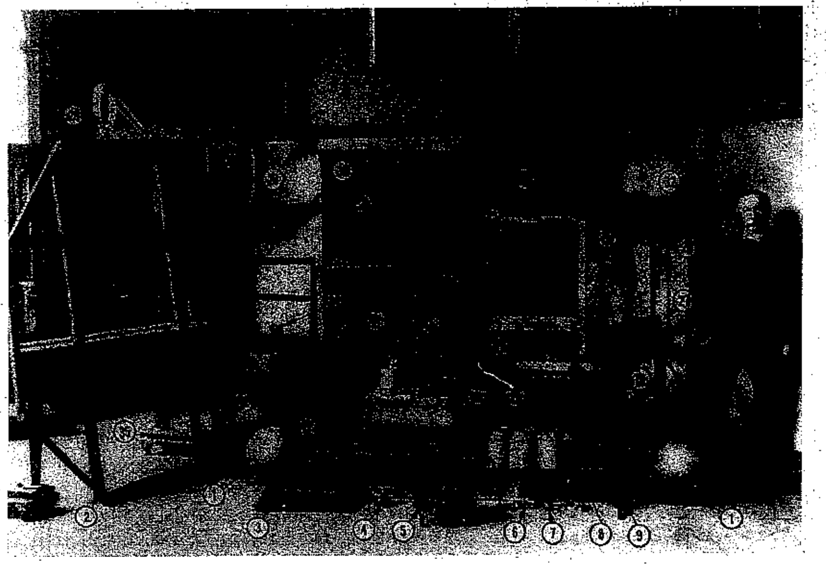

FIGURE 1.2 Original apparatus used by Hertz for his electromagnetics experiments. (1) 50 MHz transmitter spark gap and loaded dipole antenna. (2) Parallel wire grid for polarization experiments. (3) Vacuum apparatus for cathode ray experiments. (4) Hot-wire galvanometer. (5) Reiss or Knochenhauer spirals. (6) Rolled-paper galvanometer. (7) Metal sphere probe. (8) Reiss spark micrometer. (9) Coaxial transmission line. (10–12) Equipment to demonstrate dielectric polarization effects. (13) Mercury induction coil interrupter. (14) Meidinger cell. (15) Vacuum bell jar. (16) High-voltage induction coil. (17) Bunsen cells. (18) Large-area conductor for charge storage. (19) Circular loop receiving antenna. (20) Eight-sided receiver detector. (21) Rotating mirror and mercury interrupter. (22) Square loop receiving antenna. (23) Equipment for refraction and dielectric constant measurement. (24) Two square loop receiving antennas. (25) Square loop receiving antenna. (26) Transmitter dipole. (27) High-voltage induction coil. (28) Coaxial line. (29) High-voltage discharger. (30) Cylindrical parabolic reflector/receiver. (31) Cylindrical parabolic reflector/transmitter. (32) Circular loop receiving antenna. (33) Planar reflector. (34, 35) Battery of accumulators. Photographed on October 1, 1913 at the Bavarian Academy of Science, Munich, Germany, with Hertz's assistant, Julius Amman.

Photograph and identification courtesy of J. H. Bryant, University of Michigan.

It is interesting to observe that this is an instance of a discovery occurring after a prediction has been made on theoretical grounds—a characteristic of many of the major discoveries throughout the history of science. All of the practical applications of electromagnetic theory, including radio, television, and radar, owe their existence to the theoretical work of Maxwell.

Because of the lack of reliable microwave sources and other components, the rapid growth of radio technology in the early 1900s occurred primarily in the high frequency (HF) to very high frequency (VHF) range. It was not until the 1940s and the advent of radar development during World War II that microwave theory and technology received substantial interest. In the United States, the Radiation Laboratory was established at the Massachusetts Institute of Technology (MIT) to develop radar theory and practice. A number of top scientists, including N. Marcuvitz, I. I. Rabi, J. S. Schwinger, H. A. Bethe, E. M. Purcell, C. G. Montgomery, and R. H. Dicke, among others, were gathered for what turned out to be a very intensive period of development in the microwave field. Their work included the theoretical and experimental treatment of waveguide components, microwave antennas, small aperture coupling theory, and the beginnings of microwave network theory. Many of these researchers were physicists who went back to physics research after the war (many later received Nobel Prizes), but their microwave work is summarized in the classic 28-volume Radiation Laboratory Series of books that still finds application today.

Communications systems using microwave technology began to be developed soon after the birth of radar, benefitting from much of the work that was originally done for radar systems. The advantages offered by microwave systems, including wide bandwidths and line-of-sight propagation, have proved to be critical for both terrestrial and satellite communications systems and have thus provided an impetus for the continuing development of low-cost miniaturized microwave components. We refer the interested reader to the special Centennial Issue of the *IEEE Transactions on Microwave Theory and Techniques* [2] for further historical perspectives on the field of microwave engineering.

1.2 MAXWELL'S EQUATIONS

Electric and magnetic phenomena at the macroscopic level are described by Maxwell's equations, as published by Maxwell in 1873 [1]. This work summarized the state of electromagnetic science at that time and hypothesized from theoretical considerations the existence of the electrical displacement current, which led to the discovery by Hertz and Marconi of electromagnetic wave propagation. Maxwell's work was based on a large body of empirical and theoretical knowledge developed by Gauss, Ampere, Faraday, and others. A first course in electromagnetics usually follows this historical (or deductive) approach, and it is assumed that the reader has had such a course as a prerequisite to the present material. Several books are available, [3]–[9], that provide a good treatment of electromagnetic theory at the undergraduate or graduate level.

This chapter will outline the fundamental concepts of electromagnetic theory that we will require for the rest of the book. Maxwell's equations will be presented, and boundary conditions and the effect of dielectric and magnetic materials will be discussed. Wave phenomena are of essential importance in microwave engineering, so much of the chapter is spent on plane wave topics. Plane waves are the simplest form of electromagnetic waves and so serve to illustrate a number of basic properties associated with wave propagation. Although it is assumed that the reader has studied plane waves before, the present material should help to reinforce many of the basic principles in the reader's mind and perhaps to introduce some concepts that the reader has not seen previously. This material will also serve as a useful reference for later chapters.

With an awareness of the historical perspective, it is usually advantageous from a pedagogical point of view to present electromagnetic theory from the "inductive," or axiomatic, approach by beginning with Maxwell's equations. The general form of time-varying Maxwell equations, then, can be written in "point," or differential, form as

$$\nabla \times \bar{\mathcal{E}} = \frac{-\partial \bar{\mathcal{B}}}{\partial t} - \bar{\mathcal{M}}, \tag{1.1a}$$

$$\nabla \times \bar{\mathcal{H}} = \frac{\partial \bar{\mathcal{D}}}{\partial t} + \bar{\mathcal{J}}, \tag{1.1b}$$

$$\nabla \cdot \bar{\mathcal{D}} = \rho, \tag{1.1c}$$

$$\nabla \cdot \bar{\mathcal{B}} = 0. \tag{1.1d}$$

The MKS system of units is used throughout this book. The script quantities represent time-varying vector fields and are real functions of spatial coordinates x,y,z, and the time variable t. These quantities are defined as follows:

$\bar{\mathcal{E}}$ is the electric field intensity, in V/m.
$\bar{\mathcal{H}}$ is the magnetic field intensity, in A/m.
$\bar{\mathcal{D}}$ is the electric flux density, in Coul/m^2.
$\bar{\mathcal{B}}$ is the magnetic flux density, in Wb/m^2.
$\bar{\mathcal{M}}$ is the (fictitious) magnetic current density, in V/m^2.
$\bar{\mathcal{J}}$ is the electric current density, in A/m^2.
ρ is the electric charge density, in Coul/m^3.

The sources of the electromagnetic field are the currents $\bar{\mathcal{M}}$ and $\bar{\mathcal{J}}$, and the electric charge density ρ. The magnetic current $\bar{\mathcal{M}}$ is a fictitious source in the sense that it is only a mathematical convenience: the real source of a magnetic current is always a loop of electric current or some similar type of magnetic dipole, as opposed to the flow of an actual magnetic charge (magnetic monopole charges are not known to exist). The magnetic current is included here for completeness, as we will have occasion to use it in Chapter 4 when dealing with apertures. Since electric current is really the flow of charge, it can be said that the electric charge density ρ is the ultimate source of the electromagnetic field.

In free-space, the following simple relations hold between the electric and magnetic field intensities and flux densities:

$$\bar{\mathcal{B}} = \mu_0 \bar{\mathcal{H}}, \tag{1.2a}$$

$$\bar{\mathcal{D}} = \epsilon_0 \bar{\mathcal{E}}, \tag{1.2b}$$

where $\mu_0 = 4\pi \times 10^{-7}$ Henry/m is the permeability of free-space, and $\epsilon_0 = 8.854 \times 10^{-12}$ farad/m is the permittivity of free-space. We will see in the next section how media other than free-space affect these constitutive relations.

Equations (1.1a)–(1.1d) are linear but are not independent of each other. For instance, consider the divergence of (1.1a). Since the divergence of the curl of any vector is zero [vector identity (B.12), from Appendix B], we have

$$\nabla \cdot \nabla \times \bar{\mathcal{E}} = 0 = -\frac{\partial}{\partial t}(\nabla \cdot \bar{\mathcal{B}}) - \nabla \cdot \bar{\mathcal{M}}.$$

Since there is no free magnetic charge, $\nabla \cdot \bar{\mathcal{M}} = 0$, which leads to $\nabla \cdot \bar{\mathcal{B}} = 0$, or (1.1d).

The continuity equation can be similarly derived by taking the divergence of (1.1b), giving

$$\nabla \cdot \bar{\mathcal{J}} + \frac{\partial \rho}{\partial t} = 0, \tag{1.3}$$

where (1.1c) was used. This equation states that charge is conserved, or that current is continuous, since $\nabla \cdot \bar{\mathcal{J}}$ represents the outflow of current at a point, and $\partial\rho/\partial t$ represents the charge buildup with time at the same point. It is this result that led Maxwell to the conclusion that the displacement current density $\partial\bar{\mathcal{D}}/\partial t$ was necessary in (1.1b), which can be seen by taking the divergence of this equation.

The foregoing differential equations can be converted to integral form through the use of various vector integral theorems. Thus, applying the divergence theorem (B.15) to (1.1c) and (1.1d) yields

$$\oint_S \bar{\mathcal{D}} \cdot d\bar{s} = \int_V \rho \, dv = \mathcal{Q}, \tag{1.4}$$

$$\oint_S \bar{\mathcal{B}} \cdot d\bar{s} = 0, \tag{1.5}$$

where Q in (1.4) represents the total charge contained in the closed volume V (enclosed by a closed surface S). Applying Stokes' theorem (B.16) to (1.1a) gives

$$\oint_C \bar{\mathcal{E}} \cdot d\bar{l} = -\frac{\partial}{\partial t}\int_S \bar{\mathcal{B}} \cdot d\bar{s} - \int_S \bar{\mathcal{M}} \cdot d\bar{s}, \tag{1.6}$$

which, without the $\bar{\mathcal{M}}$ term, is the usual form of Faraday's law and forms the basis for Kirchhoff's voltage law. In (1.6), C represents a closed contour around the surface S, as shown in Figure 1.3. Ampere's law can be derived by applying Stokes' theorem to (1.1b):

$$\oint_C \bar{\mathcal{H}} \cdot d\bar{l} = \frac{\partial}{\partial t}\int_S \bar{\mathcal{D}} \cdot d\bar{s} + \int_S \bar{\mathcal{J}} \cdot d\bar{s} = \frac{\partial}{\partial t}\int_S \bar{\mathcal{D}} \cdot d\bar{s} + \mathcal{I}, \tag{1.7}$$

where $\mathcal{I} = \int_S \bar{\mathcal{J}} \cdot d\bar{s}$ is the total electric current flow through the surface S. Equations (1.4)–(1.7) constitute the integral forms of Maxwell's equations.

The foregoing equations are valid for arbitrary time dependence, but most of our work will be involved with fields having a sinusoidal, or harmonic, time dependence, with steady-state conditions assumed. In this case phasor notation is very convenient, and so all field quantities will be assumed to be complex vectors with an implied $e^{j\omega t}$ time dependence and written with roman (rather than script) letters. Thus, a sinusoidal electric field in the $\hat{x}$ direction of the form

$$\bar{\mathcal{E}}(x, y, z, t) = \hat{x}A(x, y, z)\cos(\omega t + \phi), \tag{1.8}$$

where A is the (real) amplitude, ω is the radian frequency, and ϕ is the phase reference of

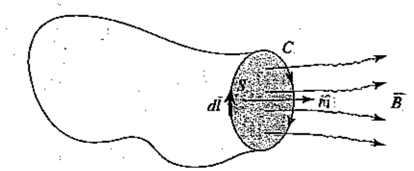

FIGURE 1.3 The closed contour C and surface S associated with Faraday's law.

the wave at $t = 0$, has the phasor form

$$\bar{E}(x, y, z) = \hat{x}A(x, y, z)e^{j\phi}. \tag{1.9}$$

We will assume cosine-based phasors in this book, so the conversion from phasor quantities to real time-varying quantities is accomplished by multiplying the phasor by $e^{j\omega t}$ and taking the real part:

$$\bar{\mathcal{E}}(x, y, z, t) = \mathrm{Re}[\bar{E}(x, y, z)e^{j\omega t}], \tag{1.10}$$

as substituting (1.9) into (1.10) to obtain (1.8) demonstrates. When working in phasor notation, it is customary to suppress the common $e^{j\omega t}$ factor on all terms.

When dealing with power and energy, we will often be interested in the time average of a quadratic quantity. This can be found very easily for time harmonic fields. For example, the average of the square of the magnitude of an electric field given by

$$\bar{\mathcal{E}} = \hat{x}E_1 \cos(\omega t + \phi_1) + \hat{y}E_2 \cos(\omega t + \phi_2) + \hat{z}E_2 \cos(\omega t + \phi_3), \tag{1.11}$$

which has the phasor form

$$\bar{E} = \hat{x}E_1 e^{j\phi_1} + \hat{y}E_2 e^{j\phi_2} + \hat{z}E_3 e^{j\phi_3}, \tag{1.12}$$

can be calculated as

$$\begin{aligned}
|\bar{\mathcal{E}}|^2_{\mathrm{av}} &= \frac{1}{T}\int_0^T \bar{\mathcal{E}} \cdot \bar{\mathcal{E}}\, dt \\
&= \frac{1}{T}\int_0^T \left[E_1^2 \cos^2(\omega t + \phi_1) + E_2^2 \cos^2(\omega t + \phi_2) + E_3^2 \cos^2(\omega t + \phi_3)\right] dt \\
&= \frac{1}{2}\left(E_1^2 + E_2^2 + E_3^2\right) = \frac{1}{2}|\bar{E}|^2 = \frac{1}{2}\bar{E} \cdot \bar{E}^*.
\end{aligned} \tag{1.13}$$

Then the root-mean-square (rms) value is $|\bar{E}|_{\mathrm{rms}} = |\bar{E}|/\sqrt{2}$.

Assuming an $e^{j\omega t}$ time dependence, the time derivatives in (1.1a)–(1.1d) can be replaced by $j\omega$. Maxwell's equations in phasor form then become

$$\nabla \times \bar{E} = -j\omega\bar{B} - \bar{M}, \tag{1.14a}$$
$$\nabla \times \bar{H} = j\omega\bar{D} + \bar{J}, \tag{1.14b}$$
$$\nabla \cdot \bar{D} = \rho, \tag{1.14c}$$
$$\nabla \cdot \bar{B} = 0. \tag{1.14d}$$

The Fourier transform can be used to convert a solution to Maxwell's equations for an arbitrary frequency ω to a solution for arbitrary time dependence.

The electric and magnetic current sources, $\bar{J}$ and $\bar{M}$, in (1.14) are volume current densities with units A/m^2 and V/m^2, respectively. In many cases, however, the actual currents will be in the form of a current sheet, a line current, or an infinitesimal dipole current. These special types of current distributions can always be written as volume current densities through the use of delta functions. Figure 1.4 shows examples of this procedure for electric and magnetic currents.

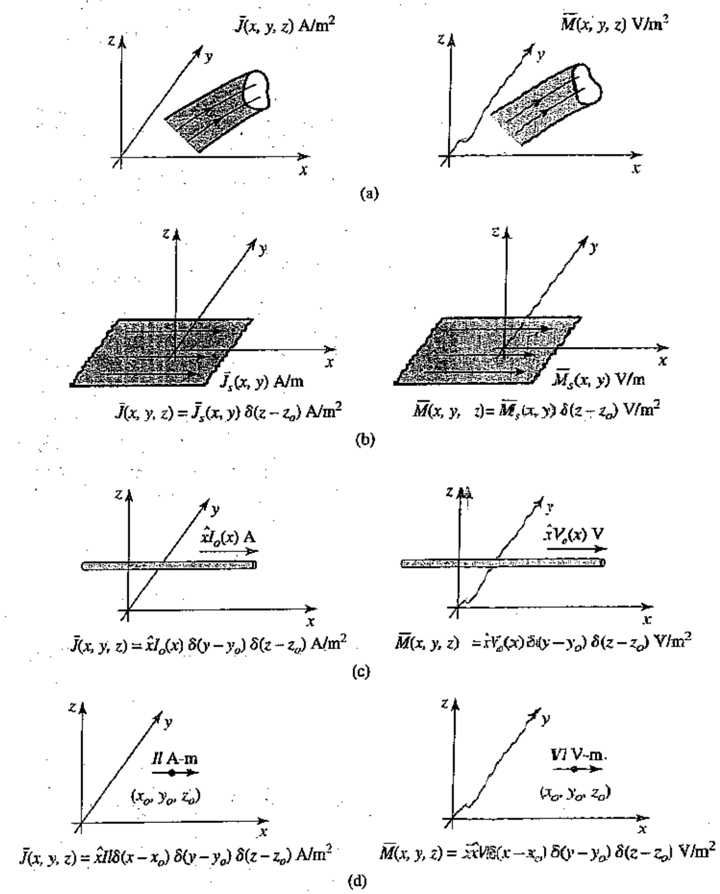

FIGURE 1.4 Arbitrary volume, surface, and line currents. (a) Arbitrary electric and magnetic volume current densities. (b) Arbitrary electric and magnetic surface current densities in the $z = z_0$ plane. (c) Arbitrary electric and magnetic line currents. (d) Infinitesimal electric and magnetic dipoles parallel to the x-axis.

1.3 FIELDS IN MEDIA AND BOUNDARY CONDITIONS

In the preceding section it was assumed that the electric and magnetic fields were in free-space, with no material bodies present. In practice, material bodies are often present; this complicates the analysis but also allows the useful application of material properties to microwave components. When electromagnetic fields exist in material media, the field vectors are related to each other by the constitutive relations.

For a dielectric material, an applied electric field $\bar{E}$ causes the polarization of the atoms or molecules of the material to create electric dipole moments that augment the total displacement flux, $\bar{D}$. This additional polarization vector is called $\bar{P}_e$, the electric polarization, where

$$\bar{D} = \epsilon_0\bar{E} + \bar{P}_e. \tag{1.15}$$

In a linear medium, the electric polarization is linearly related to the applied electric field as

$$\bar{P}_e = \epsilon_0\chi_e\bar{E}, \tag{1.16}$$

where χ_e, which may be complex, is called the *electric susceptibility*. Then,

$$\bar{D} = \epsilon_0\bar{E} + \bar{P}_e = \epsilon_0(1+\chi_e)\bar{E} = \epsilon\bar{E}, \tag{1.17}$$

where

$$\epsilon = \epsilon' - j\epsilon'' = \epsilon_0(1+\chi_e) \tag{1.18}$$

is the complex permittivity of the medium. The imaginary part of ϵ accounts for loss in the medium (heat) due to damping of the vibrating dipole moments. (Free-space, having a real ϵ, is lossless.) Due to energy conservation, as we will see in Section 1.6, the imaginary part of ϵ must be negative (ϵ'' positive). The loss of a dielectric material may also be considered as an equivalent conductor loss. In a material with conductivity σ, a conduction current density will exist:

$$\bar{J} = \sigma\bar{E}, \tag{1.19}$$

which is Ohm's law from an electromagnetic field point of view. Maxwell's curl equation for $\bar{H}$ in (1.14b) then becomes

$$\begin{aligned}\nabla\times\bar{H} &= j\omega\bar{D} + \bar{J}\\ &= j\omega\epsilon\bar{E} + \sigma\bar{E}\\ &= j\omega\epsilon'\bar{E} + (\omega\epsilon'' + \sigma)\bar{E}\\ &= j\omega\left(\epsilon' - j\epsilon'' - j\frac{\sigma}{\omega}\right)\bar{E},\end{aligned} \tag{1.20}$$

where it is seen that loss due to dielectric damping ($\omega\epsilon''$) is indistinguishable from conductivity loss (σ). The term $\omega\epsilon'' + \sigma$ can then be considered as the total effective conductivity. A related quantity of interest is the loss tangent, defined as

$$\tan\delta = \frac{\omega\epsilon'' + \sigma}{\omega\epsilon'}, \tag{1.21}$$

which is seen to be the ratio of the real to the imaginary part of the total displacement current. Microwave materials are usually characterized by specifying the real permittivity, $\epsilon' = \epsilon_r\epsilon_0$, and the loss tangent at a certain frequency. These constants are listed in Appendix G for several types of materials. It is useful to note that, after a problem has been solved assuming a lossless dielectric, loss can easily be introduced by replacing the real ϵ with a complex $\epsilon = \epsilon' - j\epsilon'' = \epsilon'(1 - j\tan\delta) = \epsilon_0\epsilon_r(1 - j\tan\delta)$.

In the preceding discussion it was assumed that $\bar{P}_e$ was a vector in the same direction as $\bar{E}$. Such materials are called isotropic materials, but not all materials have this property. Some materials are anisotropic and are characterized by a more complicated relation between $\bar{P}_e$ and $\bar{E}$, or $\bar{D}$ and $\bar{E}$. The most general linear relation between these vectors takes the form of a tensor of rank two (a dyad), which can be written in matrix form as

$$\begin{bmatrix} D_x \\ D_y \\ D_z \end{bmatrix} = \begin{bmatrix} \epsilon_{xx} & \epsilon_{xy} & \epsilon_{xz} \\ \epsilon_{yx} & \epsilon_{yy} & \epsilon_{yz} \\ \epsilon_{zx} & \epsilon_{zy} & \epsilon_{zz} \end{bmatrix} \begin{bmatrix} E_x \\ E_y \\ E_z \end{bmatrix} = [\epsilon]\begin{bmatrix} E_x \\ E_y \\ E_z \end{bmatrix}. \tag{1.22}$$

It is thus seen that a given vector component of $\bar{E}$ gives rise, in general, to three components of $\bar{D}$. Crystal structures and ionized gases are examples of anisotropic dielectrics. For a linear isotropic material, the matrix of (1.22) would reduce to a diagonal matrix with elements ϵ.

An analogous situation occurs for magnetic materials. An applied magnetic field may align magnetic dipole moments in a magnetic material to produce a magnetic polarization (or magnetization) $\bar{P}_m$. Then,

$$\bar{B} = \mu_0(\bar{H} + \bar{P}_m). \tag{1.23}$$

For a linear magnetic material, $\bar{P}_m$ is linearly related to $\bar{H}$ as

$$\bar{P}_m = \chi_m\bar{H}, \tag{1.24}$$

where χ_m is a complex magnetic susceptibility. From (1.23) and (1.24),

$$\bar{B} = \mu_0(1+\chi_m)\bar{H} = \mu\bar{H}, \tag{1.25}$$

where $\mu = \mu_0(1+\chi_m) = \mu' - j\mu''$ is the permeability of the medium. Again, the imaginary part of χ_m or μ accounts for loss due to damping forces; there is no magnetic conductivity, since there is no real magnetic current. As in the electric case, magnetic materials may be anisotropic, in which case a tensor permeability can be written as

$$\begin{bmatrix} B_x \\ B_y \\ B_z \end{bmatrix} = \begin{bmatrix} \mu_{xx} & \mu_{xy} & \mu_{xz} \\ \mu_{yx} & \mu_{yy} & \mu_{yz} \\ \mu_{zx} & \mu_{zy} & \mu_{zz} \end{bmatrix} \begin{bmatrix} H_x \\ H_y \\ H_z \end{bmatrix} = [\mu]\begin{bmatrix} H_x \\ H_y \\ H_z \end{bmatrix}. \tag{1.26}$$

An important example of anisotropic magnetic materials in microwave engineering is the class of ferrimagnetic materials known as ferrites; these materials and their applications will be discussed further in Chapter 9.

If linear media are assumed (ϵ, μ not depending on $\bar{E}$ or $\bar{H}$), then Maxwell's equations can be written in phasor form as

$$\nabla\times\bar{E} = -j\omega\mu\bar{H} - \bar{M}, \tag{1.27a}$$
$$\nabla\times\bar{H} = j\omega\epsilon\bar{E} + \bar{J}, \tag{1.27b}$$
$$\nabla\cdot\bar{D} = \rho, \tag{1.27c}$$
$$\nabla\cdot\bar{B} = 0. \tag{1.27d}$$

The constitutive relations are

$$\bar{D} = \epsilon\bar{E}, \tag{1.28a}$$
$$\bar{B} = \mu\bar{H}, \tag{1.28b}$$

where ϵ and μ may be complex and may be tensors. Note that relations like (1.28a) and (1.28b) generally cannot be written in time domain form, even for linear media, because of the possible phase shift between $\bar{D}$ and $\bar{E}$, or $\bar{B}$ and $\bar{H}$. The phasor representation accounts for this phase shift by the complex form of ϵ and μ.

Maxwell's equations (1.27a)–(1.27d) in differential form require known boundary values for a complete and unique solution. A general method used throughout this book is to solve the source-free Maxwell's equations in a certain region to obtain solutions with unknown coefficients, and then apply boundary conditions to solve for these coefficients. A number of specific cases of boundary conditions arise, as discussed below.

Fields at a General Material Interface

Consider a plane interface between two media, as shown in Figure 1.5. Maxwell's equations in integral form can be used to deduce conditions involving the normal and tangential fields

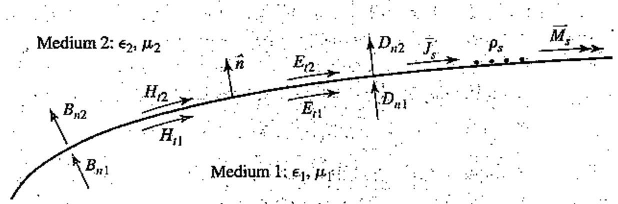

FIGURE 1.5 Fields, currents, and surface charge at a general interface between two media.

at this interface. The time-harmonic version of (1.4), where S is the closed "pillbox"-shaped surface shown in Figure 1.6, can be written as

$$\oint_S \bar{D} \cdot d\bar{s} = \int_V \rho \, dv. \tag{1.29}$$

In the limit as $h \to 0$, the contribution of $D_{\tan}$ through the sidewalls goes to zero, so (1.29) reduces to

$$\Delta S D_{2n} - \Delta S D_{1n} = \Delta S \rho_s,$$

or

$$D_{2n} - D_{1n} = \rho_s, \tag{1.30}$$

where ρ_s is the surface charge density on the interface. In vector form, we can write

$$\hat{n} \cdot (\bar{D}_2 - \bar{D}_1) = \rho_s. \tag{1.31}$$

A similar argument for $\bar{B}$ leads to the result that

$$\hat{n} \cdot \bar{B}_2 = \hat{n} \cdot \bar{B}_1, \tag{1.32}$$

since there is no free magnetic charge.

For the tangential components of the electric field we use the phasor form of (1.6),

$$\oint_C \bar{E} \cdot d\bar{l} = -j\omega \int_S \bar{B} \cdot d\bar{s} - \int_S \bar{M} \cdot d\bar{s}, \tag{1.33}$$

in connection with the closed contour C shown in Figure 1.7. In the limit as $h \to 0$, the surface integral of $\bar{B}$ vanishes (since $S = h\,\Delta\ell$ vanishes). The contribution from the surface integral of $\bar{M}$, however, may be nonzero if a magnetic surface current density $\bar{M}_s$ exists on the surface. The Dirac delta function can then be used to write

$$\bar{M} = \bar{M}_s \delta(h), \tag{1.34}$$

where h is a coordinate measured normal from the interface. Equation (1.33) then gives

$$\Delta\ell E_{t1} - \Delta\ell E_{t2} = -\Delta\ell M_s,$$

or

$$E_{t1} - E_{t2} = -M_s; \tag{1.35}$$

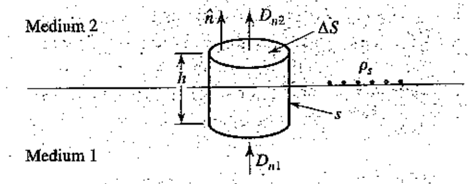

FIGURE 1.6 Closed surface S for equation (1.29).

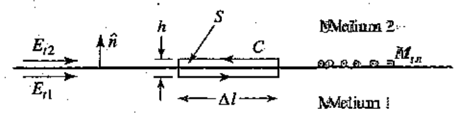

FIGURE 1.7 Closed contour C for Equation (1.33).

which can be generalized in vector form as

$$(\bar{E}_2 - \bar{E}_1) \times \hat{n} = \bar{M}_s. \tag{1.36}$$

A similar argument for the magnetic field leads to

$$\hat{n} \times (\bar{H}_2 - \bar{H}_1) = \bar{J}_s, \tag{1.37}$$

where $\bar{J}_s$ is an electric surface current density that may exist at the interface. Equations (1.31), (1.32), (1.36), and (1.37) are the most general expressions for the boundary conditions at an arbitrary interface of materials and/or surface currents.

Fields at a Dielectric Interface

At an interface between two lossless dielectric materials, no charge or surface current densities will ordinarily exist. Equations (1.31), (1.32), (1.36), and (1.37) then reduce to

$$\hat{n} \cdot \bar{D}_1 = \hat{n} \cdot \bar{D}_2, \tag{1.38a}$$
$$\hat{n} \cdot \bar{B}_1 = \hat{n} \cdot \bar{B}_2, \tag{1.38b}$$
$$\hat{n} \times \bar{E}_1 = \hat{n} \times \bar{E}_2, \tag{1.38c}$$
$$\hat{n} \times \bar{H}_1 = \hat{n} \times \bar{H}_2. \tag{1.38d}$$

In words, these equations state that the normal components of $\bar{D}$ and $\bar{B}$ are continuous across the interface, and the tangential components of $\bar{E}$ and $\bar{H}$ are continuous across the interface. Because Maxwell's equations are not all linearly independent, the six boundary conditions contained in the above equations are not all linearly independent. Thus, the enforcement of (1.38c) and (1.38d) for the four tangential field components, for example, will automatically force the satisfaction of the equations for the continuity of the normal components.

Fields at the Interface with a Perfect Conductor (Electric Wall)

Many problems in microwave engineering involve boundaries with good conductors (e.g., metals), which can often be assumed as lossless ($\sigma \to \infty$). In this case of a perfect conductor, all field components must be zero inside the conducting region. This result can be seen by considering a conductor with finite conductivity ($\sigma < \infty$) and noting that the skin depth (the depth to which most of the microwave power penetrates) goes to zero as $\sigma \to \infty$. (Such an analysis will be performed in Section 1.7.) If we also assume here that $\bar{M}_s = 0$, which would be the case if the perfect conductor filled all the space on one side of the boundary, then (1.31), (1.32), (1.36), and (1.37) reduce to the following:

$$\hat{n} \cdot \bar{D} = \rho_s, \tag{1.39a}$$
$$\hat{n} \cdot \bar{B} = 0, \tag{1.39b}$$
$$\hat{n} \times \bar{E} = 0, \tag{1.39c}$$
$$\hat{n} \times \bar{H} = \bar{J}_s, \tag{1.39d}$$

where ρ_s and $\bar{J}_s$ are the electric surface charge density and current density, respectively, on the interface, and $\hat{n}$ is the normal unit vector pointing out of the perfect conductor. Such a boundary is also known as an *electric wall*, because the tangential components of $\bar{E}$ are "shorted out," as seen from (1.39c), and must vanish at the surface of the conductor.

The Magnetic Wall Boundary Condition

Dual to the preceding boundary condition is the *magnetic wall* boundary condition, where the tangential components of $\bar{H}$ must vanish. Such a boundary does not really exist in practice, but may be approximated by a corrugated surface, or in certain planar transmission line problems. In addition, the idealization that $\hat{n} \times \bar{H} = 0$ at an interface is often a convenient simplification, as we will see in later chapters. We will also see that the magnetic wall boundary condition is analogous to the relations between the voltage and current at the end of an open-circuited transmission line, while the electric wall boundary condition is analogous to the voltage and current at the end of a short-circuited transmission line. The magnetic wall condition, then, provides a degree of completeness in our formulation of boundary conditions and is a useful approximation in several cases of practical interest.

The fields at a magnetic wall satisfy the following conditions:

$$\hat{n} \cdot \bar{D} = 0, \tag{1.40a}$$

$$\hat{n} \cdot \bar{B} = 0, \tag{1.40b}$$

$$\hat{n} \times \bar{E} = -\bar{M}_s, \tag{1.40c}$$

$$\hat{n} \times \bar{H} = 0, \tag{1.40d}$$

where $\hat{n}$ is the normal unit vector pointing out of the magnetic wall region.

The Radiation Condition

When dealing with problems that have one or more infinite boundaries, such as plane waves in an infinite medium, or infinitely long transmission lines, a condition on the fields at infinity must be enforced. This boundary condition is known as the *radiation condition*, and is essentially a statement of energy conservation. It states that, at an infinite distance from a source, the fields must either be vanishingly small (i.e., zero) or propagating in an outward direction. This result can easily be seen by allowing the infinite medium to contain a small loss factor (as any physical medium would have). Incoming waves (from infinity) of finite amplitude would then require an infinite source at infinity, and so are disallowed.

1.4 THE WAVE EQUATION AND BASIC PLANE WAVE SOLUTIONS

The Helmholtz Equation

In a source-free, linear, isotropic, homogeneous region, Maxwell's curl equations in phasor form are

$$\nabla \times \bar{E} = -j\omega\mu\bar{H}, \tag{1.41a}$$

$$\nabla \times \bar{H} = j\omega\epsilon\bar{E}, \tag{1.41b}$$

and constitute two equations for the two unknowns, $\bar{E}$ and $\bar{H}$. As such, they can be solved for either $\bar{E}$ or $\bar{H}$. Thus, taking the curl of (1.41a) and using (1.41b) gives

$$\nabla \times \nabla \times \bar{E} = -j\omega\mu\nabla \times \bar{H} = \omega^2\mu\epsilon\bar{E},$$

which is an equation for $\bar{E}$. This result can be simplified through the use of vector identity (B.14), $\nabla \times \nabla \times \bar{A} = \nabla(\nabla \cdot \bar{A}) - \nabla^2\bar{A}$, which is valid for the rectangular components of an arbitrary vector $\bar{A}$. Then,

$$\nabla^2\bar{E} + \omega^2\mu\epsilon\bar{E} = 0, \tag{1.42}$$

since $\nabla \cdot \bar{E} = 0$ in a source-free region. Equation (1.42) is the wave equation, or Helmholtz equation, for $\bar{E}$. An identical equation for $\bar{H}$ can be derived in the same manner:

$$\nabla^2\bar{H} + \omega^2\mu\epsilon\bar{H} = 0. \tag{1.43}$$

A constant $k = \omega\sqrt{\mu\epsilon}$ is defined and called the wavenumber, or propagation constant, of the medium; its units are 1/m.

As a way of introducing wave behavior, we will next study the solutions to the above wave equations in their simplest forms, first for a lossless medium and then for a lossy (conducting) medium.

Plane Waves in a Lossless Medium

In a lossless medium, ϵ and μ are real numbers, so k is real. A basic plane wave solution to the above wave equations can be found by considering an electric field with only an $\hat{x}$ component and uniform (no variation) in the x and y directions. Then, $\partial/\partial x = \partial/\partial y = 0$, and the Helmholtz equation of (1.42) reduces to

$$\frac{\partial^2 E_x}{\partial z^2} + k^2 E_x = 0. \tag{1.44}$$

The two independent solutions to this equation are easily seen, by substitution, to be of the form

$$E_x(z) = E^+e^{-jkz} + E^-e^{jkz}, \tag{1.45}$$

where E^+ and E^- are arbitrary amplitude constants.

The above solution is for the time harmonic case at frequency ω. In the time domain, this result is written as

$$\mathcal{E}_x(z, t) = E^+\cos(\omega t - kz) + E^-\cos(\omega t + kz), \tag{1.46}$$

where we have assumed that E^+ and E^- are real constants. Consider the first term in (1.46). This term represents a wave traveling in the $+z$ direction, since, to maintain a fixed point on the wave ($\omega t - kz$ = constant), one must move in the $+z$ direction as time increases. Similarly, the second term in (1.46) represents a wave traveling in the negative z direction; hence the notation E^+ and E^- for these wave amplitudes. The velocity of the wave in this sense is called the *phase velocity*, because it is the velocity at which a fixed phase point on the wave travels, and it is given by

$$v_p = \frac{dz}{dt} = \frac{d}{dt}\left(\frac{\omega t - \text{constant}}{k}\right) = \frac{\omega}{k} = \frac{1}{\sqrt{\mu\epsilon}}. \tag{1.47}$$

In free-space, we have $v_p = 1/\sqrt{\mu_0\epsilon_0} = c = 2.998 \times 10^8$ m/sec, which is the speed of light.

The wavelength, λ, is defined as the distance between two successive maxima (or minima, or any other reference points) on the wave, at a fixed instant of time.

Thus,

$$[\omega t - kz] - [\omega t - k(z + \lambda)] = 2\pi,$$

so,

$$\lambda = \frac{2\pi}{k} = \frac{2\pi v_p}{\omega} = \frac{v_p}{f}. \tag{1.48}$$

A complete specification of the plane wave electromagnetic field must include the magnetic field. In general, whenever $\bar{E}$ or $\bar{H}$ is known, the other field vector can be readily found by using one of Maxwell's curl equations. Thus, applying (1.41a) to the electric field of (1.45) gives $H_x = H_z = 0$, and

$$H_y = \frac{1}{\eta}[E^+ e^{-jkz} - E^- e^{jkz}], \tag{1.49}$$

where $\eta = \omega\mu/k = \sqrt{\mu/\epsilon}$ is the wave impedance for the plane wave, defined as the ratio of the $\bar{E}$ and $\bar{H}$ fields. For plane waves, this impedance is also the intrinsic impedance of the medium. In free-space we have $\eta_0 = \sqrt{\mu_0/\epsilon_0} = 377\ \Omega$. Note that the $\bar{E}$ and $\bar{H}$ vectors are orthogonal to each other and orthogonal to the direction of propagation ($\pm\hat{z}$); this is a characteristic of transverse electromagnetic (TEM) waves.

EXAMPLE 1.1 BASIC PLANE WAVE PARAMETERS

A plane wave propagating in a lossless dielectric medium has an electric field given as $\mathcal{E}_x = E_0 \cos(1.51 \times 10^{10} t - 61.6z)$. Determine the wavelength, phase velocity, and wave impedance for this wave, and the dielectric constant of the medium.

Solution

By comparison with (1.46) we identify $\omega = 1.51 \times 10^{10}$ rad/sec and $k = 61.6\ \text{m}^{-1}$. Using (1.48) then gives the wavelength as

$$\lambda = \frac{2\pi}{k} = \frac{2\pi}{61.6} = 0.102\ \text{m}.$$

The phase velocity can be found from (1.47):

$$v_p = \frac{\omega}{k} = \frac{1.51 \times 10^{10}}{61.6} = 2.45 \times 10^8\ \text{m/sec}.$$

This is slower than the speed of light by a factor of 1.225. The dielectric constant of the medium can be found as

$$\epsilon_r = \left(\frac{c}{v_p}\right)^2 = \left(\frac{3.0 \times 10^8}{2.45 \times 10^8}\right)^2 = 1.50.$$

The wave impedance is

$$\eta = \eta_0/\sqrt{\epsilon_r} = \frac{377}{\sqrt{1.5}} = 307.8\ \Omega.$$

Plane Waves in a General Lossy Medium

Now consider the effect of a lossy medium. If the medium is conductive, with a conductivity σ, Maxwell's curl equations can be written, from (1.41a) and (1.20) as

$$\nabla \times \bar{E} = -j\omega\mu\bar{H}, \tag{1.50a}$$

$$\nabla \times \bar{H} = j\omega\epsilon\bar{E} + \sigma\bar{E}. \tag{1.50b}$$

The resulting wave equation for $\bar{E}$ then becomes

$$\nabla^2\bar{E} + \omega^2\mu\epsilon\left(1 - j\frac{\sigma}{\omega\epsilon}\right)\bar{E} = 0, \tag{1.51}$$

where we see a similarity with (1.42), the wave equation for $\bar{E}$ in the lossless case. The difference is that the wavenumber $k^2 = \omega^2\mu\epsilon$ of (1.42) is replaced by $\omega^2\mu\epsilon[1 - j(\sigma/\omega\epsilon)]$ in (1.51). We then define a complex propagation constant for the medium as

$$\gamma = \alpha + j\beta = j\omega\sqrt{\mu\epsilon}\sqrt{1 - j\frac{\sigma}{\omega\epsilon}} \tag{1.52}$$

If we again assume an electric field with only an $\hat{x}$ component and uniform in x and y, the wave equation of (1.51) reduces to

$$\frac{\partial^2 E_x}{\partial z^2} - \gamma^2 E_x = 0, \tag{1.53}$$

which has solutions

$$E_x(z) = E^+ e^{-\gamma z} + E^- e^{\gamma z}. \tag{1.54}$$

The positive traveling wave then has a propagation factor of the form

$$e^{-\gamma z} = e^{-\alpha z}e^{-j\beta z},$$

which in the time domain is of the form

$$e^{-\alpha z}\cos(\omega t - \beta z).$$

We see that this represents a wave traveling in the $+z$ direction with a phase velocity $v_p = \omega/\beta$, a wavelength $\lambda = 2\pi/\beta$, and an exponential damping factor. The rate of decay with distance is given by the attenuation constant, α. The negative traveling wave term of (1.54) is similarly damped along the $-z$ axis. If the loss is removed, $\sigma = 0$, and we have $\gamma = jk$ and $\alpha = 0$, $\beta = k$.

As discussed in Section 1.3, loss can also be treated through the use of a complex permittivity. From (1.52) and (1.20) with $\sigma = 0$ but $\epsilon = \epsilon' - j\epsilon''$ complex, we have that

$$\gamma = j\omega\sqrt{\mu\epsilon} = jk = j\omega\sqrt{\mu\epsilon'(1 - j\tan\delta)}, \tag{1.55}$$

where $\tan\delta = \epsilon''/\epsilon'$ is the loss tangent of the material.

Next, the associated magnetic field can be calculated as

$$H_y = \frac{j}{\omega\mu}\frac{\partial E_x}{\partial z} = \frac{-j\gamma}{\omega\mu}(E^+e^{-\gamma z} - E^-e^{\gamma z}). \tag{1.56}$$

As with the lossless case, a wave impedance can be defined to relate the electric and magnetic fields:

$$\eta = \frac{j\omega\mu}{\gamma}. \tag{1.57}$$

Then (1.56) can be rewritten as

$$H_y = \frac{1}{\eta}(E^+e^{-\gamma z} - E^-e^{\gamma z}). \tag{1.58}$$

Note that η is, in general, complex and reduces to the lossless case of $\eta = \sqrt{\mu/\epsilon}$ when $\gamma = jk = j\omega\sqrt{\mu\epsilon}$.

Plane Waves in a Good Conductor

Many problems of practical interest involve loss or attenuation due to good (but not perfect) conductors. A good conductor is a special case of the preceding analysis, where the conductive current is much greater than the displacement current, which means $\sigma \gg \omega\epsilon$. Most metals can be categorized as good conductors. In terms of a complex ϵ, rather than conductivity, this condition is equivalent to $\epsilon'' \gg \epsilon'$. The propagation constant of (1.52) can then be adequately approximated by ignoring the displacement current term, to give

$$\gamma = \alpha + j\beta \simeq j\omega\sqrt{\mu\epsilon}\sqrt{\frac{\sigma}{j\omega\epsilon}} = (1+j)\sqrt{\frac{\omega\mu\sigma}{2}}. \tag{1.59}$$

The *skin depth*, or characteristic depth of penetration, is defined as

$$\delta_s = \frac{1}{\alpha} = \sqrt{\frac{2}{\omega\mu\sigma}}. \tag{1.60}$$

Then the amplitude of the fields in the conductor decay by an amount $1/e$ or 36.8%, after traveling a distance of one skin depth, since $e^{-\alpha z} = e^{-\alpha\delta_s} = e^{-1}$. At microwave frequencies, for a good conductor, this distance is very small. The practical importance of this result is that only a thin plating of a good conductor (e.g., silver or gold) is necessary for low-loss microwave components.

EXAMPLE 1.2 SKIN DEPTH AT MICROWAVE FREQUENCIES

Compute the skin depth of aluminum, copper, gold, and silver at a frequency of 10 GHz.

Solution

The conductivities for these metals are listed in Appendix F. Equation (1.60) gives the skin depths as

$$\delta_s = \sqrt{\frac{2}{\omega\mu\sigma}} = \sqrt{\frac{1}{\pi f \mu_0 \sigma}} = \sqrt{\frac{1}{\pi(10^{10})(4\pi\times10^{-7})}}\sqrt{\frac{1}{\sigma}}$$

$$= 5.03\times10^{-3}\sqrt{\frac{1}{\sigma}}.$$

For aluminum: $\delta_s = 5.03\times10^{-3}\sqrt{\frac{1}{3.816\times10^7}} = 8.14\times10^{-7}$ m.

For copper: $\delta_s = 5.03\times10^{-3}\sqrt{\frac{1}{5.813\times10^7}} = 6.60\times10^{-7}$ m.

For gold: $\delta_s = 5.03\times10^{-3}\sqrt{\frac{1}{4.098\times10^7}} = 7.86\times10^{-7}$ m.

For silver: $\delta_s = 5.03\times10^{-3}\sqrt{\frac{1}{6.173\times10^7}} = 6.40\times10^{-7}$ m.

TABLE 1.1 Summary of Results for Plane Wave Propagation in Various Media

	Type of Medium		
Quantity	Lossless ($\epsilon'' = \sigma = 0$)	General Lossy	Good Conductor $\epsilon'' \gg \epsilon'$ or $\sigma \gg \omega\epsilon'$
Complex propagation constant	$\gamma = j\omega\sqrt{\mu\epsilon}$	$\gamma = j\omega\sqrt{\mu\epsilon} = j\omega\sqrt{\mu\epsilon'}\sqrt{1 - j\frac{\sigma}{\omega\epsilon'}}$	$\gamma = (1+j)\sqrt{\omega\mu\sigma/2}$
Phase constant (wavenumber)	$\beta = k = \omega\sqrt{\mu\epsilon}$	$\beta = \mathrm{Im}(\gamma)$	$\beta = \mathrm{Im}(\gamma) = \sqrt{\omega\mu\sigma/2}$
Attenuation constant	$\alpha = 0$	$\alpha = \mathrm{Re}(\gamma)$	$\alpha = \mathrm{Re}(\gamma) = \sqrt{\omega\mu\sigma/2}$
Impedance	$\eta = \sqrt{\mu/\epsilon} = \omega\mu/k$	$\eta = j\omega\mu/\gamma$	$\eta = (1+j)\sqrt{\omega\mu/2\sigma}$
Skin depth	$\delta_s = \infty$	$\delta_s = 1/\alpha$	$\delta_s = \sqrt{2/\omega\mu\sigma}$
Wavelength	$\lambda = 2\pi/\beta$	$\lambda = 2\pi/\beta$	$\lambda = 2\pi/\beta$
Phase velocity	$v_p = \omega/\beta$	$v_p = \omega/\beta$	$v_p = \omega/\beta$

These results show that most of the current flow in a good conductor occurs in an extremely thin region near the surface of the conductor. ■

The wave impedance inside a good conductor can be obtained from (1.57) and (1.59). The result is

$$\eta = \frac{j\omega\mu}{\gamma} \simeq (1+j)\sqrt{\frac{\omega\mu}{2\sigma}} = (1+j)\frac{1}{\sigma\delta_s}. \tag{1.61}$$

Notice that the phase angle of this impedance is 45°, a characteristic of good conductors. The phase angle of the impedance for a lossless material is 0°, and the phase angle of the impedance of an arbitrary lossy medium is somewhere between 0° and 45°.

Table 1.1 summarizes the results for plane wave propagation in lossless and lossy homogeneous media.

1.5 GENERAL PLANE WAVE SOLUTIONS

Some specific features of plane waves were discussed in Section 1.4. Here we will look at plane waves again, from a more general point of view, and solve the wave equation by the method of separation of variables. This technique will find application in succeeding chapters. We will also discuss circularly polarized plane waves, which will be important for the discussion of ferrites in Chapter 9.

In free space, the Helmholtz equation for $\bar{E}$ can be written as

$$\nabla^2\bar{E} + k_0^2\bar{E} = \frac{\partial^2\bar{E}}{\partial x^2} + \frac{\partial^2\bar{E}}{\partial y^2} + \frac{\partial^2\bar{E}}{\partial z^2} + k_0^2\bar{E} = 0, \tag{1.62}$$

and this vector wave equation holds for each rectangular component of $\bar{E}$:

$$\frac{\partial^2 E_i}{\partial x^2} + \frac{\partial^2 E_i}{\partial y^2} + \frac{\partial^2 E_i}{\partial z^2} + k_0^2 E_i = 0, \tag{1.63}$$

where the index $i = x, y$, or z. This equation will now be solved by the method of separation of variables, a standard technique for treating such partial differential equations. The method begins by assuming that the solution to (1.63) for, say, E_x, can be written as a product of three functions for each of the three coordinates:

$$E_x(x, y, z) = f(x)\, g(y)\, h(z). \tag{1.64}$$

Substituting this form into (1.63) and dividing by fgh gives

$$\frac{f''}{f} + \frac{g''}{g} + \frac{h''}{h} + k_0^2 = 0, \tag{1.65}$$

where the double primes denote the second derivative. Now the key step in the argument is to recognize that each of the terms in (1.65) must be equal to a constant, since they are independent of each other. That is, f''/f is only a function of x, and the remaining terms in (1.65) do not depend on x, so f''/f must be a constant, and similarly for the other terms in (1.65). Thus, we define three separation constants, k_x, k_y, and k_z, such that

$$f''/f = -k_x^2; \quad g''/g = -k_y^2; \quad h''/h = -k_z^2;$$

or

$$\frac{d^2 f}{dx^2} + k_x^2 f = 0; \quad \frac{d^2 g}{dy^2} + k_y^2 g = 0; \quad \frac{d^2 h}{dz^2} + k_z^2 h = 0. \tag{1.66}$$

Combining (1.65) and (1.66) shows that

$$k_x^2 + k_y^2 + k_z^2 = k_0^2. \tag{1.67}$$

The partial differential equation of (1.63) has now been reduced to three separate ordinary differential equations in (1.66). Solutions to these equations are of the form $e^{\pm jk_x x}$, $e^{\pm jk_y y}$, and $e^{\pm jk_z z}$, respectively. As we have seen in the previous section, the terms with + signs result in waves traveling in the negative x, y, or z direction, while the terms with − signs result in waves traveling in the positive direction. Both solutions are possible and are valid; the amount to which these various terms are excited is dependent on the source of the fields. For our present discussion, we will select a plane wave traveling in the positive direction for each coordinate, and write the complete solution for E_x as

$$E_x(x, y, z) = Ae^{-j(k_x x + k_y y + k_z z)}, \tag{1.68}$$

where A is an arbitrary amplitude constant. Now define a wavenumber vector $\bar{k}$ as

$$\bar{k} = k_x\hat{x} + k_y\hat{y} + k_z\hat{z} = k_0\hat{n}. \tag{1.69}$$

Then from (1.67) $|\bar{k}| = k_0$, and so $\hat{n}$ is a unit vector in the direction of propagation. Also define a position vector as

$$\bar{r} = x\hat{x} + y\hat{y} + z\hat{z}; \tag{1.70}$$

then (1.68) can be written as

$$E_x(x, y, z) = Ae^{-j\bar{k}\cdot\bar{r}}. \tag{1.71}$$

Solutions to (1.63) for E_y and E_z are, of course, similar in form to E_x of (1.71), but with different amplitude constants:

$$E_y(x, y, z) = Be^{-j\bar{k}\cdot\bar{r}}, \tag{1.72}$$

$$E_z(x, y, z) = Ce^{-j\bar{k}\cdot\bar{r}}. \tag{1.73}$$

The x, y, and z dependences of the three components of $\bar{E}$ in (1.71)–(1.73) must be the same (same k_x, k_y, k_z), because the divergence condition that

$$\nabla \cdot \bar{E} = \frac{\partial E_x}{\partial x} + \frac{\partial E_y}{\partial y} + \frac{\partial E_z}{\partial z} = 0$$

must also be applied in order to satisfy Maxwell's equations, which implies that E_x, E_y, and E_z must each have the same variation in x, y, and z. (Note that the solutions in the preceding section automatically satisfied the divergence condition, since E_x was the only component of $\bar{E}$, and E_x did not vary with x.) This condition also imposes a constraint on the amplitudes A, B, and C, since if

$$\bar{E}_0 = A\hat{x} + B\hat{y} + C\hat{z},$$

we have

$$\bar{E} = \bar{E}_0 e^{-j\bar{k}\cdot\bar{r}},$$

and

$$\nabla \cdot \bar{E} = \nabla \cdot (\bar{E}_0 e^{-j\bar{k}\cdot\bar{r}}) = \bar{E}_0 \cdot \nabla e^{-j\bar{k}\cdot\bar{r}} = -j\bar{k} \cdot \bar{E}_0 e^{-j\bar{k}\cdot\bar{r}} = 0,$$

where vector identity (B.7) was used. Thus, we must have

$$\bar{k} \cdot \bar{E}_0 = 0, \tag{1.74}$$

which means that the electric field amplitude vector $\bar{E}_0$ must be perpendicular to the direction of propagation, $\bar{k}$. This condition is a general result for plane waves and implies that only two of the three amplitude constants, A, B, and C, can be chosen independently.

The magnetic field can be found from Maxwell's equation,

$$\nabla \times \bar{E} = -j\omega\mu_0 \bar{H}, \tag{1.75}$$

to give

$$\begin{aligned}
\bar{H} &= \frac{j}{\omega\mu_0} \nabla \times \bar{E} = \frac{j}{\omega\mu_0} \nabla \times (\bar{E}_0 e^{-j\bar{k}\cdot\bar{r}}) \\
&= \frac{-j}{\omega\mu_0} \bar{E}_0 \times \nabla e^{-j\bar{k}\cdot\bar{r}} \\
&= \frac{-j}{\omega\mu_0} \bar{E}_0 \times (-j\bar{k}) e^{-j\bar{k}\cdot\bar{r}} \\
&= \frac{k_0}{\omega\mu_0} \hat{n} \times \bar{E}_0 e^{-j\bar{k}\cdot\bar{r}} \\
&= \frac{1}{\eta_0} \hat{n} \times \bar{E}_0 e^{-j\bar{k}\cdot\bar{r}} \\
&= \frac{1}{\eta_0} \hat{n} \times \bar{E},
\end{aligned} \tag{1.76}$$

where vector identity (B.9) was used in obtaining the second line. This result shows that the magnetic field intensity vector $\bar{H}$ lies in a plane normal to $\bar{k}$, the direction of propagation, and that $\bar{H}$ is perpendicular to $\bar{E}$. See Figure 1.8 for an illustration of these vector relations. The quantity $\eta_0 = \sqrt{\mu_0/\epsilon_0} = 377\ \Omega$ in (1.76) is the intrinsic impedance of free-space.

The time-domain expression for the electric field can be found as

$$\begin{aligned}
\bar{\mathcal{E}}(x, y, z, t) &= \text{Re}\{\bar{E}(x, y, z)e^{j\omega t}\} \\
&= \text{Re}\{\bar{E}_0 e^{-j\bar{k}\cdot\bar{r}} e^{j\omega t}\} \\
&= \bar{E}_0 \cos(\bar{k}\cdot\bar{r} - \omega t),
\end{aligned} \tag{1.77}$$

assuming that the amplitude constants A, B, and C contained in $\bar{E}_0$ are real. If these constants are not real, their phases should be included inside the cosine term of (1.77). It

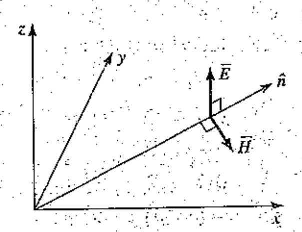

FIGURE 1.8 Orientation of the $\bar{E}$, $\bar{H}$, and $\bar{k} = k_0\hat{n}$ vectors for a general plane wave.

is easy to show that the wavelength and phase velocity for this solution are the same as obtained in Section 1.4.

EXAMPLE 1.3 CURRENT SHEETS AS SOURCES OF PLANE WAVES

An infinite sheet of surface current can be considered as a source for plane waves. If an electric surface current density $\bar{J}_s = J_o\hat{x}$ exists on the $z = 0$ plane in free-space, find the resulting fields by assuming plane waves on either side of the current sheet and enforcing boundary conditions.

Solution

Since the source does not vary with x or y, the fields will not vary with x or y but will propagate away from the source in the $\pm z$ direction. The boundary conditions to be satisfied at $z = 0$ are

$$\hat{n} \times (\bar{E}_2 - \bar{E}_1) = \hat{z} \times (\bar{E}_2 - \bar{E}_1) = 0,$$

$$\hat{n} \times (\bar{H}_2 - \bar{H}_1) = \hat{z} \times (\bar{H}_2 - \bar{H}_1) = J_o\hat{x},$$

where $\bar{E}_1$, $\bar{H}_1$ are the fields for $z < 0$, and $\bar{E}_2$, $\bar{H}_2$ are the fields for $z > 0$. To satisfy the second condition, $\bar{H}$ must have a $\hat{y}$ component. Then for $\bar{E}$ to be orthogonal to $\bar{H}$ and $\hat{z}$, $\bar{E}$ must have an $\hat{x}$ component. Thus the fields will have the following form:

$$\text{for } z < 0, \quad \bar{E}_1 = \hat{x}A\eta_0 e^{jk_0z}, \quad \bar{H}_1 = -\hat{y}Ae^{jk_0z},$$

$$\text{for } z > 0, \quad \bar{E}_2 = \hat{x}B\eta_0 e^{-jk_0z}, \quad \bar{H}_2 = \hat{y}Be^{-jk_0z},$$

where A and B are arbitrary amplitude constants. The first boundary condition, that E_x is continuous at $z = 0$, yields $A = B$, while the boundary condition for $\bar{H}$ yields the equation

$$-B - A = J_o.$$

Solving for A, B gives

$$A = B = -J_o/2,$$

which completes the solution. ■

Circularly Polarized Plane Waves

The plane waves discussed above all had their electric field vector pointing in a fixed direction and so are called *linearly polarized* waves. In general, the polarization of a plane wave refers to the orientation of the electric field vector, which may be in a fixed direction or may change with time.

Consider the superposition of an $\hat{x}$ linearly polarized wave with amplitude E_1 and a $\hat{y}$ linearly polarized wave with amplitude E_2, both traveling in the positive $\hat{z}$ direction. The total electric field can be written as

$$\bar{E} = (E_1\hat{x} + E_2\hat{y})e^{-jk_0z}. \tag{1.78}$$

A number of possibilities now arise. If $E_1 \neq 0$ and $E_2 = 0$, we have a plane wave linearly polarized in the $\hat{x}$ direction. Similarly, if $E_1 = 0$ and $E_2 \neq 0$, we have a plane wave linearly polarized in the $\hat{y}$ direction. If E_1 and E_2 are both real and nonzero, we have a plane wave linearly polarized at the angle

$$\phi = \tan^{-1}\frac{E_2}{E_1}.$$

For example, if $E_1 = E_2 = E_0$, we have

$$\bar{E} = E_0(\hat{x} + \hat{y})e^{-jk_0z},$$

which represents an electric field vector at a 45° angle from the x-axis.

Now consider the case in which $E_1 = jE_2 = E_0$, where E_0 is real, so that

$$\bar{E} = E_0(\hat{x} - j\hat{y})e^{-jk_0z}. \tag{1.79}$$

The time domain form of this field is

$$\bar{\mathcal{E}}(z, t) = E_0\{\hat{x}\cos(\omega t - k_0z) + \hat{y}\cos(\omega t - k_0z - \pi/2)\}. \tag{1.80}$$

This expression shows that the electric field vector changes with time or, equivalently, with distance along the z-axis. To see this, pick a fixed position, say $z = 0$. Equation (1.80) then reduces to

$$\bar{\mathcal{E}}(0, t) = E_0\{\hat{x}\cos\omega t + \hat{y}\sin\omega t\}, \tag{1.81}$$

so as ωt increases from zero, the electric field vector rotates counterclockwise from the x-axis. The resulting angle from the x-axis of the electric field vector at time t, at $z = 0$, is then

$$\phi = \tan^{-1}\left(\frac{\sin\omega t}{\cos\omega t}\right) = \omega t,$$

which shows that the polarization rotates at the uniform angular velocity ω. Since the fingers of the right hand point in the direction of rotation when the thumb points in the direction of propagation, this type of wave is referred to as a right hand circularly polarized (RHCP) wave. Similarly, a field of the form

$$\bar{E} = E_0(\hat{x} + j\hat{y})e^{-jk_0z} \tag{1.82}$$

constitutes a left hand circularly polarized (LHCP) wave, where the electric field vector rotates in the opposite direction. See Figure 1.9 for a sketch of the polarization vectors for RHCP and LHCP plane waves.

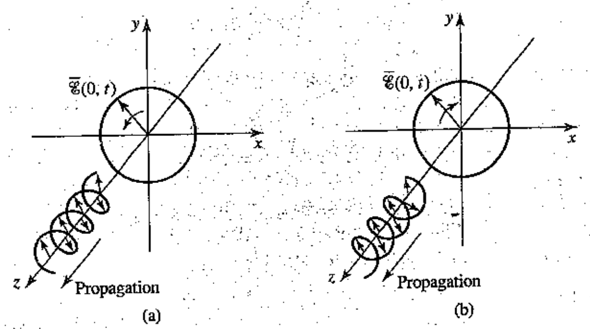

FIGURE 1.9 Electric field polarization for (a) RHCP and (b) LHCP plane waves.

The magnetic field associated with a circularly polarized wave may be found from Maxwell's equations, or by using the wave impedance applied to each component of the electric field. For example, applying (1.76) to the electric field of a RHCP wave as given in (1.79) yields

$$\bar{H} = \frac{E_0}{\eta_0}\hat{z} \times (\hat{x} - j\hat{y})e^{-jk_0 z} = \frac{E_0}{\eta_0}(\hat{y} + j\hat{x})e^{-jk_0 z} = \frac{jE_0}{\eta_0}(\hat{x} - j\hat{y})e^{-jk_0 z},$$

which is also seen to represent a vector rotating in the RHCP sense.

1.6 ENERGY AND POWER

In general, a source of electromagnetic energy sets up fields that store electric and magnetic energy and carry power that may be transmitted or dissipated as loss. In the sinusoidal steady-state case, the time-average stored electric energy in a volume V is given by,

$$W_e = \frac{1}{4}\mathrm{Re} \int_V \bar{E} \cdot \bar{D}^* \, dv, \tag{1.83}$$

which in the case of simple lossless isotropic, homogeneous, linear media, where ϵ is a real scalar constant, reduces to

$$W_e = \frac{\epsilon}{4} \int_V \bar{E} \cdot \bar{E}^* \, dv. \tag{1.84}$$

Similarly, the time-average magnetic energy stored in the volume V is

$$W_m = \frac{1}{4}\mathrm{Re} \int_V \bar{H} \cdot \bar{B}^* \, dv, \tag{1.85}$$

which becomes

$$W_m = \frac{\mu}{4} \int_V \bar{H} \cdot \bar{H}^* \, dv, \tag{1.86}$$

for a real, constant, scalar μ.

We can now derive Poynting's theorem, which leads to energy conservation for electromagnetic fields and sources. If we have an electric source current, $\bar{J}_s$, and a conduction current $\sigma\bar{E}$, as defined in (1.19), then the total electric current density is $\bar{J} = \bar{J}_s + \sigma\bar{E}$.

Then multiplying (1.27a) by $\bar{H}^*$, and multiplying the conjugate of (1.27b) by $\bar{E}$, yields

$$\bar{H}^* \cdot (\nabla \times \bar{E}) = -j\omega\mu|\bar{H}|^2 - \bar{H}^* \cdot \bar{M}_s,$$

$$\bar{E} \cdot (\nabla \times \bar{H}^*) = \bar{E} \cdot \bar{J}^* - j\omega\epsilon^*|\bar{E}|^2 = \bar{E} \cdot \bar{J}_s^* + \sigma|\bar{E}|^2 - j\omega\epsilon^*|\bar{E}|^2,$$

where $\bar{M}_s$ is the magnetic source current. Using these two results in vector identity (B.8) gives

$$\nabla \cdot (\bar{E} \times \bar{H}^*) = \bar{H}^* \cdot (\nabla \times \bar{E}) - \bar{E} \cdot (\nabla \times \bar{H}^*)$$
$$= -\sigma|\bar{E}|^2 + j\omega(\epsilon^*|\bar{E}|^2 - \mu|\bar{H}|^2) - (\bar{E} \cdot \bar{J}_s^* + \bar{H}^* \cdot \bar{M}_s).$$

Now integrate over a volume V and use the divergence theorem:

$$\int_V \nabla \cdot (\bar{E} \times \bar{H}^*) dv = \oint_S \bar{E} \times \bar{H}^* \cdot d\bar{s}$$
$$= -\sigma \int_V |\bar{E}|^2 dv + j\omega \int_V (\epsilon^*|\bar{E}|^2 - \mu|\bar{H}|^2) dv - \int_V (\bar{E} \cdot \bar{J}_s^* + \bar{H}^* \cdot \bar{M}_s) dv, \tag{1.87}$$

where S is a closed surface enclosing the volume V, as shown in Figure 1.10. Allowing $\epsilon = \epsilon' - j\epsilon''$ and $\mu = \mu' - j\mu''$ to be complex to allow for loss, and rewriting (1.87) gives

$$-\frac{1}{2}\int_V (\bar{E} \cdot \bar{J}_s^* + \bar{H}^* \cdot \bar{M}_s) dv = \frac{1}{2}\oint_S \bar{E} \times \bar{H}^* \cdot d\bar{s} + \frac{\sigma}{2}\int_V |\bar{E}|^2 dv$$
$$+ \frac{\omega}{2}\int_V (\epsilon''|\bar{E}|^2 + \mu''|\bar{H}|^2) dv + j\frac{\omega}{2}\int_V (\mu'|\bar{H}|^2 - \epsilon'|\bar{E}|^2) dv. \tag{1.88}$$

This result is known as Poynting's theorem, after the physicist J. H. Poynting (1852–1914), and is basically a power balance equation. Thus, the integral on the left-hand side represents the complex power, P_s, delivered by the sources $\bar{J}_s$ and $\bar{M}_s$, inside S:

$$P_s = -\frac{1}{2}\int_V (\bar{E} \cdot \bar{J}_s^* + \bar{H}^* \cdot \bar{M}_s) dv. \tag{1.89}$$

The first integral on the right-hand side of (1.88) represents complex power flow out of the closed surface S. If we define a quantity called the *Poynting vector*, $\bar{S}$, as

$$\bar{S} = \bar{E} \times \bar{H}^*, \tag{1.90}$$

then this power can be expressed as

$$P_o = \frac{1}{2}\oint_S \bar{E} \times \bar{H}^* \cdot d\bar{s} = \frac{1}{2}\oint_S \bar{S} \cdot d\bar{s}. \tag{1.91}$$

The surface S in (1.91) must be a closed surface in order for this interpretation to be valid. The real parts of P_s and P_o in (1.89) and (1.91) represent time-average powers.

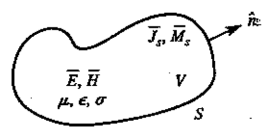

FIGURE 1.10 A volume V, enclosed by the closed surface S, containing fields $\bar{E}$, $\bar{H}$, and current sources $\bar{J}_s$, $\bar{M}_s$.

where $[\epsilon']$ is now a diagonal matrix. What are the elements of $[\epsilon']$? Using this result, derive wave equations for E_+ and E_-, and find the resulting propagation constants.

1.17 Show that the reciprocity theorem expressed in (1.157) also applies to a region enclosed by a closed surface S, where a surface impedance boundary condition applies.

1.18 Consider an electric surface current density of $\bar{J}_s = \hat{y} J_o e^{-\beta x}$ A/m, located on the $z = d$ plane. If a perfectly conducting ground plane is placed at $z = 0$, use image theory to find the total fields for $z > 0$.

C h a p t e r T w o

Transmission Line Theory

In many ways transmission line theory bridges the gap between field analysis and basic circuit theory, and so is of significant importance in microwave network analysis. As we will see, the phenomenon of wave propagation on transmission lines can be approached from an extension of circuit theory or from a specialization of Maxwell's equations; we shall present both viewpoints and show how this wave propagation is described by equations very similar to those used in Chapter 1 for plane wave propagation.

2.1 THE LUMPED-ELEMENT CIRCUIT MODEL FOR A TRANSMISSION LINE

The key difference between circuit theory and transmission line theory is electrical size. Circuit analysis assumes that the physical dimensions of a network are much smaller than the electrical wavelength, while transmission lines may be a considerable fraction of a wavelength, or many wavelengths, in size. Thus a transmission line is a distributed-parameter network, where voltages and currents can vary in magnitude and phase over its length.

As shown in Figure 2.1a, a transmission line is often schematically represented as a two-wire line, since transmission lines (for TEM wave propagation) always have at least two conductors. The piece of line of infinitesimal length Δz of Figure 2.1a can be modeled as a lumped-element circuit, as shown in Figure 2.1b, where R, L, G, C are per unit length quantities defined as follows:

R = series resistance per unit length, for both conductors, in Ω/m.
L = series inductance per unit length, for both conductors, in H/m.
G = shunt conductance per unit length, in S/m.
C = shunt capacitance per unit length, in F/m.

The series inductance L represents the total self-inductance of the two conductors, and the shunt capacitance C is due to the close proximity of the two conductors. The series

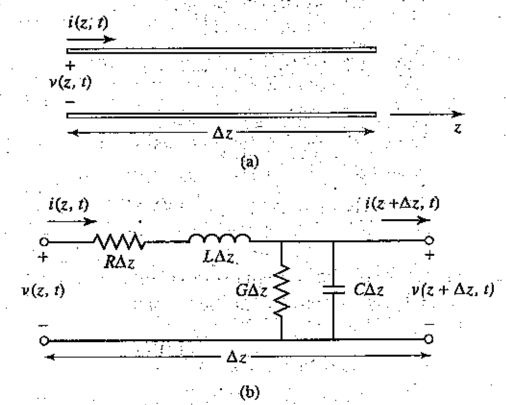

FIGURE 2.1 Voltage and current definitions and equivalent circuit for an incremental length of transmission line. (a) Voltage and current definitions. (b) Lumped-element equivalent circuit.

resistance R represents the resistance due to the finite conductivity of the conductors, and the shunt conductance G is due to dielectric loss in the material between the conductors. R and G, therefore, represent loss. A finite length of transmission line can be viewed as a cascade of sections of the form shown in Figure 2.1b.

From the circuit of Figure 2.1b, Kirchhoff's voltage law can be applied to give

$$v(z,t) - R\Delta z i(z,t) - L\Delta z \frac{\partial i(z,t)}{\partial t} - v(z+\Delta z, t) = 0, \tag{2.1a}$$

and Kirchhoff's current law leads to

$$i(z,t) - G\Delta z v(z+\Delta z,t) - C\Delta z \frac{\partial v(z+\Delta z,t)}{\partial t} - i(z+\Delta z,t) = 0. \tag{2.1b}$$

Dividing (2.1a) and (2.1b) by Δz and taking the limit as $\Delta z \to 0$ gives the following differential equations:

$$\frac{\partial v(z,t)}{\partial z} = -Ri(z,t) - L\frac{\partial i(z,t)}{\partial t}, \tag{2.2a}$$

$$\frac{\partial i(z,t)}{\partial z} = -Gv(z,t) - C\frac{\partial v(z,t)}{\partial t}. \tag{2.2b}$$

These equations are the time-domain form of the transmission line, or telegrapher, equations.

For the sinusoidal steady-state condition, with cosine-based phasors, (2.2) simplify to

$$\frac{dV(z)}{dz} = -(R + j\omega L)I(z), \tag{2.3a}$$

$$\frac{dI(z)}{dz} = -(G + j\omega C)V(z). \tag{2.3b}$$

Note the similarity in the form of (2.3) and Maxwell's curl equations of (1.41a) and (1.41b).

Wave Propagation on a Transmission Line

The two equations of (2.3) can be solved simultaneously to give wave equations for $V(z)$ and $I(z)$:

$$\frac{d^2V(z)}{dz^2} - \gamma^2 V(z) = 0, \tag{2.4a}$$

$$\frac{d^2I(z)}{dz^2} - \gamma^2 I(z) = 0, \tag{2.4b}$$

where

$$\gamma = \alpha + j\beta = \sqrt{(R + j\omega L)(G + j\omega C)} \tag{2.5}$$

is the complex propagation constant, which is a function of frequency. Traveling wave solutions to (2.4) can be found as

$$V(z) = V_o^+ e^{-\gamma z} + V_o^- e^{\gamma z}, \tag{2.6a}$$

$$I(z) = I_o^+ e^{-\gamma z} + I_o^- e^{\gamma z}, \tag{2.6b}$$

where the $e^{-\gamma z}$ term represents wave propagation in the $+z$ direction, and the $e^{\gamma z}$ term represents wave propagation in the $-z$ direction. Applying (2.3a) to the voltage of (2.6a) gives the current on the line:

$$I(z) = \frac{\gamma}{R + j\omega L}\left[V_o^+ e^{-\gamma z} - V_o^- e^{\gamma z}\right].$$

Comparison with (2.6b) shows that a characteristic impedance, Z_0, can be defined as

$$Z_0 = \frac{R + j\omega L}{\gamma} = \sqrt{\frac{R + j\omega L}{G + j\omega C}} \tag{2.7}$$

to relate the voltage and current on the line as

$$\frac{V_o^+}{I_o^+} = Z_0 = \frac{-V_o^-}{I_o^-}.$$

Then (2.6b) can be rewritten in the following form:

$$I(z) = \frac{V_o^+}{Z_0} e^{-\gamma z} - \frac{V_o^-}{Z_0} e^{\gamma z}. \tag{2.8}$$

Converting back to the time domain, the voltage waveform can be expressed as

$$\begin{aligned} v(z,t) = &|V_o^+| \cos(\omega t - \beta z + \phi^+) e^{-\alpha z} \\ &+ |V_o^-| \cos(\omega t + \beta z + \phi^-) e^{\alpha z}, \end{aligned} \tag{2.9}$$

where $\phi^\pm$ is the phase angle of the complex voltage $V_o^\pm$. Using arguments similar to those in Section 1.4, we find that the wavelength on the line is

$$\lambda = \frac{2\pi}{\beta}, \tag{2.10}$$

and the phase velocity is

$$v_p = \frac{\omega}{\beta} = \lambda f. \tag{2.11}$$

The Lossless Line

The above solution was for a general transmission line, including loss effects, and it was seen that the propagation constant and characteristic impedance were complex. In many practical cases, however, the loss of the line is very small and so can be neglected, resulting in a simplification of the above results. Setting $R = G = 0$ in (2.5) gives the propagation constant as

$$\gamma = \alpha + j\beta = j\omega\sqrt{LC},$$

or

$$\beta = \omega\sqrt{LC}, \tag{2.12a}$$

$$\alpha = 0. \tag{2.12b}$$

As expected for the lossless case, the attenuation constant α is zero. The characteristic impedance of (2.7) reduces to

$$Z_0 = \sqrt{\frac{L}{C}}, \tag{2.13}$$

which is now a real number. The general solutions for voltage and current on a lossless transmission line can then be written as

$$V(z) = V_o^+ e^{-j\beta z} + V_o^- e^{j\beta z}, \tag{2.14a}$$

$$I(z) = \frac{V_o^+}{Z_0} e^{-j\beta z} - \frac{V_o^-}{Z_0} e^{j\beta z}. \tag{2.14b}$$

The wavelength is

$$\lambda = \frac{2\pi}{\beta} = \frac{2\pi}{\omega\sqrt{LC}}, \tag{2.15}$$

and the phase velocity is

$$v_p = \frac{\omega}{\beta} = \frac{1}{\sqrt{LC}}. \tag{2.16}$$

2.2 FIELD ANALYSIS OF TRANSMISSION LINES

In this section we will rederive the time-harmonic form of the telegrapher's equations, starting with Maxwell's equations. We will begin by deriving the transmission line parameters (R, L, G, C) in terms of the electric and magnetic fields of the transmission line and then derive the telegrapher equations using these parameters for the specific case of a coaxial line.

Transmission Line Parameters

Consider a 1 m section of a uniform transmission line with fields $\bar{E}$ and $\bar{H}$, as shown in Figure 2.2, where S is the cross-sectional surface area of the line. Let the voltage between the conductors be $V_o e^{\pm j\beta z}$ and the current be $I_o e^{\pm j\beta z}$. The time-average stored magnetic energy for this 1 m section of line can be written, from (1.86), as

$$W_m = \frac{\mu}{4}\int_S \bar{H}\cdot\bar{H}^*\, ds,$$

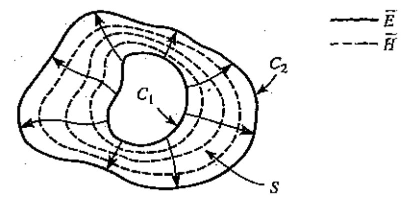

FIGURE 2.2 Field lines on an arbitrary TEM transmission line.

and circuit theory gives $W_m = L|I_o|^2/4$, in terms of the current on the line. We can thus identify the self-inductance per unit length as

$$L = \frac{\mu}{|I_o|^2}\int_S \bar{H}\cdot\bar{H}^*\, ds \text{ H/m}. \tag{2.17}$$

Similarly, the time-average stored electric energy per unit length can be found from (1.84) as

$$W_e = \frac{\epsilon}{4}\int_S \bar{E}\cdot\bar{E}^*\, ds,$$

and circuit theory gives $W_e = C|V_o|^2/4$, resulting in the following expression for the capacitance per unit length:

$$C = \frac{\epsilon}{|V_o|^2}\int_S \bar{E}\cdot\bar{E}^*\, ds \text{ F/m}. \tag{2.18}$$

From (1.130), the power loss per unit length due to the finite conductivity of the metallic conductors is

$$P_c = \frac{R_s}{2}\int_{C_1+C_2} \bar{H}\cdot\bar{H}^*\, d\ell$$

(assuming $\bar{H}$ is tangential to S), and circuit theory gives $P_c = R|I_o|^2/2$, so the series resistance R per unit length of line is

$$R = \frac{R_s}{|I_o|^2}\int_{C_1+C_2} \bar{H}\cdot\bar{H}^*\, dl \;\Omega/\text{m}. \tag{2.19}$$

In (2.19), $R_s = 1/\sigma\delta_s$ is the surface resistance of the conductors, and $C_1 + C_2$ represent integration paths over the conductor boundaries. From (1.92), the time-average power dissipated per unit length in a lossy dielectric is

$$P_d = \frac{\omega\epsilon''}{2}\int_S \bar{E}\cdot\bar{E}^*\, ds,$$

where ϵ'' is the imaginary part of the complex dielectric constant $\epsilon = \epsilon' - j\epsilon'' = \epsilon'(1 - j\tan\delta)$. Circuit theory gives $P_d = G|V_o|^2/2$, so the shunt conductance per unit length can be written as

$$G = \frac{\omega\epsilon''}{|V_o|^2}\int_S \bar{E}\cdot\bar{E}^*\, ds \text{ S/m}. \tag{2.20}$$

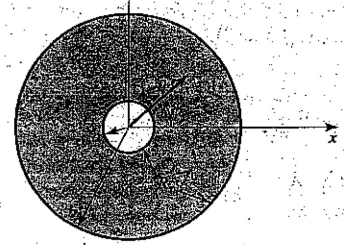

FIGURE 2.3 Geometry of a coaxial line with surface resistance R_s on the inner and outer conductors.

EXAMPLE 2.1 TRANSMISSION LINE PARAMETERS OF A COAXIAL LINE

The fields of a traveling TEM wave inside the coaxial line shown in Figure 2.3 can be expressed as

$$\bar{E} = \frac{V_o \hat{\rho}}{\rho \ln b/a} e^{-\gamma z},$$

$$\bar{H} = \frac{I_o \hat{\phi}}{2\pi\rho} e^{-\gamma z},$$

where γ is the propagation constant of the line. The conductors are assumed to have a surface resistivity R_s, and the material filling the space between the conductors is assumed to have a complex permittivity $\epsilon = \epsilon' - j\epsilon''$ and a permeability $\mu = \mu_0\mu_r$. Determine the transmission line parameters.

Solution

From (2.17)–(2.20) and the above fields the parameters of the coaxial line can be calculated as

$$L = \frac{\mu}{(2\pi)^2} \int_{\phi=\phi}^{2\pi} \int_{\rho=a}^{b} \frac{1}{\rho^2} \rho \, d\rho \, d\phi = \frac{\mu}{2\pi} \ln b/a \text{ H/m},$$

$$C = \frac{\epsilon'}{(\ln b/a)^2} \int_{\phi=0}^{2\pi} \int_{\rho=a}^{b} \frac{1}{\rho^2} \rho \, d\rho \, d\phi = \frac{2\pi\epsilon'}{\ln b/a} \text{ F/m},$$

$$R = \frac{R_s}{(2\pi)^2} \left\{ \int_{\phi=0}^{2\pi} \frac{1}{a^2} a \, d\phi + \int_{\phi=0}^{2\pi} \frac{1}{b^2} b \, d\phi \right\} = \frac{R_s}{2\pi} \left(\frac{1}{a} + \frac{1}{b} \right) \ \Omega\text{/m},$$

$$G = \frac{\omega\epsilon''}{(\ln b/a)^2} \int_{\phi=0}^{2\pi} \int_{\rho=a}^{b} \frac{1}{\rho^2} \rho \, d\rho \, d\phi = \frac{2\pi\omega\epsilon''}{\ln b/a} \text{ S/m}. \quad \blacksquare$$

Table 2.1 summarizes the parameters for coaxial, two-wire, and parallel plate lines. As we will see in the next chapter, the propagation constant, characteristic impedance, and attenuation ~~of most~~ transmission lines are derived directly from a field theory solution; the approach here of first finding the equivalent circuit parameters (L, C, R, G) is useful only for relatively simple lines. Nevertheless, it provides a helpful intuitive concept, and relates a transmission line to its equivalent circuit model.

TABLE 2.1 Transmission Line Parameters for Some Common Lines

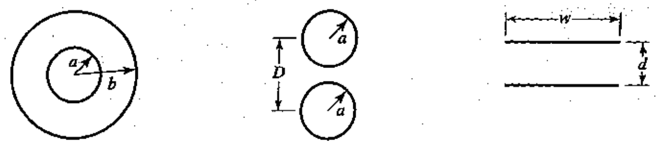

	COAX	TWO-WIRE	PARALLEL PLATE
L	$\frac{\mu}{2\pi} \ln \frac{b}{a}$	$\frac{\mu}{\pi} \cosh^{-1}\left(\frac{D}{2a}\right)$	$\frac{\mu d}{w}$
C	$\frac{2\pi\epsilon'}{\ln b/a}$	$\frac{\pi\epsilon'}{\cosh^{-1}(D/2a)}$	$\frac{\epsilon' w}{d}$
R	$\frac{R_s}{2\pi}\left(\frac{1}{a}+\frac{1}{b}\right)$	$\frac{R_s}{\pi a}$	$\frac{2R_s}{w}$
G	$\frac{2\pi\omega\epsilon''}{\ln b/a}$	$\frac{\pi\omega\epsilon''}{\cosh^{-1}(D/2a)}$	$\frac{\omega\epsilon'' w}{d}$

The Telegrapher Equations Derived from Field Analysis of a Coaxial Line

We now show that the telegrapher equations of (2.3), derived using circuit theory, can also be obtained from Maxwell's equations. We will consider the specific geometry of the coaxial line of Figure 2.3. Although we will treat TEM wave propagation more generally in the next chapter, the present discussion should provide some insight into the relationship of circuit and field quantities.

A TEM wave on the coaxial line of Figure 2.3 will be characterized by $E_z = H_z = 0$; furthermore, due to azimuthal symmetry, the fields will have no ϕ-variation, and so $\partial/\partial\phi = 0$. The fields inside the coaxial line will satisfy Maxwell's curl equations,

$$\nabla \times \bar{E} = -j\omega\mu\bar{H}, \tag{2.21a}$$

$$\nabla \times \bar{H} = j\omega\epsilon\bar{E}, \tag{2.21b}$$

where $\epsilon = \epsilon' - j\epsilon''$ may be complex to allow for a lossy dielectric filling. Conductor loss will be ignored here. A rigorous field analysis of conductor loss can be carried out, but at this point would tend to obscure our purpose; the interested reader is referred to references [1] or [2].

Expanding (2.21a) and (2.21b) then gives the following vector equations:

$$-\hat{\rho}\frac{\partial E_\phi}{\partial z} + \hat{\phi}\frac{\partial E_\rho}{\partial z} + \hat{z}\frac{1}{\rho}\frac{\partial}{\partial\rho}(\rho E_\phi) = -j\omega\mu(\hat{\rho}H_\rho + \hat{\phi}H_\phi), \tag{2.22a}$$

$$-\hat{\rho}\frac{\partial H_\phi}{\partial z} + \hat{\phi}\frac{\partial H_\rho}{\partial z} + \hat{z}\frac{1}{\rho}\frac{\partial}{\partial\rho}(\rho H_\phi) = j\omega\epsilon(\hat{\rho}E_\rho + \hat{\phi}E_\phi). \tag{2.22b}$$

Since the $\hat{z}$ components of these two equations must vanish, it is seen that E_ϕ and H_ϕ must have the forms

$$E_\phi = \frac{f(z)}{\rho}, \tag{2.23a}$$

$$H_\phi = \frac{g(z)}{\rho}. \tag{2.23b}$$

To satisfy the boundary condition that $E_\phi = 0$ at $\rho = a, b$, we must have $E_\phi = 0$ everywhere, due to the form of E_ϕ in (2.23a). Then from the $\hat{\rho}$ component of (2.22a), it is seen that $H_\rho = 0$. With these results, (2.22) can be reduced to

$$\frac{\partial E_\rho}{\partial z} = -j\omega\mu H_\phi, \tag{2.24a}$$

$$\frac{\partial H_\phi}{\partial z} = -j\omega\epsilon E_\rho. \tag{2.24b}$$

From the form of H_ϕ in (2.23b) and (2.24a), E_ρ must be of the form

$$E_\rho = \frac{h(z)}{\rho}. \tag{2.25}$$

Using (2.23b) and (2.25) in (2.24) gives

$$\frac{\partial h(z)}{\partial z} = -j\omega\mu g(z), \tag{2.26a}$$

$$\frac{\partial g(z)}{\partial z} = -j\omega\epsilon h(z). \tag{2.26b}$$

Now the voltage between the two conductors can be evaluated as

$$V(z) = \int_{\rho=a}^{b} E_\rho(\rho, z)\,d\rho = h(z)\int_{\rho=a}^{b} \frac{d\rho}{\rho} = h(z)\ln\frac{b}{a}, \tag{2.27a}$$

and the total current on the inner conductor at $\rho = a$ can be evaluated using (2.23b) as

$$I(z) = \int_{\phi=0}^{2\pi} H_\phi(a, z)a\,d\phi = 2\pi g(z). \tag{2.27b}$$

Then $h(z)$ and $g(z)$ can be eliminated from (2.26) by using (2.27) to give

$$\frac{\partial V(z)}{\partial z} = -j\frac{\omega\mu\ln b/a}{2\pi}I(z),$$

$$\frac{\partial I(z)}{\partial z} = -j\omega(\epsilon' - j\epsilon'')\frac{2\pi V(z)}{\ln b/a}.$$

Finally, using the results for L, G, and C for a coaxial line as derived above, we obtain the telegrapher equations as

$$\frac{\partial V(z)}{\partial z} = -j\omega L I(z), \tag{2.28a}$$

$$\frac{\partial I(z)}{\partial z} = -(G + j\omega C)V(z) \tag{2.28b}$$

(excluding R, the series resistance, since the conductors were assumed to have perfect conductivity). A similar analysis can be carried out for other simple transmission lines.

Propagation Constant, Impedance, and Power Flow for the Lossless Coaxial Line

Equations (2.24a) and (2.24b) for E_ρ and H_ϕ can be simultaneously solved to yield a wave equation for E_ρ (or H_ϕ):

$$\frac{\partial^2 E_\rho}{\partial z^2} + \omega^2\mu\epsilon E_\rho = 0, \tag{2.29}$$

from which it is seen that the propagation constant is $\gamma^2 = -\omega^2\mu\epsilon$, which, for lossless media, reduces to

$$\beta = \omega\sqrt{\mu\epsilon} = \omega\sqrt{LC}, \tag{2.30}$$

where the last result is from (2.12). Observe that this propagation constant is of the same form as that for plane waves in a lossless dielectric medium. This is a general result for TEM transmission lines.

The wave impedance is defined as $Z_w = E_\rho/H_\phi$, which can be calculated from (2.24a) assuming an $e^{-j\beta z}$ dependence to give

$$Z_w = \frac{E_\rho}{H_\phi} = \frac{\omega\mu}{\beta} = \sqrt{\mu/\epsilon} = \eta. \tag{2.31}$$

This wave impedance is then seen to be identical to the intrinsic impedance of the medium, η, and again is a general result for TEM transmission lines.

The characteristic impedance of the coaxial line is defined as

$$Z_0 = \frac{V_o}{I_o} = \frac{E_\rho \ln b/a}{2\pi H_\phi} = \frac{\eta\ln b/a}{2\pi} = \sqrt{\frac{\mu}{\epsilon}}\frac{\ln b/a}{2\pi}, \tag{2.32}$$

where the forms for E_ρ and H_ϕ from Example 2.1 have been used. The characteristic impedance is geometry dependent and will be different for other transmission line configurations.

Finally, the power flow (in the z direction) on the coaxial line may be computed from the Poynting vector as

$$P = \frac{1}{2}\int_s \bar{E}\times\bar{H}^*\cdot d\bar{s} = \frac{1}{2}\int_{\phi=0}^{2\pi}\int_{\rho=a}^{b}\frac{V_o I_o^*}{2\pi\rho^2\ln b/a}\rho\,d\rho\,d\phi = \frac{1}{2}V_o I_o^*, \tag{2.33}$$

a result that is in clear agreement with circuit theory. This shows that the flow of power in a transmission line takes place entirely via the electric and magnetic fields between the two conductors; power is not transmitted through the conductors themselves. As we will see later, for the case of finite conductivity, power may enter the conductors, but this power is then lost as heat and is not delivered to the load.

2.3 THE TERMINATED LOSSLESS TRANSMISSION LINE

Figure 2.4 shows a lossless transmission line terminated in an arbitrary load impedance Z_L. This problem will illustrate wave reflection on transmission lines, a fundamental property of distributed systems.

Assume that an incident wave of the form $V_o^+ e^{-j\beta z}$ is generated from a source at $z < 0$. We have seen that the ratio of voltage to current for such a traveling wave is Z_0, the characteristic impedance. But when the line is terminated in an arbitrary load $Z_L \neq Z_0$, the ratio of voltage to current at the load must be Z_L. Thus, a reflected wave must

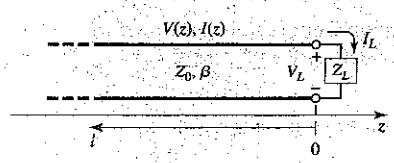

FIGURE 2.4 A transmission line terminated in a load impedance Z_L.

be excited with the appropriate amplitude to satisfy this condition. The total voltage on the line can then be written as in (2.14a), as a sum of incident and reflected waves:

$$V(z) = V_o^+ e^{-j\beta z} + V_o^- e^{j\beta z}. \tag{2.34a}$$

Similarly, the total current on the line is described by (2.14b):

$$I(z) = \frac{V_o^+}{Z_0} e^{-j\beta z} - \frac{V_o^-}{Z_0} e^{j\beta z}. \tag{2.34b}$$

The total voltage and current at the load are related by the load impedance, so at $z = 0$ we must have

$$Z_L = \frac{V(0)}{I(0)} = \frac{V_o^+ + V_o^-}{V_o^+ - V_o^-} Z_0.$$

Solving for V_o^- gives

$$V_o^- = \frac{Z_L - Z_0}{Z_L + Z_0} V_o^+.$$

The amplitude of the reflected voltage wave normalized to the amplitude of the incident voltage wave is defined as the *voltage reflection coefficient*, Γ:

$$\Gamma = \frac{V_o^-}{V_o^+} = \frac{Z_L - Z_0}{Z_L + Z_0}. \tag{2.35}$$

The total voltage and current waves on the line can then be written as

$$V(z) = V_o^+ \left[e^{-j\beta z} + \Gamma e^{j\beta z}\right], \tag{2.36a}$$

$$I(z) = \frac{V_o^+}{Z_0} \left[e^{-j\beta z} - \Gamma e^{j\beta z}\right]. \tag{2.36b}$$

From these equations it is seen that the voltage and current on the line consist of a superposition of an incident and reflected wave; such waves are called standing waves. Only when $\Gamma = 0$ is there no reflected wave. To obtain $\Gamma = 0$, the load impedance Z_L must be equal to the characteristic impedance Z_0 of the transmission line, as seen from (2.35). Such a load is then said to be *matched* to the line, since there is no reflection of the incident wave.

Now consider the time-average power flow along the line at the point z:

$$P_{av} = \frac{1}{2}\text{Re}\left[V(z)I(z)^*\right] = \frac{1}{2}\frac{|V_o^+|^2}{Z_0}\text{Re}\left\{1 - \Gamma^* e^{-2j\beta z} + \Gamma e^{2j\beta z} - |\Gamma|^2\right\},$$

where (2.36) has been used. The middle two terms in the brackets are of the form $A - A^* = 2j\,\text{Im}(A)$ and so are purely imaginary. This simplifies the result to

$$P_{av} = \frac{1}{2}\frac{|V_o^+|^2}{Z_0}\left(1 - |\Gamma|^2\right), \tag{2.37}$$

which shows that the average power flow is constant at any point on the line, and that the total power delivered to the load (P_{av}) is equal to the incident power ($|V_o^+|^2/2Z_0$), minus the reflected power ($|V_o|^2|\Gamma|^2/2Z_0$). If $\Gamma = 0$, maximum power is delivered to the load, while no power is delivered for $|\Gamma| = 1$. The above discussion assumes that the generator is matched, so that there is no rereflection of the reflected wave from $z < 0$.

When the load is mismatched, not all of the available power from the generator is delivered to the load. This "loss" is called *return loss* (RL), and is defined (in dB) as

$$\text{RL} = -20 \log |\Gamma| \text{ dB}, \tag{2.38}$$

so that a matched load ($\Gamma = 0$) has a return loss of ∞ dB (no reflected power), whereas a total reflection ($|\Gamma| = 1$) has a return loss of 0 dB (all incident power is reflected).

If the load is matched to the line, $\Gamma = 0$ and the magnitude of the voltage on the line is $|V(z)| = |V_o^+|$, which is a constant. Such a line is sometimes said to be "flat." When the load is mismatched, however, the presence of a reflected wave leads to standing waves where the magnitude of the voltage on the line is not constant. Thus, from (2.36a),

$$\begin{aligned} |V(z)| &= |V_o^+||1 + \Gamma e^{2j\beta z}| = |V_o^+||1 + \Gamma e^{-2j\beta\ell}| \\ &= |V_o^+||1 + |\Gamma|e^{j(\theta - 2\beta\ell)}|, \end{aligned} \tag{2.39}$$

where $\ell = -z$ is the positive distance measured from the load at $z = 0$, and θ is the phase of the reflection coefficient ($\Gamma = |\Gamma|e^{j\theta}$). This result shows that the voltage magnitude oscillates with position z along the line. The maximum value occurs when the phase term $e^{j(\theta - 2\beta\ell)} = 1$, and is given by

$$V_{max} = |V_o^+|(1 + |\Gamma|). \tag{2.40a}$$

The minimum value occurs when the phase term $e^{j(\theta - 2\beta\ell)} = -1$, and is given by

$$V_{min} = |V_o^+|(1 - |\Gamma|). \tag{2.40b}$$

As $|\Gamma|$ increases, the ratio of V_{max} to V_{min} increases, so a measure of the mismatch of a line, called the *standing wave ratio* (SWR), can be defined as

$$\text{SWR} = \frac{V_{max}}{V_{min}} = \frac{1 + |\Gamma|}{1 - |\Gamma|}. \tag{2.41}$$

This quantity is also known as the *voltage standing wave ratio*, and is sometimes identified as VSWR. From (2.41) it is seen that SWR is a real number such that $1 \le \text{SWR} \le \infty$, where SWR = 1 implies a matched load.

From (2.39), it is seen that the distance between two successive voltage maxima (or minima) is $\ell = 2\pi/2\beta = \pi\lambda/2\pi = \lambda/2$, while the distance between a maximum and a minimum is $\ell = \pi/2\beta = \lambda/4$, where λ is the wavelength on the transmission line.

The reflection coefficient of (2.35) was defined as the ratio of the reflected to the incident voltage wave amplitudes at the load ($\ell = 0$), but this quantity can be generalized to any point ℓ on the line as follows. From (2.34a), with $z = -\ell$, the ratio of the reflected component to the incident component is

$$\Gamma(\ell) = \frac{V_o^- e^{-j\beta\ell}}{V_o^+ e^{j\beta\ell}} = \Gamma(0)e^{-2j\beta\ell}, \tag{2.42}$$

where $\Gamma(0)$ is the reflection coefficient at $z = 0$, as given by (2.35). This form is useful when transforming the effect of a load mismatch down the line.

We have seen that the real power flow on the line is a constant but that the voltage amplitude, at least for a mismatched line, is oscillatory with position on the line. The perceptive reader may therefore have concluded that the impedance seen looking into the line must vary with position, and this is indeed the case. At a distance $\ell = -z$ from the load, the input impedance seen looking toward the load is

$$Z_{in} = \frac{V(-\ell)}{I(-\ell)} = \frac{V_o^+\left[e^{j\beta\ell} + \Gamma e^{-j\beta\ell}\right]}{V_o^+\left[e^{j\beta\ell} - \Gamma e^{-j\beta\ell}\right]} Z_0 = \frac{1 + \Gamma e^{-2j\beta\ell}}{1 - \Gamma e^{-2j\beta\ell}} Z_0, \qquad (2.43)$$

where (2.36a,b) have been used for $V(z)$ and $I(z)$. A more usable form may be obtained by using (2.35) for Γ in (2.43):

$$\begin{aligned} Z_{in} &= Z_0 \frac{(Z_L + Z_0)e^{j\beta\ell} + (Z_L - Z_0)e^{-j\beta\ell}}{(Z_L + Z_0)e^{j\beta\ell} - (Z_L - Z_0)e^{-j\beta\ell}} \\ &= Z_0 \frac{Z_L \cos\beta\ell + jZ_0 \sin\beta\ell}{Z_0 \cos\beta\ell + jZ_L \sin\beta\ell} \\ &= Z_0 \frac{Z_L + jZ_0 \tan\beta\ell}{Z_0 + jZ_L \tan\beta\ell}. \end{aligned} \qquad (2.44)$$

This is an important result giving the input impedance of a length of transmission line with an arbitrary load impedance. We will refer to this result as the *transmission line impedance equation;* some special cases will be considered next.

Special Cases of Lossless Terminated Lines

A number of special cases of lossless terminated transmission lines will frequently appear in our work, so it is appropriate to consider the properties of such cases here.

Consider first the transmission line circuit shown in Figure 2.5, where a line is terminated in a short circuit, $Z_L = 0$. From (2.35) it is seen that the reflection coefficient for a short circuit load is $\Gamma = -1$; it then follows from (2.41) that the standing wave ratio is infinite. From (2.36) the voltage and current on the line are

$$V(z) = V_o^+\left[e^{-j\beta z} - e^{j\beta z}\right] = -2jV_o^+ \sin\beta z, \qquad (2.45a)$$

$$I(z) = \frac{V_o^+}{Z_0}\left[e^{-j\beta z} + e^{j\beta z}\right] = \frac{2V_o^+}{Z_0} \cos\beta z, \qquad (2.45b)$$

which shows that $V = 0$ at the load (as expected, for a short circuit), while the current is a maximum there. From (2.44), or the ratio $V(-\ell)/I(-\ell)$, the input impedance is

$$Z_{in} = jZ_0 \tan\beta\ell, \qquad (2.45c)$$

which is seen to be purely imaginary for any length, ℓ, and to take on all values between $+j\infty$ and $-j\infty$. For example, when $\ell = 0$ we have $Z_{in} = 0$, but for $\ell = \lambda/4$ we have $Z_{in} = \infty$

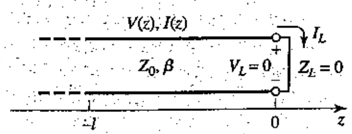

FIGURE 2.5 A transmission line terminated in a short circuit.

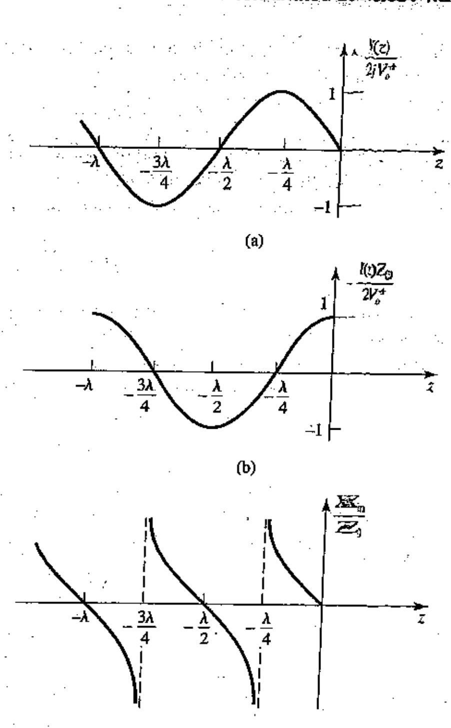

FIGURE 2.6 (a) Voltage, (b) current, and (c) impedance ($R_{in} = 0$ or ∞) variation along a short-circuited transmission line.

(open circuit). Equation (2.45c) also shows that the impedance is periodic in ℓ, repeating for multiples of $\lambda/2$. The voltage, current, and input reactance for the short-circuited line are plotted in Figure 2.6.

Next consider the open-circuited line shown in Figure 2.7, where $Z_L = \infty$. Dividing the numerator and denominator of (2.35) by Z_L and allowing $Z_L \to \infty$ shows that the reflection coefficient for this case is $\Gamma = 1$, and the standing wave ratio is again infinite. From (2.36) the voltage and current on the line are

$$V(z) = V_o^+\left[e^{-j\beta z} + e^{j\beta z}\right] = 2V_o^+ \cos\beta z, \qquad (2.46a)$$

$$I(z) = \frac{V_o^+}{Z_0}\left[e^{-j\beta z} - e^{j\beta z}\right] = \frac{-2jV_o^+}{Z_0} \sin\beta z, \qquad (2.46b)$$

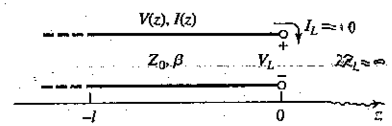

FIGURE 2.7 A transmission line terminated in an open circuit.

2.22 Use the Smith chart to find the shortest lengths of a short-circuited 75 Ω line to give the follo[wing] input impedance:
(a) $Z_{in} = 0$.
(b) $Z_{in} = \infty$.
(c) $Z_{in} = j75\ \Omega$.
(d) $Z_{in} = -j50\ \Omega$.
(e) $Z_{in} = j10\ \Omega$.

2.23 Repeat Problem 2.22 for an open-circuited length of 75 Ω line.

2.24 A slotted-line experiment is performed with the following results: distance between successive mini[ma] = 2.1 cm; distance of first voltage minimum from load = 0.9 cm; SWR of load = 2.5. If $Z_0 = 50$ [Ω], find the load impedance.

2.25 Design a quarter-wave matching transformer to match a 40 Ω load to a 75 Ω line. Plot the SWR [for] $0.5 \leq f/f_o \leq 2.0$, where f_o is the frequency at which the line is $\lambda/4$ long.

2.26 Consider the quarter-wave matching transformer circuit shown below. Derive expressions for V^+ [and] V^-, the amplitudes of the forward and reverse traveling waves on the quarter-wave line section, [in] terms of V^i, the incident voltage amplitude.

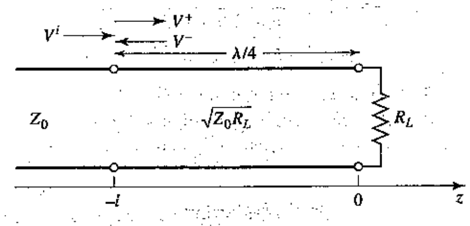

2.27 Derive Equation (2.71) from (2.70).

2.28 In Example 2.7, the attenuation of a coaxial line due to finite conductivity is

$$\alpha_c = \frac{R_s}{2\eta \ln b/a}\left(\frac{1}{a} + \frac{1}{b}\right).$$

Show that α_c is minimized for conductor radii such that $x \ln x = 1 + x$, where $x = b/a$. Solve this equation for x, and show that the corresponding characteristic impedance for $\epsilon_r = 1$ is 77 Ω.

2.29 Compute and plot the factor by which attenuation is increased due to surface roughness, for rms roughness ranging from zero to 0.01 mm. Assume copper conductors at 10 GHz.

2.30 A 50 Ω transmission line is matched to a 10 V source and feeds a load $Z_L = 100\ \Omega$. If the line is 2.3λ long and has an attenuation constant $\alpha = 0.5$ dB/λ, find the powers that are delivered by the source, lost in the line, and delivered to the load.

2.31 Consider a nonreciprocal transmission line having different propagation constants, β^+ and β^-, fo[r] propagation in the forward and reverse directions, with corresponding characteristic impedances Z_0^+ and Z_0^-. (An example of such a line could be a microstrip transmission line on a magnetized ferrite substrate.) If the line is terminated as shown below, derive expressions for the reflection coefficien[t] and impedance seen at the input of the line.

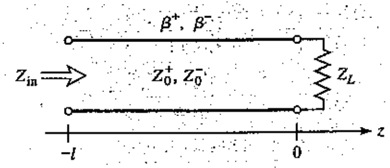

C h a p t e r   T h r e e

Transmission Lines and Waveguides

One of the early milestones in microwave engineering was the development of waveguide and other transmission lines for the low-loss tranmission of microwave power. Although Heaviside considered the possibility of propagation of electromagnetic waves inside a closed hollow tube in 1893, he rejected the idea because he believed that two conductors were necessary for the transfer of electromagnetic energy [1]. In 1897, Lord Rayleigh (John William Strutt) [2] mathematically proved that wave propagation in waveguides was possible, for both circular and rectangular cross sections. Rayleigh also noted the infinite set of modes of the TE and TM type that were possible and the existence of a cutoff frequency, but no experimental verification was made at the time. The waveguide was essentially forgotten until it was rediscovered independently in 1936 by two men [3]. After preliminary experiments in 1932, George C. Southworth of the AT&T Company in New York presented a paper on the waveguide in 1936. At the same meeting, W. L. Barrow of MIT presented a paper on the circular waveguide, with experimental confirmation of propagation.

Early microwave systems relied on waveguide and coaxial lines for transmission line media. Waveguide has the advantage of high power-handling capability and low loss but is bulky and expensive. Coaxial line has very high bandwidth and is convenient for test applications, but is a difficult medium in which to fabricate complex microwave components. Planar transmission lines provide an alternative, in the form of stripline, microstrip, slotline, coplanar waveguide, and many other types of related geometries. Such transmission lines are compact, low in cost, and are capable of being easily integrated with active devices such as diodes and transistors to form microwave integrated circuits. The first planar transmission line may have been a flat-strip coaxial line, similar to stripline, used in a production power divider network in World War II [4]. But planar lines did not receive intensive development until the 1950s. Microstrip line was developed at ITT laboratories [5] and was a competitor of stripline. The first microstrip lines used a relatively thick dielectric substrate, which accentuated the non-TEM mode behavior and frequency dispersion of the line. This characteristic made it less desirable than stripline until the 1960s, when much thinner substrates began to be used. This reduced the frequency dependence of the line, and now microstrip is often the preferred medium for microwave integrated circuits.

In this chapter we will study the properties of several types of transmission lines and waveguides that are in common use today. As we know from Chapter 2, a transmission line is characterized by a propagation constant and a characteristic impedance; if the line is lossy, attenuation is also of interest. These quantities will be derived by a field theory analysis for the various lines and waveguides treated here.

We will begin with a general discussion of the different types of wave propagation and modes that can exist on transmission lines and waveguides. Transmission lines that consist of two or more conductors may support transverse electromagnetic (TEM) waves, characterized by the lack of longitudinal field components. TEM waves have a uniquely defined voltage, current, and characteristic impedance. Waveguides, often consisting of a single conductor, support transverse electric (TE) and/or transverse magnetic (TM) waves, characterized by the presence of longitudinal magnetic or electric, respectively, field components. As we will see in Chapter 4, a unique definition of characteristic impedance is not possible for such waves, although definitions can be chosen so that the characteristic impedance concept can be used for waveguides with meaningful results.

3.1 GENERAL SOLUTIONS FOR TEM, TE, AND TM WAVES

In this section we will find general solutions to Maxwell's equations for the specific cases of TEM, TE, and TM wave propagation in cylindrical transmission lines or waveguides. The geometry of an arbitrary transmission line or waveguide is shown in Figure 3.1, and is characterized by conductor boundaries that are parallel to the z-axis. These structures are assumed to be uniform in the z direction and infinitely long. The conductors will initially be assumed to be perfectly conducting, but attenuation can be found by the perturbation method discussed in Chapter 2.

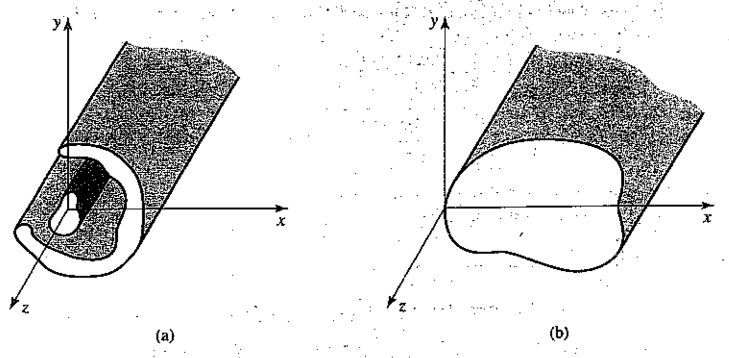

FIGURE 3.1 (a) General two-conductor transmission line and (b) closed waveguide.

We assume time-harmonic fields with an $e^{j\omega t}$ dependence and wave propagation along the z-axis. The electric and magnetic fields can then be written as

$$\bar{E}(x, y, z) = [\bar{e}(x, y) + \hat{z}e_z(x, y)]e^{-j\beta z}, \tag{3.1a}$$

$$\bar{H}(x, y, z) = [\bar{h}(x, y) + \hat{z}h_z(x, y)]e^{-j\beta z}, \tag{3.1b}$$

where $\bar{e}(x, y)$ and $\bar{h}(x, y)$ represent the transverse ($\hat{x}, \hat{y}$) electric and magnetic field components, while e_z and h_z are the longitudinal electric and magnetic field components. In the above, the wave is propagating in the $+z$ direction; $-z$ propagation can be obtained by replacing β with $-\beta$. Also, if conductor or dielectric loss is present, the propagation constant will be complex; $j\beta$ should then be replaced with $\gamma = \alpha + j\beta$.

Assuming that the transmission line or waveguide region is source free, Maxwell's equations can be written as

$$\nabla \times \bar{E} = -j\omega\mu\bar{H}, \tag{3.2a}$$

$$\nabla \times \bar{H} = j\omega\epsilon\bar{E}. \tag{3.2b}$$

With an $e^{-j\beta z}$ dependence, the three components of each of the above vector equations can be reduced to the following:

$$\frac{\partial E_z}{\partial y} + j\beta E_y = -j\omega\mu H_x, \tag{3.3a}$$

$$-j\beta E_x - \frac{\partial E_z}{\partial x} = -j\omega\mu H_y, \tag{3.3b}$$

$$\frac{\partial E_y}{\partial x} - \frac{\partial E_x}{\partial y} = -j\omega\mu H_z, \tag{3.3c}$$

$$\frac{\partial H_z}{\partial y} + j\beta H_y = j\omega\epsilon E_x, \tag{3.4a}$$

$$-j\beta H_x - \frac{\partial H_z}{\partial x} = j\omega\epsilon E_y, \tag{3.4b}$$

$$\frac{\partial H_y}{\partial x} - \frac{\partial H_x}{\partial y} = j\omega\epsilon E_z. \tag{3.4c}$$

The above six equations can be solved for the four transverse field components in terms of E_z and H_z (for example, H_x can be derived by eliminating E_y from (3.3a) and (3.4b)) as follows:

$$H_x = \frac{j}{k_c^2}\left(\omega\epsilon\frac{\partial E_z}{\partial y} - \beta\frac{\partial H_z}{\partial x}\right), \tag{3.5a}$$

$$H_y = \frac{-j}{k_c^2}\left(\omega\epsilon\frac{\partial E_z}{\partial x} + \beta\frac{\partial H_z}{\partial y}\right), \tag{3.5b}$$

$$E_x = \frac{-j}{k_c^2}\left(\beta\frac{\partial E_z}{\partial x} + \omega\mu\frac{\partial H_z}{\partial y}\right), \tag{3.5c}$$

$$E_y = \frac{j}{k_c^2}\left(-\beta\frac{\partial E_z}{\partial y} + \omega\mu\frac{\partial H_z}{\partial x}\right), \tag{3.5d}$$

where

$$k_c^2 = k^2 - \beta^2 \tag{3.6}$$

has been defined as the cutoff wavenumber; the reason for this terminology will become clear later. As in previous chapters,

$$k = \omega\sqrt{\mu\epsilon} = 2\pi/\lambda \quad (3$$

is the wavenumber of the material filling the transmission line or waveguide region. dielectric loss is present, ϵ can be made complex by using $\epsilon = \epsilon_0\epsilon_r(1 - j\tan\delta)$, wh tan δ is the loss tangent of the material.

Equations (3.5a–d) are very useful general results that can be applied to a variety waveguiding systems. We will now specialize these results to specific wave types.

TEM Waves

Transverse electromagnetic (TEM) waves are characterized by $E_z = H_z = 0$. Observe fro (3.5) that if $E_z = H_z = 0$, then the transverse fields are also all zero, unless $k_c^2 = 0$ (k^2 β^2), in which case we have an indeterminate result. Thus, we can return to (3.3)–(3.4) an apply the condition that $E_z = H_z = 0$. Then from (3.3a) and (3.4b), we can eliminate H to obtain

$$\beta^2 E_y = \omega^2\mu\epsilon E_y,$$

or

$$\beta = \omega\sqrt{\mu\epsilon} = k, \quad (3.8)$$

as noted earlier. (This result can also be obtained from (3.3b) and (3.4a).) The cutoff wavenumber, $k_c = \sqrt{k^2 - \beta^2}$, is thus zero for TEM waves.

Now the Helmholtz wave equation for E_x is, from (1.42),

$$\left(\frac{\partial^2}{\partial x^2} + \frac{\partial^2}{\partial y^2} + \frac{\partial^2}{\partial z^2} + k^2\right) E_x = 0, \quad (3.9)$$

but for $e^{-j\beta z}$ dependence, $(\partial^2/\partial z^2)E_x = -\beta^2 E_x = -k^2 E_x$, so (3.9) reduces to

$$\left(\frac{\partial^2}{\partial x^2} + \frac{\partial^2}{\partial y^2}\right) E_x = 0. \quad (3.10)$$

A similar result also applies to E_y, so using the form of $\bar{E}$ assumed in (3.1a) we can write

$$\nabla_t^2 \bar{e}(x, y) = 0, \quad (3.11)$$

where $\nabla_t^2 = \partial^2/\partial x^2 + \partial^2/\partial y^2$ is the Laplacian operator in the two transverse dimensions.

The result of (3.11) shows that the transverse electric fields, $\bar{e}(x, y)$, of a TEM wave satisfy Laplace's equation. It is easy to show in the same way that the transverse magnetic fields also satisfy Laplace's equation:

$$\nabla_t^2 \bar{h}(x, y) = 0. \quad (3.12)$$

The transverse fields of a TEM wave are thus the same as the static fields that can exist between the conductors. In the electrostatic case, we know that the electric field can be expressed as the gradient of a scalar potential, $\Phi(x, y)$:

$$\bar{e}(x, y) = -\nabla_t \Phi(x, y), \quad (3.13)$$

where $\nabla_t = \hat{x}(\partial/\partial x) + \hat{y}(\partial/\partial y)$ is the transverse gradient operator in two dimensions. In order for the relation in (3.13) to be valid, the curl of $\bar{e}$ must vanish, and this is indeed the case here since

$$\nabla_t \times \bar{e} = -j\omega\mu h_z \hat{z} = 0.$$

Using the fact that $\nabla \cdot \bar{D} = \epsilon\nabla_t \cdot \bar{e} = 0$ with (3.13) shows that $\Phi(x, y)$ also satisfies Laplace's equation,

$$\nabla_t^2 \Phi(x, y) = 0, \quad (3.14)$$

as expected from electrostatics. The voltage between two conductors can be found as

$$V_{12} = \Phi_1 - \Phi_2 = \int_1^2 \bar{E} \cdot d\bar{\ell}, \quad (3.15)$$

where Φ_1 and Φ_2 represent the potential at conductors 1 and 2 respectively. The current flow on a conductor can be found from Ampere's law as

$$I = \oint_C \bar{H} \cdot d\bar{\ell}, \quad (3.16)$$

where C is the cross-sectional contour of the conductor.

TEM waves can exist when two or more conductors are present. Plane waves are also examples of TEM waves, since there are no field components in the direction of propagation; in this case the transmission line conductors may be considered to be two infinitely large plates separated to infinity. The above results show that a closed conductor (such as a rectangular waveguide) cannot support TEM waves, since the corresponding static potential in such a region would be zero (or possibly a constant), leading to $\bar{e} = 0$.

The wave impedance of a TEM mode can be found as the ratio of the transverse electric and magnetic fields:

$$Z_{\mathrm{TEM}} = \frac{E_x}{H_y} = \frac{\omega\mu}{\beta} = \sqrt{\frac{\mu}{\epsilon}} = \eta, \quad (3.17a)$$

where (3.4a) was used. The other pair of transverse field components, from (3.3a), give

$$Z_{\mathrm{TEM}} = \frac{-E_y}{H_x} = \sqrt{\frac{\mu}{\epsilon}} = \eta. \quad (3.17b)$$

Combining the results of (3.17a) and (3.17b) gives a general expression for the transverse fields as

$$\bar{h}(x, y) = \frac{1}{Z_{\mathrm{TEM}}} \hat{z} \times \bar{e}(x, y). \quad (3.18)$$

Note that the wave impedance is the same as that for a plane wave in a lossless medium, as derived in Chapter 1; the reader should not confuse this impedance with the characteristic impedance, Z_0, of a transmission line. The latter relates an incident voltage and current and is a function of the line geometry as well as the material filling the line, while the wave impedance relates transverse field components and is dependent only on the material constants. From (2.32), the characteristic impedance of the TEM line is $Z_0 = V/I$, where V and I are the amplitudes of the incident voltage and current waves.

The procedure for analyzing a TEM line can be summarized as follows:

1. Solve Laplace's equation, (3.14), for $\Phi(x, y)$. The solution will contain several unknown constants.
2. Find these constants by applying the boundary conditions for the known voltages on the conductors.
3. Compute $\bar{e}$ and $\bar{E}$ from (3.13), (3.1a). Compute $\bar{h}$ and $\bar{H}$ from (3.18), (3.1b).
4. Compute V from (3.15), I from (3.16).
5. The propagation constant is given by (3.8), and the characteristic impedance is given by $Z_0 = V/I$.

TE Waves

Transverse electric (TE) waves, (also referred to as H-waves) are characterized by $E_z = 0$ and $H_z \neq 0$. Equations (3.5) then reduce to

$$H_x = \frac{-j\beta}{k_c^2}\frac{\partial H_z}{\partial x}, \tag{3.19a}$$

$$H_y = \frac{-j\beta}{k_c^2}\frac{\partial H_z}{\partial y}, \tag{3.19b}$$

$$E_x = \frac{-j\omega\mu}{k_c^2}\frac{\partial H_z}{\partial y}, \tag{3.19c}$$

$$E_y = \frac{j\omega\mu}{k_c^2}\frac{\partial H_z}{\partial x}. \tag{3.19d}$$

In this case, $k_c \neq 0$, and the propagation constant $\beta = \sqrt{k^2 - k_c^2}$ is generally a function of frequency and the geometry of the line or guide. To apply (3.19), one must first find H_z from the Helmholtz wave equation,

$$\left(\frac{\partial^2}{\partial x^2} + \frac{\partial^2}{\partial y^2} + \frac{\partial^2}{\partial z^2} + k^2\right)H_z = 0, \tag{3.20}$$

which, since $H_z(x, y, z) = h_z(x, y)e^{-j\beta z}$, can be reduced to a two-dimensional wave equation for h_z:

$$\left(\frac{\partial^2}{\partial x^2} + \frac{\partial^2}{\partial y^2} + k_c^2\right)h_z = 0, \tag{3.21}$$

since $k_c^2 = k^2 - \beta^2$. This equation must be solved subject to the boundary conditions of the specific guide geometry.

The TE wave impedance can be found as

$$Z_{\text{TE}} = \frac{E_x}{H_y} = \frac{-E_y}{H_x} = \frac{\omega\mu}{\beta} = \frac{k\eta}{\beta}, \tag{3.22}$$

which is seen to be frequency dependent. TE waves can be supported inside closed conductors, as well as between two or more conductors.

TM Waves

Transverse magnetic (TM) waves (also referred to as E-waves) are characterized by $E_z \neq 0$ and $H_z = 0$. Equations (3.5) then reduce to

$$H_x = \frac{j\omega\epsilon}{k_c^2}\frac{\partial E_z}{\partial y}, \tag{3.23a}$$

$$H_y = \frac{-j\omega\epsilon}{k_c^2}\frac{\partial E_z}{\partial x}, \tag{3.23b}$$

$$E_x = \frac{-j\beta}{k_c^2}\frac{\partial E_z}{\partial x}, \tag{3.23c}$$

$$E_y = \frac{-j\beta}{k_c^2}\frac{\partial E_z}{\partial y}. \tag{3.23d}$$

As in the TE case, $k_c \neq 0$, and the propagation constant $\beta = \sqrt{k^2 - k_c^2}$ is a function of frequency and the geometry of the line or guide. E_z is found from the Helmholtz wave equation,

$$\left(\frac{\partial^2}{\partial x^2} + \frac{\partial^2}{\partial y^2} + \frac{\partial^2}{\partial z^2} + k^2\right)E_z = 0, \tag{3.24}$$

which, since $E_z(x, y, z) = e_z(x, y)e^{-j\beta z}$, can be reduced to a two-dimensional wave equation for e_z:

$$\left(\frac{\partial^2}{\partial x^2} + \frac{\partial^2}{\partial y^2} + k_c^2\right)e_z = 0, \tag{3.25}$$

since $k_c^2 = k^2 - \beta^2$. This equation must be solved subject to the boundary conditions of the specific guide geometry.

The TM wave impedance can be found as

$$Z_{\text{TM}} = \frac{E_x}{H_y} = \frac{-E_y}{H_x} = \frac{\beta}{\omega\epsilon} = \frac{\beta\eta}{k}, \tag{3.26}$$

which is frequency dependent. As for TE waves, TM waves can be supported inside closed conductors, as well as between two or more conductors.

The procedure for analyzing TE and TM waveguides can be summarized as follows:

1. Solve the reduced Helmholtz equation, (3.21) or (3.25), for h_z or e_z. The solution will contain several unknown constants, and the unknown cutoff wavenumber, k_c.
2. Use (3.19) or (3.23) to find the transverse fields from h_z or e_z.
3. Apply the boundary conditions to the appropriate field components to find the unknown constants and k_c.
4. The propagation constant is given by (3.6), and the wave impedance by (3.22) or (3.26).

Attenuation Due to Dielectric Loss

Attenuation in a transmission line or waveguide can be caused by either dielectric loss or conductor loss. If α_d is the attenuation constant due to dielectric loss, and α_c is the attenuation constant due to conductor loss, then the total attenuation constant is $\alpha = \alpha_d + \alpha_c$.

Attenuation caused by conductor loss can be calculated using the perturbation method of Section 2.7; this loss depends on the field distribution in the guide and so must be evaluated separately for each type of transmission line or waveguide. But if the line or guide is completely filled with a homogeneous dielectric, the attenuation due to lossy dielectric can be calculated from the propagation constant, and this result will apply to any guide or line with a homogeneous dielectric filling.

Thus, using the complex dielectric constant allows the complex propagation constant to be written as

$$\begin{aligned} \gamma &= \alpha_d + j\beta = \sqrt{k_c^2 - k^2} \\ &= \sqrt{k_c^2 - \omega^2\mu_0\epsilon_0\epsilon_r(1 - j\tan\delta)}. \end{aligned} \tag{3.27}$$

In practice, most dielectric materials have a very small loss ($\tan\delta \ll 1$), so this expression can be simplified by using the first two terms of the Taylor expansion,

$$\sqrt{a^2+x^2} \simeq a + \frac{1}{2}\left(\frac{x^2}{a}\right), \qquad \text{for } x \ll a.$$

Then (3.27) reduces to

$$\begin{aligned}\gamma &= \sqrt{k_c^2 - k^2 + jk^2 \tan\delta} \\ &\simeq \sqrt{k_c^2 - k^2} + \frac{jk^2 \tan\delta}{2\sqrt{k_c^2-k^2}} \\ &= \frac{k^2 \tan\delta}{2\beta} + j\beta, \end{aligned} \tag{3.28}$$

since $\sqrt{k_c^2 - k^2} = j\beta$. In these results, $k^2 = \omega^2\mu_0\epsilon_0\epsilon_r$ is the (real) wavenumber in the absence of loss. Equation (3.28) shows that when the loss is small the phase constant, β, is unchanged, while the attenuation constant due to dielectric loss is given by

$$\alpha_d = \frac{k^2 \tan\delta}{2\beta} \text{ Np/m (TE or TM waves).} \tag{3.29}$$

This result applies to any TE or TM wave, as long as the guide is completely filled with the dielectric. It can also be used for TEM lines, where $k_c = 0$, by letting $\beta = k$:

$$\alpha_d = \frac{k \tan\delta}{2} \text{ Np/m (TEM waves).} \tag{3.30}$$

3.2 PARALLEL PLATE WAVEGUIDE

The parallel plate waveguide is probably the simplest type of guide that can support TM and TE modes; it can also support a TEM mode, since it is formed from two flat plates, or strips, as shown in Figure 3.2. Although an idealization, this guide is also important for practical reasons, since its operation is quite similar to that of a variety of other waveguides, and models the propagation of higher order modes in stripline.

In the geometry of the parallel plate waveguide in Figure 3.2, the strip width W is assumed to be much greater than the separation, d, so that fringing fields and any x variation can be ignored. A material with permittivity ϵ and permeability μ is assumed to fill the region between the two plates. We will discuss solutions for TEM, TM, and TE waves.

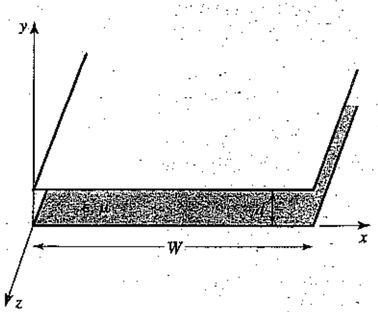

FIGURE 3.2 Geometry of a parallel plate waveguide.

TEM Modes

As discussed in Section 3.1, the TEM mode solution can be obtained by solving Laplace's equation, (3.14), for the electrostatic potential $\Phi(x, y)$ between the two plates. Thus,

$$\nabla_t^2 \Phi(x, y) = 0, \qquad \text{for } 0 \le x \le W,\ 0 \le y \le d. \tag{3.31}$$

If we assume that the bottom plate is at ground (zero) potential and the top plate at a potential of V_o, then the boundary conditions for $\Phi(x, y)$ are

$$\Phi(x, 0) = 0, \tag{3.32a}$$

$$\Phi(x, d) = V_o. \tag{3.32b}$$

Since there is no variation in x, the general solution to (3.31) for $\Phi(x, y)$ is

$$\Phi(x, y) = A + By,$$

and the constants A, B can be evaluated from the boundary conditions of (3.32) to give the final solution as

$$\Phi(x, y) = V_o y/d. \tag{3.33}$$

The transverse electric field is, from (3.13),

$$\bar{e}(x, y) = -\nabla_t \Phi(x, y) = -\hat{y}\frac{V_o}{d}, \tag{3.34}$$

so that the total electric field is

$$\bar{E}(x, y, z) = \bar{e}(x, y)e^{-jkz} = -\hat{y}\frac{V_o}{d}e^{-jkz}, \tag{3.35}$$

where $k = \omega\sqrt{\mu\epsilon}$ is the propagation constant of the TEM wave, as in (3.8). The magnetic field, from (3.18), is

$$\bar{H}(x, y, z) = \frac{1}{\eta}\hat{z} \times \bar{E}(x, y, z) = \hat{x}\frac{V_o}{\eta d}e^{-jkz}, \tag{3.36}$$

where $\eta = \sqrt{\mu/\epsilon}$ is the intrinsic impedance of the medium between the parallel plates. Note that $E_z = H_z = 0$ and that the fields are similar in form to a plane wave in a homogeneous region.

The voltage of the top plate with respect to the bottom plate can be calculated from (3.15) and (3.35) as

$$V = -\int_{y=0}^{d} E_y \, dy = V_o e^{-jkz}, \tag{3.37}$$

as expected. The total current on the top plate can be found from Ampere's law or the surface current density:

$$I = \int_{x=0}^{w} \bar{J}_s \cdot \hat{z}\,dx = \int_{x=0}^{w} (-\hat{y} \times \bar{H}) \cdot \hat{z}\,dx = \int_{x=0}^{w} H_x dx = \frac{wV_o}{\eta d} e^{-jkz}. \tag{3.38}$$

Thus the characteristic impedance can be found as

$$Z_0 = \frac{V}{I} = \frac{\eta d}{w}, \tag{3.39}$$

which is seen to be a constant dependent only on the geometry and material parameters of the guide. The phase velocity is also a constant:

$$v_p = \frac{\omega}{\beta} = \frac{1}{\sqrt{\mu\epsilon}}, \tag{3.40}$$

which is the speed of light in the material medium.

Attenuation due to dielectric loss is given by (3.30). The formula for conductor attenuation will be derived in the next subsection, as a special case of TM mode attenuation.

TM Modes

As discussed in Section 3.1, TM waves are characterized by $H_z = 0$ and a nonzero E_z field that satisfies the reduced wave equation of (3.25), with $\partial/\partial x = 0$:

$$\left(\frac{\partial^2}{\partial y^2} + k_c^2\right) e_z(x, y) = 0, \tag{3.41}$$

where $k_c^2 = k^2 - \beta^2$ is the cutoff wavenumber, and $E_z(x, y, z) = e_z(x, y)e^{-j\beta z}$. The general solution to (3.41) is of the form

$$e_z(x, y) = A \sin k_c y + B \cos k_c y, \tag{3.42}$$

subject to the boundary conditions that

$$e_z(x, y) = 0, \quad \text{at } y = 0, d. \tag{3.43}$$

This implies that $B = 0$ and $k_c d = n\pi$, for $n = 0, 1, 2, 3 \ldots$, or

$$k_c = \frac{n\pi}{d}, \quad n = 0, 1, 2, 3 \ldots. \tag{3.44}$$

Thus the cutoff wavenumber k_c is constrained to discrete values as given by (3.44); this implies that the propagation constant β is given by

$$\beta = \sqrt{k^2 - k_c^2} = \sqrt{k^2 - (n\pi/d)^2}. \tag{3.45}$$

The solution for $e_z(x, y)$ is then

$$e_z(x, y) = A_n \sin \frac{n\pi y}{d}, \tag{3.46}$$

thus,

$$E_z(x, y, z) = A_n \sin \frac{n\pi y}{d} e^{-j\beta z}. \tag{3.47}$$

The transverse field components can be found, using (3.23), to be

$$H_x = \frac{j\omega\epsilon}{k_c} A_n \cos \frac{n\pi y}{d} e^{-j\beta z}, \tag{3.48a}$$

$$E_y = \frac{-j\beta}{k_c} A_n \cos \frac{n\pi y}{d} e^{-j\beta z}, \tag{3.48b}$$

$$E_x = H_y = 0. \tag{3.48c}$$

Observe that for $n = 0$, $\beta = k = \omega\sqrt{\mu\epsilon}$, and that $E_z = 0$. The E_y and H_x fields are then constant in y, so that the TM_0 mode is actually identical to the TEM mode. For $n \geq 1$, however, the situation is different. Each value of n corresponds to a different TM mode, denoted as the TM_n mode, and each mode has its own propagation constant given by (3.45), and field expressions as given by (3.48).

From (3.45) it can be seen that β is real only when $k > k_c$. Since $k = \omega\sqrt{\mu\epsilon}$ is proportional to frequency, the TM_n modes (for $n > 0$) exhibit a cutoff phenomenon, whereby no propagation will occur until the frequency is such that $k > k_c$. The cutoff frequency of the TM_n mode can then be deduced as

$$f_c = \frac{k_c}{2\pi\sqrt{\mu\epsilon}} = \frac{n}{2d\sqrt{\mu\epsilon}}. \tag{3.49}$$

Thus, the TM mode that propagates at the lowest frequency is the TM_1 mode, with a cutoff frequency of $f_c = 1/2d\sqrt{\mu\epsilon}$; the TM_2 mode has a cutoff frequency equal to twice this value, and so on. At frequencies below the cutoff frequency of a given mode, the propagation constant is purely imaginary, corresponding to a rapid exponential decay of the fields. Such modes are referred to as cutoff, or evanescent, modes. TM_n mode propagation is analogous to a high-pass filter response.

The wave impedance of the TM modes, from (3.26), is a function of frequency:

$$Z_{TM} = \frac{-E_y}{H_x} = \frac{\beta}{\omega\epsilon} = \frac{\beta\eta}{k}, \tag{3.50}$$

which we see is pure real for $f > f_c$, but pure imaginary for $f < f_c$. The phase velocity is also a function of frequency:

$$v_p = \frac{\omega}{\beta}, \tag{3.51}$$

and is seen to be greater than $1/\sqrt{\mu\epsilon} = \omega/k$, the speed of light in the medium, since $\beta < k$. The guide wavelength is defined as

$$\lambda_g = \frac{2\pi}{\beta}, \tag{3.52}$$

and is the distance between equiphase planes along the z-axis. Note that $\lambda_g > \lambda = 2\pi/k$, the wavelength of a plane wave in the material. The phase velocity and guide wavelength are defined only for a propagating mode, for which β is real. One may also define a cutoff wavelength for the TM_n mode as

$$\lambda_c = \frac{2d}{n}. \tag{3.53}$$

and applying the boundary conditions shows that $A = 0$ and

$$k_c = \frac{n\pi}{d}, \quad n = 1, 2, 3 \ldots, \tag{3.65}$$

as for the TM case. The final solution for H_z is then

$$H_z(x, y) = B_n \cos\frac{n\pi y}{d} e^{-j\beta z}. \tag{3.66}$$

The transverse fields can be computed from (3.19) as

$$E_x = \frac{j\omega\mu}{k_c} B_n \sin\frac{n\pi y}{d} e^{-j\beta z}, \tag{3.67a}$$

$$H_y = \frac{j\beta}{k_c} B_n \sin\frac{n\pi y}{d} e^{-j\beta z}, \tag{3.67b}$$

$$E_y = H_x = 0. \tag{3.67c}$$

The propagation constant of the TE_n mode is thus,

$$\beta = \sqrt{k^2 - \left(\frac{n\pi}{d}\right)^2}, \tag{3.68}$$

which is the same as the propagation constant of the TM_n mode. The cutoff frequency of the TE_n mode is

$$f_c = \frac{n}{2d\sqrt{\mu\epsilon}}, \tag{3.69}$$

which is also identical to that of the TM_n mode. The wave impedance of the TE_n mode is, from (3.22),

$$Z_{TE} = \frac{E_x}{H_y} = \frac{\omega\mu}{\beta} = \frac{k\eta}{\beta}, \tag{3.70}$$

which is seen to be real for propagating modes and imaginary for nonpropagating, or cutoff, modes. The phase velocity, guide wavelength, and cutoff wavelength are similar to the results for the TM modes.

The power flow down the guide for a TE_n mode can be calculated as

$$P_o = \frac{1}{2}\mathrm{Re}\int_{x=0}^{w}\int_{y=0}^{d} \bar{E} \times \bar{H}^* \cdot \hat{z}\, dy\, dx = \frac{1}{2}\mathrm{Re}\int_{x=0}^{w}\int_{y=0}^{d} E_x H_y^*\, dy\, dx$$

$$= \frac{\omega\mu d w}{4k_c^2}|B_n|^2 \mathrm{Re}(\beta), \qquad \text{for } n > 0, \tag{3.71}$$

which is zero if the operating frequency is below the cutoff frequency (β imaginary).

Note that if $n = 0$, then $E_x = H_y = 0$ from (3.67), and thus $P_o = 0$, implying that there is no TE_0 mode.

Attenuation can be calculated in the same way as for the TM modes. The attenuation due to dielectric loss is given by (3.29). It is left as a problem to show that the attenuation due to conductor loss for TE modes is given by

$$\alpha_c = \frac{2k_c^2 R_s}{\omega\mu\beta d} = \frac{2k_c^2 R_s}{k\beta\eta d}\ \mathrm{Np/m}. \tag{3.72}$$

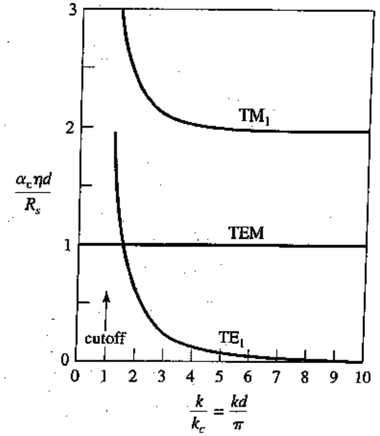

FIGURE 3.4 Attenuation due to conductor loss for the TEM, TM_1, and TE_1 modes of a parallel plate waveguide.

Figure 3.4 shows the attenuation due to conductor loss for the TEM, TM_1, and TE_1 modes. Observe that $\alpha_c \to \infty$ as cutoff is approached for the TM and TE modes.

Table 3.1 summarizes a number of useful results for TEM, TM, and TE mode propagation on parallel plate waveguides. Field lines for the TEM, TM_1, and TE_1 modes are shown in Figure 3.5.

TABLE 3.1 Summary of Results for Parallel Plate Waveguide

Quantity	TEM Mode	TM_n Mode	TE_n Mode
k	$\omega\sqrt{\mu\epsilon}$	$\omega\sqrt{\mu\epsilon}$	$\omega\sqrt{\mu\epsilon}$
k_c	0	$n\pi/d$	$n\pi/d$
β	$k = \omega\sqrt{\mu\epsilon}$	$\sqrt{k^2 - k_c^2}$	$\sqrt{k^2 - k_c^2}$
λ_c	∞	$2\pi/k_c = 2d/n$	$2\pi/k_c = 2d/n$
λ_g	$2\pi/k$	$2\pi/\beta$	$2\pi/\beta$
v_p	$\omega/k = 1/\sqrt{\mu\epsilon}$	ω/β	ω/β
α_d	$(k \tan\delta)/2$	$(k^2 \tan\delta)/2\beta$	$(k^2 \tan\delta)/2\beta$
α_c	$R_s/\eta d$	$2kR_s/\beta\eta d$	$2k_c^2 R_s/k\beta\eta d$
E_z	0	$A_n \sin(n\pi y/d)e^{-j\beta z}$	0
H_z	0	0	$B_n \cos(n\pi y/d)e^{-j\beta z}$
E_x	0	0	$(j\omega\mu/k_c)B_n \sin(n\pi y/d)e^{-j\beta z}$
E_y	$(-V_o/d)e^{-j\beta z}$	$(-j\beta/k_c)A_n \cos(n\pi y/d)e^{-j\beta z}$	0
H_x	$(V_o/\eta d)e^{-j\beta z}$	$(j\omega\epsilon/k_c)A_n \cos(n\pi y/d)e^{-j\beta z}$	0
H_y	0	0	$(j\beta/k_c)B_n \sin(n\pi y/d)e^{-j\beta z}$
Z	$Z_{TEM} = \eta d/w$	$Z_{TM} = \beta\eta/k$	$Z_{TE} = k\eta/\beta$

The surface charge density on the strip at $y = b/2$ is

$$\begin{aligned}\rho_s &= D_y(x, y = b/2^+) - D_y(x, y = b/2^-)\\ &= \epsilon_0\epsilon_r[E_y(x, y = b/2^+) - E_y(x, y = b/2^-)]\\ &= 2\epsilon_0\epsilon_r \sum_{\substack{n=1\\ \text{odd}}}^{\infty} A_n \left(\frac{n\pi}{a}\right)\cos\frac{n\pi x}{a}\cosh\frac{n\pi b}{2a},\end{aligned} \qquad (3.1$$

which is seen to be a Fourier series in x for the surface charge density, ρ_s. If we k the surface charge density, we could easily find the unknown constants, A_n, and then capacitance. We do not know the exact surface charge density, but we can make a guess by approximating it as a constant over the width of the strip

$$\rho_s(x) = \begin{cases} 1 & \text{for } |x| < W/2\\ 0 & \text{for } |x| > W/2.\end{cases} \qquad (3.18$$

Equating this to (3.187) and using the orthogonality properties of the $\cos(n\pi x/a)$ functi gives the constants A_n as

$$A_n = \frac{2a\sin(n\pi W/2a)}{(n\pi)^2\epsilon_0\epsilon_r\cosh(n\pi b/2a)}. \qquad (3.1$$

The voltage of the center strip relative to the bottom conductor is

$$V = -\int_0^{b/2} E_y(x = 0, y)\,dy = \sum_{\substack{n=1\\ \text{odd}}}^{\infty} A_n \sinh\frac{n\pi b}{2a}. \qquad (3.19$$

The total charge, per unit length, on the center conductor is

$$Q = \int_{-W/2}^{W/2} \rho_s(x)\,dx = W \text{ C/m}, \qquad (3.19$$

so that the capacitance per unit length of the stripline is

$$C = \frac{Q}{V} = \frac{W}{\displaystyle\sum_{\substack{n=1\\ \text{odd}}}^{\infty} \frac{2a\sin(n\pi W/2a)\sinh(n\pi b/2a)}{(n\pi)^2\epsilon_0\epsilon_r\cosh(n\pi b/2a)}} \text{ Fd/m}. \qquad (3.192)$$

The characteristic impedance is then found as

$$Z_0 = \sqrt{\frac{L}{C}} = \frac{\sqrt{LC}}{C} = \frac{1}{v_pC} = \frac{\sqrt{\epsilon_r}}{cC},$$

where $c = 3 \times 10^8$ m/sec.

EXAMPLE 3.6 NUMERICAL CALCULATION OF STRIPLINE PARAMETERS

Evaluate the above expressions for a stripline having $\epsilon_r = 2.55$ and $a = 100b$, to find the characteristic impedance for $W/b = 0.25$ to 5.0. Compare with the results from (3.179).

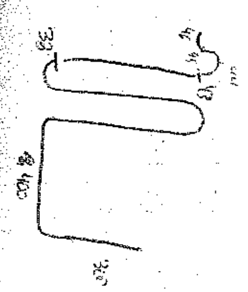

written to evaluate (3.192). The series was truncated ults are shown below.

	Numerical Eq. (3.192)	Formula Eq. (3.179)
	98.8 Ω	86.6 Ω
	73.3	62.7
	49.0	41.0
	28.4	24.2
	16.8	15.0
5.0	11.8	10.8

We see that the results are in reasonable agreement with the closed-form equations of (3.179), particularly for wider strips. Better results could be obtained if more sophisticated estimates were used for the charge density, ρ_s. ■

3.8 MICROSTRIP

Microstrip line is one of the most popular types of planar transmission lines, primarily because it can be fabricated by photolithographic processes and is easily integrated with other passive and active microwave devices. The geometry of a microstrip line is shown in Figure 3.25a. A conductor of width W is printed on a thin, grounded dielectric substrate of thickness d and relative permittivity ϵ_r; a sketch of the field lines is shown in Figure 3.25b.

If the dielectric were not present ($\epsilon_r = 1$), we could think of the line as a two-wire line consisting of two flat strip conductors of width W, separated by a distance $2d$ (the

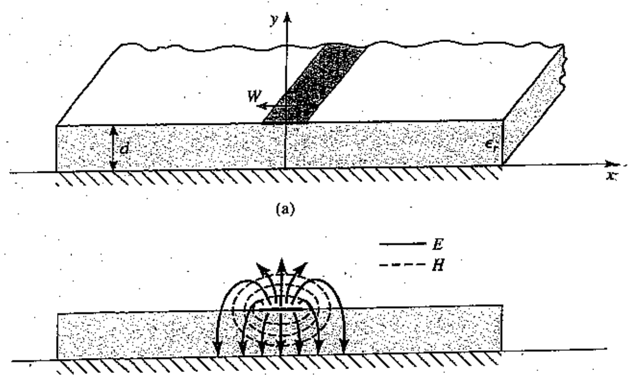

FIGURE 3.25 Microstrip transmission line. (a) Geometry. (b) Electric and magnetic field lines.

ground plane can be removed via image theory). In this case we would have a simple
transmission line, with $v_p = c$ and $\beta = k_0$.

The presence of the dielectric, and particularly the fact that the dielectric doe
fill the air region above the strip ($y > d$), complicates the behavior and analysis of
crostrip line. Unlike stripline, where all the fields are contained within a homogen
dielectric region, microstrip has some (usually most) of its field lines in the dielectri
gion, concentrated between the strip conductor and the ground plane, and some fract
in the air region above the substrate. For this reason the microstrip line cannot supp
a pure TEM wave, since the phase velocity of TEM fields in the dielectric region wou
be $c/\sqrt{\epsilon_r}$, but the phase velocity of TEM fields in the air region would be c. Thus
phase match at the dielectric-air interface would be impossible to attain for a TEM-ty
wave.

In actuality, the exact fields of a microstrip line constitute a hybrid TM-TE wave, an
require more advanced analysis techniques than we are prepared to deal with here. In mo
practical applications, however, the dielectric substrate is electrically very thin ($d \ll$
and so the fields are quasi-TEM. In other words, the fields are essentially the same as thos
of the static case. Thus, good approximations for the phase velocity, propagation constan
and characteristic impedance can be obtained from static or quasi-static solutions. Then th
phase velocity and propagation constant can be expressed as

$$v_p = \frac{c}{\sqrt{\epsilon_e}}, \tag{3.193}$$

$$\beta = k_0\sqrt{\epsilon_e}, \tag{3.194}$$

where ϵ_e is the effective dielectric constant of the microstrip line. Since some of the field lines are in the dielectric region and some are in air, the effective dielectric constant satisfies the relation

$$1 < \epsilon_e < \epsilon_r,$$

and is dependent on the substrate thickness, d, and conductor width, W.

We will first present design formulas for the effective dielectric constant and charac-
teristic impedance of microstrip line; these results are curve-fit approximations to rigorous
quasi-static solutions [8], [9]. Then we will outline a numerical method of solution (simi-
lar to that used in the previous section for stripline) for the capacitance per unit length of
microstrip line.

Formulas for Effective Dielectric Constant, Characteristic Impedance, and Attenuation

The effective dielectric constant of a microstrip line is given approximately by

$$\epsilon_e = \frac{\epsilon_r + 1}{2} + \frac{\epsilon_r - 1}{2}\frac{1}{\sqrt{1 + 12d/W}}. \tag{3.195}$$

The effective dielectric constant can be interpreted as the dielectric constant of a homogeneous medium that replaces the air and dielectric regions of the microstrip, as shown in Figure 3.26. The phase velocity and propagation constant are then given by (3.193) and (3.194).

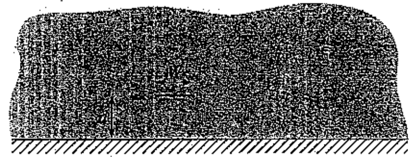

FIGURE 3.26 Equivalent geometry of quasi-TEM microstrip line, where the dielectric slab of thickness d and relative permittivity ϵ_r has been replaced with a homogeneous medium of effective relative permittivity, ϵ_e.

Given the dimensions of the microstrip line, the characteristic impedance can be calculated as

$$Z_0 = \begin{cases} \dfrac{60}{\sqrt{\epsilon_e}} \ln\left(\dfrac{8d}{W} + \dfrac{W}{4d}\right) & \text{for } W/d \le 1 \\[2ex] \dfrac{120\pi}{\sqrt{\epsilon_e}\left[W/d + 1.393 + 0.667\ln(W/d + 1.444)\right]} & \text{for } W/d \ge 1. \end{cases} \tag{3.196}$$

For a given characteristic impedance Z_0 and dielectric constant ϵ_r, the W/d ratio can be found as

$$\frac{W}{d} = \begin{cases} \dfrac{8e^A}{e^{2A} - 2} & \text{for } W/d < 2 \\[2ex] \dfrac{2}{\pi}\left[B - 1 - \ln(2B - 1) + \dfrac{\epsilon_r - 1}{2\epsilon_r}\left\{\ln(B - 1) + 0.39 - \dfrac{0.61}{\epsilon_r}\right\}\right] & \text{for } W/d > 2, \end{cases} \tag{3.197}$$

where

$$A = \frac{Z_0}{60}\sqrt{\frac{\epsilon_r + 1}{2}} + \frac{\epsilon_r - 1}{\epsilon_r + 1}\left(0.23 + \frac{0.11}{\epsilon_r}\right)$$

$$B = \frac{377\pi}{2Z_0\sqrt{\epsilon_r}}.$$

Considering microstrip as a quasi-TEM line, the attenuation due to dielectric loss can be determined as

$$\alpha_d = \frac{k_0 \epsilon_r(\epsilon_e - 1)\tan\delta}{2\sqrt{\epsilon_e}(\epsilon_r - 1)} \text{ Np/m}, \tag{3.198}$$

where $\tan\delta$ is the loss tangent of the dielectric. This result is derived from (3.30) by multiplying by a "filling factor,"

$$\frac{\epsilon_r(\epsilon_e - 1)}{\epsilon_e(\epsilon_r - 1)},$$

which accounts for the fact that the fields around the microstrip line are partly in air (lossless) and partly in the dielectric. The attenuation due to conductor loss is given approximately by [8]

$$\alpha_c = \frac{R_s}{Z_0 W} \text{ Np/m}, \tag{3.199}$$

where $R_s = \sqrt{\omega\mu_0/2\sigma}$ is the surface resistivity of the conductor. For most microstrip substrates, conductor loss is much more significant than dielectric loss; exceptions occur with some semiconductor substrates, however.

EXAMPLE 3.7 MICROSTRIP DESIGN

Calculate the width and length of a microstrip line for a 50 Ω characteristic impedance and a 90° phase shift at 2.5 GHz. The substrate thickness is $d = 0.127$ cm, with $\epsilon_r = 2.20$.

Solution

We first find W/d for $Z_0 = 50\ \Omega$, and initially guess that $W/d > 2$. From (3.197),

$$B = 7.985, \qquad W/d = 3.081.$$

So $W/d > 2$; otherwise we would use the expression for $W/d < 2$. Then $W = 3.081d = 0.391$ cm. From (3.195) the effective dielectric constant is

$$\epsilon_e = 1.87.$$

The line length, ℓ, for a 90° phase shift is found as

$$\phi = 90^\circ = \beta\ell = \sqrt{\epsilon_e}k_0\ell,$$

$$k_0 = \frac{2\pi f}{c} = 52.35\ \text{m}^{-1},$$

$$\ell = \frac{90^\circ(\pi/180^\circ)}{\sqrt{\epsilon_e}k_0} = 2.19\ \text{cm}.$$

An Approximate Electrostatic Solution

We now look at an approximate quasi-static solution for the microstrip line, so that the appearance of design equations like those of (3.195)–(3.197) is not a complete mystery. This analysis is very similar to that carried out for stripline in the previous section. As in that analysis, it is again convenient to place conducting sidewalls on the microstrip line, as shown in Figure 3.27. The sidewalls are placed at $x = \pm a/2$, where $a \gg d$, so that the walls should not perturb the field lines localized around the strip conductor. We then can solve Laplace's equation in the region between the sidewalls:

$$\nabla_t^2\Phi(x, y) = 0, \quad \text{for } |x| \le a/2,\ 0 \le y < \infty, \tag{3.200}$$

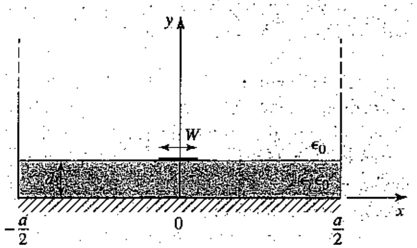

FIGURE 3.27 Geometry of a microstrip line with conducting sidewalls.

with boundary conditions,

$$\Phi(x, y) = 0, \qquad \text{at } x = \pm a/2, \tag{3.201a}$$

$$\Phi(x, y) = 0, \qquad \text{at } y = 0, \infty. \tag{3.201b}$$

Since there are two regions defined by the air/dielectric interface, with a charge discontinuity on the strip, we will have separate expressions for $\Phi(x, y)$ in these regions. Solving (3.200) by the method of separation of variables and applying the boundary conditions of (3.201a,b) gives the general solutions as

$$\Phi(x, y) = \begin{cases} \displaystyle\sum_{\substack{n=1\\ \text{odd}}}^{\infty} A_n \cos\frac{n\pi x}{a}\sinh\frac{n\pi y}{a} & \text{for } 0 \le y \le d \\ \displaystyle\sum_{\substack{n=1\\ \text{odd}}}^{\infty} B_n \cos\frac{n\pi x}{a} e^{-n\pi y/a} & \text{for } d \le y < \infty. \end{cases} \tag{3.202}$$

Now the potential must be continuous at $y = d$, so from (3.202) we have that

$$A_n \sinh\frac{n\pi d}{a} = B_n e^{-n\pi d/a}, \tag{3.203}$$

so $\Phi(x, y)$ can be written as

$$\Phi(x, y) = \begin{cases} \displaystyle\sum_{\substack{n=1\\ \text{odd}}}^{\infty} A_n \cos\frac{n\pi x}{a}\sinh\frac{n\pi y}{a} & \text{for } 0 \le y \le d \\ \displaystyle\sum_{\substack{n=1\\ \text{odd}}}^{\infty} A_n \cos\frac{n\pi x}{a}\sinh\frac{n\pi d}{a} e^{-n\pi(y-d)/a} & \text{for } d \le y < \infty. \end{cases} \tag{3.204}$$

The remaining constants, A_n, can be found by considering the surface charge density on the strip. We first find $E_y = -\partial\Phi/\partial y$:

$$E_y = \begin{cases} \displaystyle -\sum_{\substack{n=1\\ \text{odd}}}^{\infty} A_n\left(\frac{n\pi}{a}\right)\cos\frac{n\pi x}{a}\cosh\frac{n\pi y}{a} & \text{for } 0 \le y < d \\ \displaystyle\sum_{\substack{n=1\\ \text{odd}}}^{\infty} A_n\left(\frac{n\pi}{a}\right)\cos\frac{n\pi x}{a}\sinh\frac{n\pi d}{a} e^{-n\pi(y-d)/a} & \text{for } d \le y < \infty. \end{cases} \tag{3.205}$$

Then the surface charge density on the strip at $y = d$ is

$$\begin{aligned} \rho_s &= D_y(x, y = d^+) - D_y(x, y = d^-) \\ &= \epsilon_0 E_y(x, y = d^+) - \epsilon_0\epsilon_r E_y(x, y = d^-) \\ &= \epsilon_0 \sum_{\substack{n=1\\ \text{odd}}}^{\infty} A_n\left(\frac{n\pi}{a}\right)\cos\frac{n\pi x}{a}\left[\sinh\frac{n\pi d}{a} + \epsilon_r\cosh\frac{n\pi d}{a}\right], \end{aligned} \tag{3.206}$$

which is seen to be a Fourier series in x for the surface charge density, ρ_s. As for the stripline case, we can approximate the charge density on the microstrip line by a uniform distribution:

$$\rho_s(x) = \begin{cases} 1 & \text{for } |x| < W/2 \\ 0 & \text{for } |x| > W/2. \end{cases} \tag{3.207}$$

Equating (3.207) to (3.206) and using the orthogonality of the $\cos n\pi x/a$ functions gives the constants A_n as

$$A_n = \frac{4a \sin n\pi W/2a}{(n\pi)^2 \epsilon_0 [\sinh(n\pi d/a) + \epsilon_r \cosh(n\pi d/a)]}. \tag{3.208}$$

The voltage of the strip relative to the ground plane is

$$V = -\int_0^d E_y(x = 0, y)\, dy = \sum_{\substack{n=1\\ \text{odd}}}^{\infty} A_n \sinh \frac{n\pi d}{a}. \tag{3.209}$$

The total charge, per unit length, on the center strip is

$$Q = \int_{-W/2}^{W/2} \rho_s(x)\, dx = W \text{ C/m}, \tag{3.210}$$

so the static capacitance per unit length of the microstrip line is

$$C = \frac{Q}{V} = \frac{1}{\displaystyle\sum_{\substack{n=1\\ \text{odd}}}^{\infty} \frac{4a \sin(n\pi W/2a) \sinh(n\pi d/a)}{(n\pi)^2 W \epsilon_0 [\sinh(n\pi d/a) + \epsilon_r \cosh(n\pi d/a)]}}. \tag{3.211}$$

Now to find the effective dielectric constant, we consider two cases of capacitance:

Let C = capacitance per unit length of the microstrip line with a dielectric substrate ($\epsilon_r \neq 1$)

Let C_o = capacitance per unit length of the microstrip line with an air dielectric ($\epsilon_r = 1$)

Since capacitance is proportional to the dielectric constant of the material homogeneously filling the region around the conductors, we have that

$$\epsilon_e = \frac{C}{C_o}. \tag{3.212}$$

So (3.212) can be evaluated by computing (3.211) twice; once with ϵ_r equal to the dielectric constant of the substrate (for C), and then with $\epsilon_r = 1$ (for C_o). The characteristic impedance is then

$$Z_0 = \frac{1}{v_p C} = \frac{\sqrt{\epsilon_e}}{cC}, \tag{3.213}$$

where $c = 3 \times 10^8$ m/sec.

EXAMPLE 3.8 NUMERICAL CALCULATION OF MICROSTRIP PARAMETERS

Evaluate the above expressions for a microstrip line on a substrate with $\epsilon_r = 2.55$. Calculate the effective dielectric constant and characteristic impedance for $W/d = 0.5$ to 10.0, and compare with the results from (3.195) and (3.196). Let $a = 100d$.

Solution

A computer program was written to evaluate (3.211) for $\epsilon = \epsilon_0$ and then $\epsilon = \epsilon_r \epsilon_0$. Then (3.212) was used to evaluate the effective dielectric constant, ϵ_e, and (3.213) to evaluate the characteristic impedance, Z_0. The series was truncated after 50 terms, and the results are shown in the following table.

	Numerical Solutions		Formulas	
W/d	ϵ_e	$Z_0(\Omega)$	ϵ_e	$Z_0(\Omega)$
0.5	1.977	100.9	1.938	119.8
1.0	1.989	94.9	1.990	89.8
2.0	2.036	75.8	2.068	62.2
4.0	2.179	45.0	2.163	39.3
7.0	2.287	29.5	2.245	25.6
10.0	2.351	21.7	2.198	19.1

The comparison is reasonably good, although better results could be obtained from the approximate numerical solution by using a better estimate of the charge density on the strip. ■

3.9 THE TRANSVERSE RESONANCE TECHNIQUE

According to the general solutions to Maxwell's equations for TE or TM waves given in Section 3.1, a uniform waveguide structure always has a propagation constant of the form

$$\beta = \sqrt{k^2 - k_c^2} = \sqrt{k^2 - k_x^2 - k_y^2}, \tag{3.214}$$

where $k_c = \sqrt{k_x^2 + k_y^2}$ is the cutoff wavenumber of the guide and, for a given mode, is a fixed function of the cross-sectional geometry of the guide. Thus, if we know k_c we can determine the propagation constant of the guide. In previous sections we determined k_c by solving the wave equation in the guide, subject to the appropriate boundary conditions; this technique is very powerful and general, but can be complicated for complex waveguides, especially if dielectric layers are present. In addition, the wave equation solution gives a complete field description inside the waveguide, which is much more information than we really need if we are only interested in the propagation constant of the guide. The transverse resonance technique employs a transmission line model of the transverse cross section of the waveguide, and gives a much simpler and more direct solution for the cutoff frequency. This is another example where circuit and transmission line theory can be used to simplify the field theory solution.

The transverse resonance procedure is based on the fact that in a waveguide at cutoff, the fields form standing waves in the transverse plane of the guide, as can be inferred from the "bouncing plane wave" interpretation of waveguide modes discussed in Section 3.2. This situation can be modeled with an equivalent transmission line circuit operating at resonance. One of the conditions of such a resonant line is the fact that, at any point on the line, the sum of the input impedances seen looking to either side must be zero. That is,

$$Z_{\text{in}}^r(x) + Z_{\text{in}}^\ell(x) = 0, \qquad \text{for all } x, \tag{3.215}$$

where $Z_{\text{in}}^r(x)$ and $Z_{\text{in}}^\ell(x)$ are the input impedances seen looking to the right and left, respectively, at the point x on the resonant line.

3.19 Design a stripline transmission line for a 70 Ω characteristic impedance. The ground plane separation is 0.316 cm, and the dielectric constant of the filling material is 2.20. What is the guide wavelength on this transmission line if the frequency is 3.0 GHz?

3.20 Design a microstrip transmission line for a 100 Ω characteristic impedance. The substrate thickness is 0.158 cm, with $\epsilon_r = 2.20$. What is the guide wavelength on this transmission line if the frequency is 4.0 GHz?

3.21 A 100 Ω microstrip line is printed on a substrate of thickness 0.0762 cm, with a dielectric constant of 2.2. Ignoring losses and fringing fields, find the shortest length of this line that appears at its input as a capacitor of 5 pF at 2.5 GHz. Repeat for an inductance of 5 nH. Using a microwave CAD package with a physical model for the microstrip line, compute the actual input impedance seen when losses are included (assume copper conductors and $\tan\delta = 0.001$).

3.22 A microwave antenna feed network operating at 5 GHz requires a 50 Ω printed transmission line that is 16λ long. Possible choices are (1) copper microstrip, with $d = 0.16$ cm, $\epsilon_r = 2.20$, and $\tan\delta = 0.001$, or (2) copper stripline, with $b = 0.32$ cm, $\epsilon_r = 2.20$, $t = 0.01$ mm, and $\tan\delta = 0.001$. Which line should be used, if attenuation is to be minimized?

3.23 Consider the TE modes of an arbitrary uniform waveguiding structure, where the transverse fields are related to H_z as in (3.19). If H_z is of the form $H_z(x, y, z) = h_z(x, y)e^{-j\beta z}$, where $h_z(x, y)$ is a real function, compute the Poynting vector and show that real power flow occurs only in the z direction. Assume that β is real, corresponding to a propagating mode.

3.24 A piece of rectangular waveguide is air filled for $z < 0$ and dielectric filled for $z > 0$. Assume that both regions can support only the dominant TE_{10} mode, and that a TE_{10} mode is incident on the interface from $z < 0$. Using a field analysis, write general expressions for the transverse field components of the incident, reflected, and transmitted waves in the two regions, and enforce the boundary conditions at the dielectric interface to find the reflection and transmission coefficients. Compare these results to those obtained with an impedance approach, using Z_{TE} for each region.

3.25 Use the transverse resonance technique to derive a transcendental equation for the propagation constant of the TM modes of a rectangular waveguide that is air filled for $0 < x < d$ and dielectric filled for $d < x < a$.

3.26 Apply the transverse resonance technique to find the propagation constants for the TE surface waves that can be supported by the structure of Problem 3.17.

3.27 An X-band waveguide filled with Teflon is operating at 9.5 GHz. Calculate the speed of light in this material and the phase and group velocities in the waveguide.

3.28 As discussed in the Point of Interest on the power handling capacity of transmission lines, the maximum power capacity of a coaxial line is limited by voltage breakdown, and is given by

$$P_{\max} = \frac{\pi a^2 E_d^2}{\eta_0} \ln \frac{b}{a}$$

where E_d is the field strength at breakdown. Find the value of b/a that maximizes the maximum power capacity and show that the corresponding characteristic impedance is about 30 Ω.

C h a p t e r F o u r

Microwave Network Analysis

Circuits operating at low frequencies, for which the circuit dimensions are small relative to the wavelength, can be treated as an interconnection of lumped passive or active components with unique voltages and currents defined at any point in the circuit. In this situation the circuit dimensions are small enough so that there is negligible phase change from one point in the circuit to another. In addition, the fields can be considered as TEM fields supported by two or more conductors. This leads to a quasi-static type of solution to Maxwell's equations, and to the well-known Kirchhoff voltage and current laws and impedance concepts of circuit theory [1]. As the reader is aware, there exists a powerful and useful set of techniques for analyzing low-frequency circuits. In general, these techniques cannot be directly applied to microwave circuits. It is the purpose of the present chapter, however, to show how circuit and network concepts can be extended to handle many microwave analysis and design problems of practical interest.

The main reason for doing this is that it is usually much easier to apply the simple and intuitive ideas of circuit analysis to a microwave problem than it is to solve Maxwell's equations for the same problem. In a way, field analysis gives us much more information about the particular problem under consideration than we really want or need. That is, because the solution to Maxwell's equations for a given problem is complete, it gives the electric and magnetic fields at all points in space. But usually we are interested in only the voltage or current at a set of terminals, the power flow through a device, or some other type of "global" quantity, as opposed to a minute description of the response at all points in space. Another reason for using circuit or network analysis is that it is then very easy to modify the original problem, or combine several elements together and find the response, without having to analyze in detail the behavior of each element in combination with its neighbors. A field analysis using Maxwell's equations for such problems would be hopelessly difficult. There are situations, however, where such circuit analysis techniques are an oversimplification, leading to erroneous results. In such cases one must resort to a field analysis approach, using Maxwell's equations. It is part of the education of a microwave engineer to be able to determine when circuit analysis concepts apply, and when they should be cast aside.

The basic procedure for microwave network analysis is as follows. We first treat a set of basic, canonical problems rigorously, using field analysis and Maxwell's equations (as we have done in Chapters 2 and 3, for a variety of transmission line and waveguide problems). W[illegible] so doing, we try to obtain quantities that can be directly related to a circuit or transmission [illegible] parameter. For example, when we treated various transmission lines and waveguides in Chap[illegible] we derived the propagation constant and characteristic impedance of the line. This allowe[illegible] transmission line or waveguide to be treated as a distributed component characterized b[illegible] length, propagation constant, and characteristic impedance. At this point, we can interco[illegible] various components and use network and/or transmission line theory to analyze the behavi[illegible] the entire system of components, including effects such as multiple reflections, loss, impeda[illegible] transformations, and transitions from one type of transmission medium to another (e.g., coa[illegible] microstrip). As we will see, a transition between different transmission lines, or a discontin[illegible] on a transmission line, generally cannot be treated as a simple junction between two transmiss[illegible] lines, but must be augmented with some type of equivalent circuit to account for reactan[illegible] associated with the transition or discontinuity.

Microwave network theory was originally developed in the service of radar system[illegible] component development at the MIT Radiation Lab in the 1940s. This work was continued [illegible] extended at the Polytechnic Institute of Brooklyn by researchers such as E. Weber, N. Marcu[illegible] A. A. Oliner, L. B. Felsen, A. Hessel, and others [2].

4.1 IMPEDANCE AND EQUIVALENT VOLTAGES AND CURRENTS

Equivalent Voltages and Currents

At microwave frequencies the measurement of voltage or current is difficult (or impossib[illegible] unless a clearly defined terminal pair is available. Such a terminal pair may be present [illegible] the case of TEM-type lines (such as coaxial cable, microstrip, or stripline), but does [illegible] strictly exist for non-TEM lines (such as rectangular, circular, or surface waveguides).

Figure 4.1 shows the electric and magnetic field lines for an arbitrary two-conduc[illegible] TEM transmission line. As in Chapter 3, the voltage, V, of the + conductor relative to the [illegible] conductor can be found as

$$V = \int_{+}^{-} \bar{E} \cdot d\bar{\ell}, \qquad (4[illegible]$$

where the integration path begins on the + conductor and ends on the − conductor. I[illegible] important to realize that, because of the electrostatic nature of the transverse fields betw[illegible] the two conductors, the voltage defined in (4.1) is unique and does not depend on the sha[illegible] of the integration path. The total current flowing on the + conductor can be determi[illegible] from an application of Ampere's law as

$$I = \oint_{C+} \bar{H} \cdot d\bar{\ell}, \qquad (4[illegible]$$

where the integration contour is any closed path enclosing the + conductor (but n[illegible]

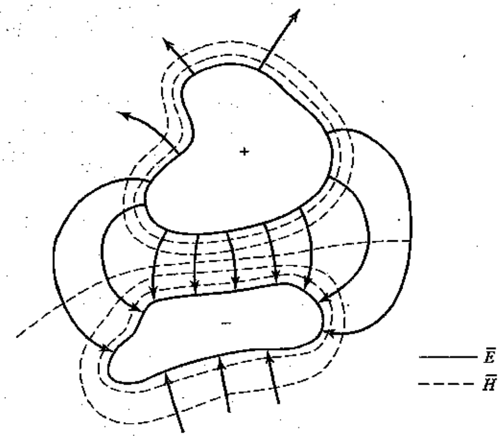

FIGURE 4.1 Electric and magnetic field lines for an arbitrary two-conductor TEM line.

the − conductor). A characteristic impedance Z_0 can then be defined for traveling waves as

$$Z_0 = \frac{V}{I}. \qquad (4.3)$$

At this point, after having defined and determined a voltage, current, and characteristic impedance (and assuming we know the propagation constant for the line), we can proceed to apply the circuit theory for transmission lines developed in Chapter 2 to characterize this line as a circuit element.

The situation is more difficult for waveguides. To see why, we will look at the case of a rectangular waveguide, as shown in Figure 4.2. For the dominant TE_{10} mode, the transverse fields can be written, from Table 3.2, as

$$E_y(x, y, z) = \frac{j\omega\mu a}{\pi} A \sin\frac{\pi x}{a} e^{-j\beta z} = Ae_y(x, y)e^{-j\beta z}, \qquad (4.4a)$$

$$H_x(x, y, z) = \frac{j\beta a}{\pi} A \sin\frac{\pi x}{a} e^{-j\beta z} = Ah_x(x, y)e^{-j\beta z}. \qquad (4.4b)$$

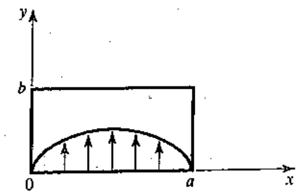

FIGURE 4.2 Electric field lines for the TE_{10} mode of a rectangular waveguide.

Applying (4.1) to the electric field of (4.4a) gives

$$V = \frac{-j\omega\mu a}{\pi} A \sin\frac{\pi x}{a} e^{-j\beta z} \int_y dy. \quad (4.\ldots)$$

Thus it is seen that this voltage depends on the position, x, as well as the length of the integration contour along the y direction. Integrating from $y = 0$ to b for $x = a/2$ gives a voltage that is quite different from that obtained by integrating from $y = 0$ to b for $x = 0$, for example. What, then, is the correct voltage? The answer is that there is no "correct" voltage in the sense of being unique or pertinent for all applications. A similar problem arises with current, and also impedance. We will now show how we can define voltages, currents, and impedances that can be useful for non-TEM lines.

There are many ways to define equivalent voltage, current, and impedance for waveguides, since these quantities are not unique for non-TEM lines, but the following considerations usually lead to the most useful results [1], [3], [4]:

- Voltage and current are defined only for a particular waveguide mode, and are defined so that the voltage is proportional to the transverse electric field, and the current is proportional to the transverse magnetic field.
- In order to be used in a manner similar to voltages and currents of circuit theory, the equivalent voltages and currents should be defined so that their product gives the power flow of the mode.
- The ratio of the voltage to the current for a single traveling wave should be equal to the characteristic impedance of the line. This impedance may be chosen arbitrarily, but is usually selected as equal to the wave impedance of the line, or else normalized to unity.

For an arbitrary waveguide mode with both positively and negatively traveling waves, the transverse fields can be written as

$$\bar{E}_t(x, y, z) = \bar{e}(x, y)(A^+e^{-j\beta z} + A^-e^{j\beta z}) = \frac{\bar{e}(x, y)}{C_1}(V^+e^{-j\beta z} + V^-e^{j\beta z}), \quad (4.6a)$$

$$\bar{H}_t(x, y, z) = \bar{h}(x, y)(A^+e^{-j\beta z} - A^-e^{j\beta z}) = \frac{\bar{h}(x, y)}{C_2}(I^+e^{-j\beta z} - I^-e^{j\beta z}), \quad (4.6b)$$

where $\bar{e}$ and $\bar{h}$ are the transverse field variations of the mode, and A^+, A^- are the field amplitudes of the traveling waves. Since $\bar{E}_t$ and $\bar{H}_t$ are related by the wave impedance, Z_w, according to (3.22) or (3.26), we also have that

$$\bar{h}(x, y) = \frac{\hat{z} \times \bar{e}(x, y)}{Z_w}. \quad (4.7)$$

Equation (4.6) also defines equivalent voltage and current waves as

$$V(z) = V^+e^{-j\beta z} + V^-e^{j\beta z}, \quad (4.8a)$$

$$I(z) = I^+e^{-j\beta z} - I^-e^{j\beta z}, \quad (4.8b)$$

with $V^+/I^+ = V^-/I^- = Z_0$. This definition embodies the idea of making the equivalent voltage and current proportional to the transverse electric and magnetic fields, respectively.

The proportionality constants for this relationship are $C_1 = V^+/A^+ = V^-/A^-$ and $C_2 = I^+/A^+ = I^-/A^-$, and can be determined from the remaining two conditions for power and impedance.

The complex power flow for the incident wave is given by

$$P^+ = \frac{1}{2}|A^+|^2 \iint_S \bar{e} \times \bar{h}^* \cdot \hat{z}\, ds = \frac{V^+I^{+*}}{2C_1C_2^*} \iint_S \bar{e} \times \bar{h}^* \cdot \hat{z}\, ds. \quad (4.9)$$

Since we want this power to be equal to $(1/2)V^+I^{+*}$, we have the result that

$$C_1C_2^* = \iint_S \bar{e} \times \bar{h}^* \cdot \hat{z}\, ds, \quad (4.10)$$

where the surface integration is over the cross section of the waveguide. The characteristic impedance is

$$Z_0 = \frac{V^+}{I^+} = \frac{V^-}{I^-} = \frac{C_1}{C_2}, \quad (4.11)$$

since $V^+ = C_1A$ and $I^+ = C_2A$, from (4.6a,b). If it is desired to have $Z_0 = Z_w$, the wave impedance (Z_{TE} or Z_{TM}) of the mode, then

$$\frac{C_1}{C_2} = Z_w \ (Z_{TE} \text{ or } Z_{TM}). \quad (4.12a)$$

Alternatively, it may be desirable to normalize the characteristic impedance to unity ($Z_0 = 1$), in which case we have

$$\frac{C_1}{C_2} = 1. \quad (4.12b)$$

So for a given waveguide mode, (4.10) and (4.12) can be solved for the constants C_1 and C_2, and equivalent voltages and currents defined. Higher order modes can be treated in the same way, so that a general field in a waveguide can be expressed in the following form:

$$\bar{E}_t(x, y, z) = \sum_{n=1}^{N} \left(\frac{V_n^+}{C_{1n}} e^{-j\beta_n z} + \frac{V_n^-}{C_{1n}} e^{j\beta_n z} \right) \bar{e}_n(x, y), \quad (4.13a)$$

$$\bar{H}_t(x, y, z) = \sum_{n=1}^{N} \left(\frac{I_n^+}{C_{2n}} e^{-j\beta_n z} - \frac{I_n^-}{C_{2n}} e^{j\beta_n z} \right) \bar{h}_n(x, y), \quad (4.13b)$$

where $V_n^\pm$ and $I_n^\pm$ are the equivalent voltages and currents for the nth mode, and C_{1n} and C_{2n} are the proportionality constants for each mode.

EXAMPLE 4.1 EQUIVALENT VOLTAGE AND CURRENT FOR A RECTANGULAR WAVEGUIDE

Find the equivalent voltages and currents for a TE_{10} mode in a rectangular waveguide.

Solution
The transverse field components and power flow of the TE_{10} rectangular waveguide mode and the equivalent transmission line model of this mode can be written as follows:

Waveguide Fields	Transmission Line Model
$E_y = \left(A^+e^{-j\beta z} + A^-e^{j\beta z}\right)\sin(\pi x/a)$	$V(z) = V^+e^{-j\beta z} + V^-e^{j\beta z}$
$H_x = \dfrac{-1}{Z_{TE}}\left(A^+e^{-j\beta z} - A^-e^{j\beta z}\right)\sin(\pi x/a)$	$I(z) = I^+e^{-j\beta z} - I^-e^{j\beta z}$ $= \dfrac{1}{Z_0}\left(V^+e^{-j\beta z} - V^-e^{j\beta z}\right)$
$P^+ = \dfrac{-1}{2}\int_S E_y H_x^* dx\,dy = \dfrac{ab}{4Z_{TE}}\lvert A^+\rvert^2$	$P^+ = \dfrac{1}{2}V^+I^{+*}$

We now find the constants $C_1 = V^+/A^+ = V^-/A^-$ and $C_2 = I^+/A^+ = I^-/A^-$ that relate the equivalent voltages $V^\pm$ and currents $I^\pm$ to the field amplitudes, $A^\pm$. Equating incident powers gives

$$\frac{ab|A^+|^2}{4Z_{TE}} = \frac{1}{2}V^+I^{+*} = \frac{1}{2}A^+C_1C_2^*.$$

If we choose $Z_0 = Z_{TE}$, then we also have that

$$\frac{V^+}{I^+} = \frac{C_1}{C_2} = Z_{TE}.$$

Solving for C_1, C_2 gives

$$C_1 = \sqrt{\frac{ab}{2}},$$

$$C_2 = \frac{1}{Z_{TE}}\sqrt{\frac{ab}{2}},$$

which completes the transmission line equivalence for the TE_{10} mode. ■

The Concept of Impedance

We have used the idea of impedance in several different applications, so it may be useful at this point to summarize this important concept. The term *impedance* was first used by Oliver Heaviside in the nineteenth century to describe the complex ratio V/I in AC circuits consisting of resistors, inductors, and capacitors; the impedance concept quickly became indispensable in the analysis of AC circuits. It was then applied to transmission lines, in terms of lumped-element equivalent circuits and the distributed series impedance and shunt admittance of the line. In the 1930s, Schelkunoff recognized that the impedance concept could be extended to electromagnetic fields in a systematic way, and noted that impedance should be regarded as characteristic of the type of field, as well as the medium [2]. And, in relation to the analogy between transmission lines and plane wave propagation, impedance may even be dependent on direction. The concept of impedance, then, forms an important link between field theory and transmission line or circuit theory.

Below we summarize the various types of impedance we have used so far and their notation:

- $\eta = \sqrt{\mu/\epsilon}$ = intrinsic impedance of the medium. This impedance is dependent only on the material parameters of the medium, and is equal to the wave impedance for plane waves.
- $Z_w = E_t/H_t = 1/Y_w$ = wave impedance. This impedance is a characteristic of the particular type of wave. TEM, TM, and TE waves each have different wave impedances (Z_{TEM}, Z_{TM}, Z_{TE}), which may depend on the type of line or guide, the material, and the operating frequency.
- $Z_0 = 1/Y_0 = \sqrt{L/C}$ = characteristic impedance. Characteristic impedance is the ratio of voltage to current for a traveling wave on a transmission line. Since voltage and current are uniquely defined for TEM waves, the characteristic impedance of a TEM wave is unique. TE and TM waves, however, do not have a uniquely defined voltage and current, so the characteristic impedance for such waves may be defined in various ways.

EXAMPLE 4.2 APPLICATION OF WAVEGUIDE IMPEDANCE

Consider a rectangular waveguide with $a = 2.286$ cm and $b = 1.016$ cm (X-band guide), air filled for $z < 0$ and Rexolite filled ($\epsilon_r = 2.54$) for $z > 0$, as shown in Figure 4.3. If the operating frequency is 10 GHz, use an equivalent transmission line model to compute the reflection coefficient of a TE_{10} wave incident on the interface from $z < 0$.

Solution
The propagation constants in the air ($z < 0$) and the dielectric ($z > 0$) regions are

$$\beta_a = \sqrt{k_0^2 - \left(\frac{\pi}{a}\right)^2} = 158.0\ \text{m}^{-1},$$

$$\beta_d = \sqrt{\epsilon_r k_0^2 - \left(\frac{\pi}{a}\right)^2} = 304.1\ \text{m}^{-1},$$

where $k_0 = 209.4\ \text{m}^{-1}$.

The reader may verify that the TE_{10} mode is the only propagating mode in either waveguide region. Now we can set up an equivalent transmission line for the TE_{10} mode in each waveguide and treat the problem as the reflection of an incident voltage wave at the junction of two infinite transmission lines.

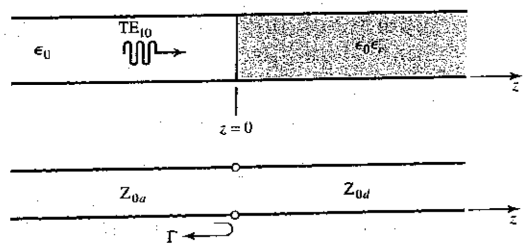

FIGURE 4.3 Geometry of a partially filled waveguide and its transmission line equivalent for Example 4.2.

By Example 4.1 and Table 3.2, the equivalent characteristic impedances for the two lines are

$$Z_{0_a} = \frac{k_0\eta_0}{\beta_a} = \frac{(209.4)(377)}{158.0} = 500.0\ \Omega,$$

$$Z_{0_d} = \frac{k\eta}{\beta_d} = \frac{k_0\eta_0}{\beta_d} = \frac{(209.4)(377)}{304.1} = 259.6\ \Omega.$$

The reflection coefficient seen looking into the dielectric filled region is then

$$\Gamma = \frac{Z_{0_d} - Z_{0_a}}{Z_{0_d} + Z_{0_a}} = -0.316.$$

With this result, expressions for the incident, reflected, and transmitted waves can be written in terms of fields, or in terms of equivalent voltages and currents. ■

We now consider the arbitrary one-port network shown in Figure 4.4, and derive a general relation between its impedance properties and electromagnetic energy stored in, and the power dissipated by, the network. The complex power delivered to this network is given by (1.91):

$$P = \frac{1}{2}\oint_S \bar{E} \times \bar{H}^* \cdot d\bar{s} = P_\ell + 2j\omega(W_m - W_e), \tag{4.14}$$

where P_ℓ is real and represents the average power dissipated by the network, and W_m and W_e represent the stored magnetic and electric energy, respectively. Note that the unit normal vector in Figure 4.4 is pointing into the volume.

If we define real transverse modal fields, $\bar{e}$ and $\bar{h}$, over the terminal plane of the network such that

$$\bar{E}_t(x, y, z) = V(z)\bar{e}(x, y)e^{-j\beta z}, \tag{4.15a}$$

$$\bar{H}_t(x, y, z) = I(z)\bar{h}(x, y)e^{-j\beta z}, \tag{4.15b}$$

with a normalization such that

$$\int_S \bar{e} \times \bar{h} \cdot d\bar{s} = 1,$$

then (4.14) can be expressed in terms of the terminal voltage and current:

$$P = \frac{1}{2}\int_S V I^* \bar{e} \times \bar{h} \cdot d\bar{s} = \frac{1}{2} V I^*. \tag{4.16}$$

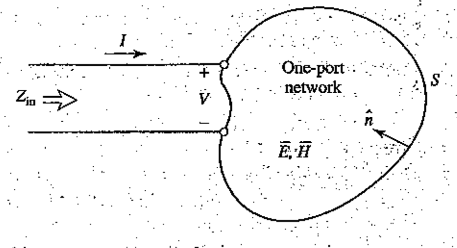

FIGURE 4.4 An arbitrary one-port network.

Then the input impedance is

$$Z_{in} = R + jX = \frac{V}{I} = \frac{VI^*}{|I|^2} = \frac{P}{\frac{1}{2}|I|^2} = \frac{P_\ell + 2j\omega(W_m - W_e)}{\frac{1}{2}|I|^2}. \tag{4.17}$$

Thus we see that the real part, R, of the input impedance is related to the dissipated power, while the imaginary part, X, is related to the net energy stored in the network. If the network is lossless, then $P_\ell = 0$ and $R = 0$. Then Z_{in} is purely imaginary, with a reactance

$$X = \frac{4\omega(W_m - W_e)}{|I|^2}, \tag{4.18}$$

which is positive for an inductive load ($W_m > W_e$), and negative for a capacitive load ($W_m < W_e$).

Even and Odd Properties of $Z(\omega)$ and $\Gamma(\omega)$

Consider the driving point impedance, $Z(\omega)$, at the input port of an electrical network. The voltage and current at this port are related as $V(\omega) = Z(\omega)I(\omega)$. For an arbitrary frequency dependence, we can find the time-domain voltage by taking the inverse Fourier transform of $V(\omega)$:

$$v(t) = \frac{1}{2\pi}\int_{-\infty}^{\infty} V(\omega)e^{j\omega t}d\omega. \tag{4.19}$$

Since $v(t)$ must be real, we have that $v(t) = v^*(t)$, or

$$\int_{-\infty}^{\infty} V(\omega)e^{j\omega t}\,d\omega = \int_{-\infty}^{\infty} V^*(\omega)e^{-j\omega t}\,d\omega = \int_{-\infty}^{\infty} V^*(-\omega)e^{j\omega t}\,d\omega,$$

where the last term was obtained by a change of variable from ω to $-\omega$. This shows that $V(\omega)$ must satisfy the relation

$$V(-\omega) = V^*(\omega), \tag{4.20}$$

which means that $\text{Re}\{V(\omega)\}$ is even in ω, while $\text{Im}\{V(\omega)\}$ is odd in ω. Similar results hold for $I(\omega)$, and for $Z(\omega)$ since

$$V^*(-\omega) = Z^*(-\omega)I^*(-\omega) = Z^*(-\omega)I(\omega) = V(\omega) = Z(\omega)I(\omega).$$

Thus, if $Z(\omega) = R(\omega) + jX(\omega)$, then $R(\omega)$ is even in ω and $X(\omega)$ is odd in ω. These results can also be inferred from (4.17).

Now consider the reflection coefficient at the input port:

$$\Gamma(\omega) = \frac{Z(\omega) - Z_0}{Z(\omega) + Z_0} = \frac{R(\omega) - Z_0 + jX(\omega)}{R(\omega) + Z_0 + jX(\omega)}. \tag{4.21}$$

Then,

$$\Gamma(-\omega) = \frac{R(\omega) - Z_0 - jX(\omega)}{R(\omega) + Z_0 - jX(\omega)} = \Gamma^*(\omega), \tag{4.22}$$

which shows that the real and imaginary parts of $\Gamma(\omega)$ are even and odd, respectively, in ω. Finally, the magnitude of the reflection coefficient is

$$|\Gamma(\omega)|^2 = \Gamma(\omega)\Gamma^*(\omega) = \Gamma(\omega)\Gamma(-\omega) = |\Gamma(-\omega)|^2, \tag{4.23}$$

which shows that $|\Gamma(\omega)|^2$ and $|\Gamma(\omega)|$ are even functions of ω. This result implies that only even series of the form $a + b\omega^2 + c\omega^4 + \cdots$ can be used to represent $|\Gamma(\omega)|$ or $|\Gamma(\omega)|^2$.

4.2 IMPEDANCE AND ADMITTANCE MATRICES

In the previous section we have seen how equivalent voltages and currents can be defined for TEM and non-TEM waves. Once such voltages and currents have been defined at various points in a microwave network, we can use the impedance and/or admittance matrices of circuit theory to relate these terminal or "port" quantities to each other, and thus to essentially arrive at a matrix description of the network. This type of representation lends itself to the development of equivalent circuits of arbitrary networks, which will be quite useful when we discuss the design of passive components such as couplers and filters.

We begin by considering an arbitrary N-port microwave network, as depicted in Figure 4.5. The ports in Figure 4.5 may be any type of transmission line or transmission line equivalent of a single propagating waveguide mode. (The term *port* was introduced by H. A. Wheeler in the 1950s to replace the less descriptive and more cumbersome phrase "two-terminal pair" [3], [2].) If one of the physical ports of the network is a waveguide supporting more than one propagating mode, additional electrical ports can be added to account for these modes. At a specific point on the nth port, a terminal plane, t_n, is defined along with equivalent voltages and currents for the incident (V_n^+, I_n^+) and reflected (V_n^-, I_n^-) waves. The terminal planes are important in providing a phase reference for the voltage and current phasors. Now at the nth terminal plane, the total voltage and current is given by

$$V_n = V_n^+ + V_n^-, \tag{4.24a}$$

$$I_n = I_n^+ - I_n^-, \tag{4.24b}$$

as seen from (4.8) when $z = 0$.

The impedance matrix $[Z]$ of the microwave network then relates these voltages and currents:

$$\begin{bmatrix} V_1 \\ V_2 \\ \vdots \\ V_N \end{bmatrix} = \begin{bmatrix} Z_{11} & Z_{12} & \cdots & Z_{1N} \\ Z_{21} & & & \vdots \\ \vdots & & & \vdots \\ Z_{N1} & \cdots & \cdots & Z_{NN} \end{bmatrix} \begin{bmatrix} I_1 \\ I_2 \\ \vdots \\ I_N \end{bmatrix},$$

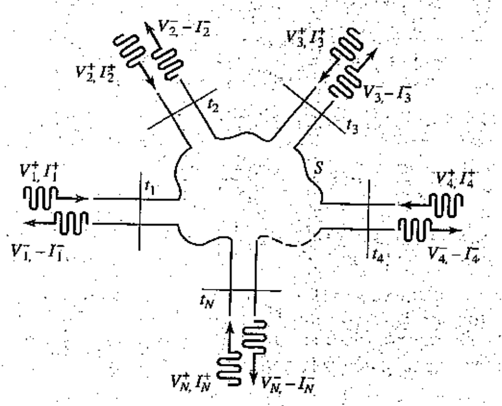

FIGURE 4.5 An arbitrary N-port microwave network.

or in matrix form as

$$[V] = [Z][I]. \tag{4.25}$$

Similarly, we can define an admittance matrix $[Y]$ as

$$\begin{bmatrix} I_1 \\ I_2 \\ \vdots \\ I_N \end{bmatrix} = \begin{bmatrix} Y_{11} & Y_{12} & \cdots & Y_{1N} \\ Y_{21} & & & \vdots \\ \vdots & & & \vdots \\ Y_{N1} & \cdots & \cdots & Y_{NN} \end{bmatrix} \begin{bmatrix} V_1 \\ V_2 \\ \vdots \\ V_N \end{bmatrix},$$

or in matrix form as

$$[I] = [Y][V]. \tag{4.26}$$

Of course, the $[Z]$ and $[Y]$ matrices are the inverses of each other:

$$[Y] = [Z]^{-1}. \tag{4.27}$$

Note that both the $[Z]$ and $[Y]$ matrices relate the total port voltages and currents.

From (4.25), we see that Z_{ij} can be found as

$$Z_{ij} = \left.\frac{V_i}{I_j}\right|_{I_k=0 \text{ for } k\neq j}. \tag{4.28}$$

In words, (4.28) states that Z_{ij} can be found by driving port j with the current I_j, open-circuiting all other ports (so $I_k = 0$ for $k \neq j$), and measuring the open-circuit voltage at port i. Thus, Z_{ii} is the input impedance seen looking into port i when all other ports are open-circuited, and Z_{ij} is the transfer impedance between ports i and j when all other ports are open-circuited.

Similarly, from (4.26), Y_{ij} can be found as

$$Y_{ij} = \left.\frac{I_i}{V_j}\right|_{V_k=0 \text{ for } k\neq j}, \tag{4.29}$$

which states that Y_{ij} can be determined by driving port j with the voltage V_j, short-circuiting all other ports (so $V_k = 0$ for $k \neq j$), and measuring the short-circuit current at port i.

In general, each Z_{ij} or Y_{ij} element may be complex. For an arbitrary N-port network, the impedance and admittance matrices are $N \times N$ in size, so there are $2N^2$ independent quantities or degrees of freedom. In practice, however, many networks are either reciprocal or lossless, or both. If the network is reciprocal (not containing any nonreciprocal media such as ferrites or plasmas, or active devices), we will show that the impedance and admittance matrices are symmetric, so that $Z_{ij} = Z_{ji}$, and $Y_{ij} = Y_{ji}$. If the network is lossless, we can show that all the Z_{ij} or Y_{ij} elements are purely imaginary. Either of these special cases serves to reduce the number of independent quantities or degrees of freedom that an N-port network may have. We now derive the above characteristics for reciprocal and lossless networks.

Reciprocal Networks

Consider the arbitrary network of Figure 4.5 to be reciprocal (no active devices, ferrites, or plasmas), with short circuits placed at all terminal planes except those of ports 1 and 2. Now let $\bar{E}_a$, $\bar{H}_a$ and $\bar{E}_b$, $\bar{H}_b$ be the fields anywhere in the network due to two independent sources, a and b, located somewhere in the network. Then the reciprocity theorem of (1.156) states that

$$\oint_S \bar{E}_a \times \bar{H}_b \cdot d\bar{s} = \oint_S \bar{E}_b \times \bar{H}_a \cdot d\bar{s}, \tag{4.30}$$

where we will take S as the closed surface along the boundaries of the network and through the terminal planes of the ports. If the boundary walls of the network and transmission lines are metal, then $\bar{E}_{\tan} = 0$ on these walls (assuming perfect conductors). If the network or the transmission lines are open structures, like microstrip or slotline, the boundaries of the network can be taken arbitrarily far from the lines so that $\bar{E}_{\tan}$ is negligible. Then the only nonzero contribution to the integrals of (4.30) come from the cross-sectional areas of ports 1 and 2.

From Section 4.1, the fields due to sources a and b can be evaluated at the terminal planes t_1 and t_2 as

$$\begin{aligned} \bar{E}_{1a} &= V_{1a}\bar{e}_1 & \bar{H}_{1a} &= I_{1a}\bar{h}_1 \\ \bar{E}_{1b} &= V_{1b}\bar{e}_1 & \bar{H}_{1b} &= I_{1b}\bar{h}_1 \\ \bar{E}_{2a} &= V_{2a}\bar{e}_2 & \bar{H}_{2a} &= I_{2a}\bar{h}_2 \\ \bar{E}_{2b} &= V_{2b}\bar{e}_2 & \bar{H}_{2b} &= I_{2b}\bar{h}_2, \end{aligned} \tag{4.31}$$

where $\bar{e}_1, \bar{h}_1$ and $\bar{e}_2, \bar{h}_2$ are the transverse modal fields of ports 1 and 2, respectively, and the Vs and Is are the equivalent total voltages and currents. (For instance, $\bar{E}_{1b}$ is the transverse electric field at terminal plane t_1 of port 1 due to source b.) Substituting the fields of (4.31) into (4.30) gives

$$(V_{1a}I_{1b} - V_{1b}I_{1a}) \int_{S_1} \bar{e}_1 \times \bar{h}_1 \cdot d\bar{s} + (V_{2a}I_{2b} - V_{2b}I_{2a}) \int_{S_2} \bar{e}_2 \times \bar{h}_2 \cdot d\bar{s} = 0, \tag{4.32}$$

where S_1, S_2 are the cross-sectional areas at the terminal planes of ports 1 and 2.

As in Section 4.1, the equivalent voltages and currents have been defined so that the power through a given port can be expressed as $VI^*/2$; then comparing (4.31) to (4.6) implies that $C_1 = C_2 = 1$ for each port, so that

$$\int_{S_1} \bar{e}_1 \times \bar{h}_1 \cdot d\bar{s} = \int_{S_2} \bar{e}_2 \times \bar{h}_2 \cdot d\bar{s} = 1. \tag{4.33}$$

This reduces (4.32) to

$$V_{1a}I_{1b} - V_{1b}I_{1a} + V_{2a}I_{2b} - V_{2b}I_{2a} = 0. \tag{4.34}$$

Now use the 2×2 admittance matrix of the (effectively) two-port network to eliminate the Is:

$$\begin{aligned} I_1 &= Y_{11}V_1 + Y_{12}V_2, \\ I_2 &= Y_{21}V_1 + Y_{22}V_2. \end{aligned}$$

Substitution into (4.34) gives

$$(V_{1a}V_{2b} - V_{1b}V_{2a})(Y_{12} - Y_{21}) = 0. \tag{4.35}$$

Since the sources a and b are independent, the voltages V_{1a}, V_{1b}, V_{2a}, and V_{2b} can take on arbitrary values. So in order for (4.35) to be satisfied for any choice of sources, we must have $Y_{12} = Y_{21}$, and since the choice of which ports are labeled as 1 and 2 is arbitrary, we have the general result that

$$Y_{ij} = Y_{ji}. \tag{4.36}$$

Then if $[Y]$ is a symmetric matrix, its inverse, $[Z]$, is also symmetric.

Lossless Networks

Now consider a reciprocal lossless N-port junction; we will show that the elements of the impedance and admittance matrices must be pure imaginary. If the network is lossless, then the net real power delivered to the network must be zero. Thus, $\mathrm{Re}\{P_{av}\} = 0$, where

$$\begin{aligned} P_{av} &= \frac{1}{2}[V]^t[I]^* = \frac{1}{2}([Z][I])^t[I]^* = \frac{1}{2}[I]^t[Z][I]^* \\ &= \frac{1}{2}(I_1 Z_{11} I_1^* + I_1 Z_{12} I_2^* + I_2 Z_{21} I_1^* + \cdots) \\ &= \frac{1}{2}\sum_{n=1}^{N}\sum_{m=1}^{N} I_m Z_{mn} I_n^*. \end{aligned} \tag{4.37}$$

(We have used the result from matrix algebra that $([A][B])^t = [B]^t[A]^t$.) Since the I_ns are independent, we must have the real part of each self term $(I_n Z_{nn} I_n^*)$ equal to zero, since we could set all port currents equal to zero except for the nth current. So,

$$\mathrm{Re}\{I_n Z_{nn} I_n^*\} = |I_n|^2 \mathrm{Re}\{Z_{nn}\} = 0,$$

or

$$\mathrm{Re}\{Z_{nn}\} = 0. \tag{4.38}$$

Now let all port currents be zero except for I_m and I_n. Then (4.37) reduces to

$$\mathrm{Re}\{(I_n I_m^* + I_m I_n^*) Z_{mn}\} = 0,$$

since $Z_{mn} = Z_{nm}$. But $(I_n I_m^* + I_m I_n^*)$ is a purely real quantity which is, in general, nonzero. Thus we must have that

$$\mathrm{Re}\{Z_{mn}\} = 0. \tag{4.39}$$

Then (4.38) and (4.39) imply that $\mathrm{Re}\{Z_{mn}\} = 0$ for any m, n. The reader can verify that this also leads to an imaginary $[Y]$ matrix.

EXAMPLE 4.3 EVALUATION OF IMPEDANCE PARAMETERS

Find the Z parameters of the two-port T-network shown in Figure 4.6.

Solution

From (4.28), Z_{11} can be found as the input impedance of port 1 when port 2 is open-circuited:

$$Z_{11} = \left.\frac{V_1}{I_1}\right|_{I_2=0} = Z_A + Z_C.$$

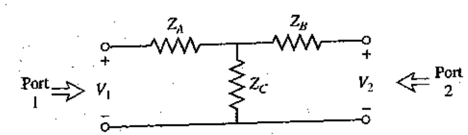

FIGURE 4.6 A two-port T-network.

The transfer impedance Z_{12} can be found measuring the open-circuit voltage at port 1 when a current I_2 is applied at port 2. By voltage division,

$$Z_{12} = \left.\frac{V_1}{I_2}\right|_{I_1=0} = \frac{V_2}{I_2}\frac{Z_C}{Z_B + Z_C} = Z_C.$$

The reader can verify that $Z_{21} = Z_{12}$, indicating that the circuit is reciprocal. Finally, Z_{22} is found as

$$Z_{22} = \left.\frac{V_2}{I_2}\right|_{I_1=0} = Z_B + Z_C.$$

■

4.3 THE SCATTERING MATRIX

We have already discussed the difficulty in defining voltages and currents for non-TEM lines. In addition, a practical problem exists when trying to measure voltages and currents at microwave frequencies because direct measurements usually involve the magnitude (inferred from power) and phase of a wave traveling in a given direction, or of a standing wave. Thus, equivalent voltages and currents, and the related impedance and admittance matrices, become somewhat of an abstraction when dealing with high-frequency networks. A representation more in accord with direct measurements, and with the ideas of incident, reflected, and transmitted waves, is given by the scattering matrix.

Like the impedance or admittance matrix for an N-port network, the scattering matrix provides a complete description of the network as seen at its N ports. While the impedance and admittance matrices relate the total voltages and currents at the ports, the scattering matrix relates the voltage waves incident on the ports to those reflected from the ports. For some components and circuits, the scattering parameters can be calculated using network analysis techniques. Otherwise, the scattering parameters can be measured directly with a vector network analyzer; a photograph of a modern network analyzer is shown in Figure 4.7. Once the scattering parameters of the network are known, conversion to other matrix parameters can be performed, if needed.

Consider the N-port network shown in Figure 4.5, where V_n^+ is the amplitude of the voltage wave incident on port n, and V_n^- is the amplitude of the voltage wave reflected from port n. The scattering matrix, or $[S]$ matrix, is defined in relation to these incident and reflected voltage waves as

$$\begin{bmatrix} V_1^- \\ V_2^- \\ \vdots \\ V_N^- \end{bmatrix} = \begin{bmatrix} S_{11} & S_{12} & \cdots & S_{1N} \\ S_{21} & & & \vdots \\ \vdots & & & \\ S_{N1} & \cdots & & S_{NN} \end{bmatrix} \begin{bmatrix} V_1^+ \\ V_2^+ \\ \vdots \\ V_N^+ \end{bmatrix},$$

or

$$[V^-] = [S][V^+]. \tag{4.40}$$

A specific element of the $[S]$ matrix can be determined as

$$S_{ij} = \left.\frac{V_i^-}{V_j^+}\right|_{V_k^+=0 \text{ for } k\neq j}. \tag{4.41}$$

In words, (4.41) says that S_{ij} is found by driving port j with an incident wave of voltage V_j^+, and measuring the reflected wave amplitude, V_i^-, coming out of port i. The incident waves on all ports except the jth port are set to zero, which means that all ports should be terminated in matched loads to avoid reflections. Thus, S_{ii} is the reflection coefficient seen looking into port i when all other ports are terminated in matched loads, and S_{ij} is the transmission coefficient from port j to port i when all other ports are terminated in matched loads.

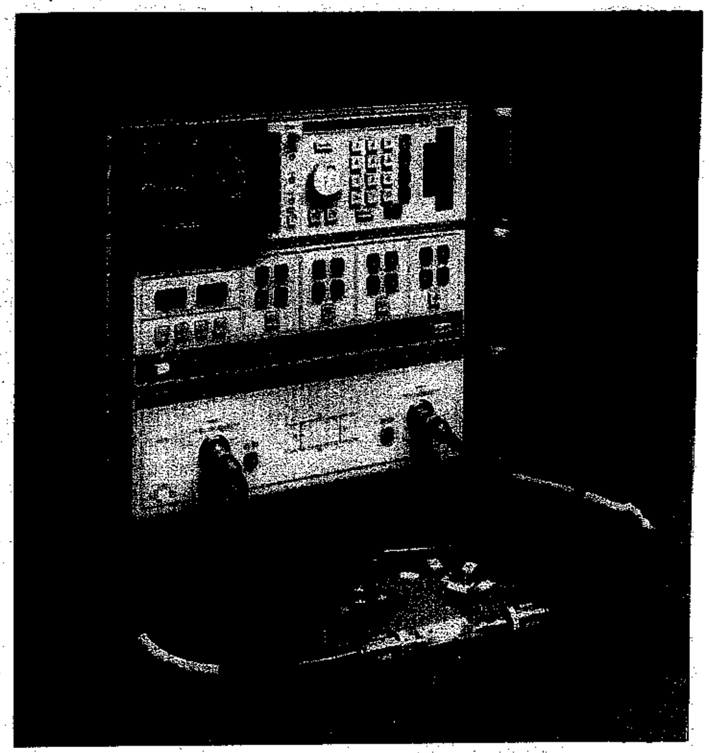

FIGURE 4.7 A photograph of the Hewlett-Packard HP8510B Network Analyzer. This test instrument is used to measure the scattering parameters (magnitude and phase) of a one- or two-port microwave network from 0.05 GHz to 26.5 GHz. Built-in microprocessors provide error correction, a high degree of accuracy, and a wide choice of display formats. This analyzer can also perform a fast Fourier transform of the frequency domain data to provide a time domain response of the network under test.
Courtesy of Agilent Technologies, Santa Rosa, Calif.

EXAMPLE 4.4 EVALUATION OF SCATTERING PARAMETERS

Find the S parameters of the 3 dB attenuator circuit shown in Figure 4.8.

Solution
From (4.41), S_{11} can be found as the reflection coefficient seen at port 1 when port 2 is terminated in a matched load ($Z_0 = 50\ \Omega$):

$$S_{11} = \left.\frac{V_1^-}{V_1^+}\right|_{V_2^+=0} = \Gamma^{(1)}|_{V_2^+=0} = \left.\frac{Z_{in}^{(1)} - Z_0}{Z_{in}^{(1)} + Z_0}\right|_{Z_0 \text{ on port } 2},$$

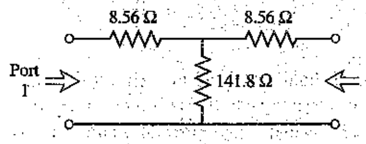

FIGURE 4.8 A matched 3 dB attenuator with a 50 Ω characteristic impedance (Example

but, $Z_{in}^{(1)} = 8.56 + [141.8(8.56 + 50)]/(141.8 + 8.56 + 50) = 50\ \Omega$, so $S_{11} = 0$. Because of the symmetry of the circuit, $S_{22} = 0$.

S_{21} can be found by applying an incident wave at port 1, V_1^+, and measuring the outcoming wave at port 2, V_2^-. This is equivalent to the transmission coefficient from port 1 to port 2:

$$S_{21} = \left.\frac{V_2^-}{V_1^+}\right|_{V_2^+=0}.$$

From the fact that $S_{11} = S_{22} = 0$, we know that $V_1^- = 0$ when port 2 is terminated in $Z_0 = 50\ \Omega$, and that $V_2^+ = 0$. In this case we then have that $V_1^+ = V_1$ and $V_2^- = V_2$. So by applying a voltage V_1 at port 1 and using voltage division twice we find $V_2^- = V_2$ as the voltage across the 50 Ω load resistor at port 2:

$$V_2^- = V_2 = V_1\left(\frac{41.44}{41.44 + 8.56}\right)\left(\frac{50}{50 + 8.56}\right) = 0.707V_1,$$

where $41.44 = 141.8(58.56)/(141.8 + 58.56)$ is the resistance of the parallel combination of the 50 Ω load and the 8.56 Ω resistor with the 141.8 Ω resistor. Thus, $S_{12} = S_{21} = 0.707$.

If the input power is $|V_1^+|^2/2Z_0$, then the output power is $|V_2^-|^2/2Z_0 = |S_{21}V_1^+|^2/2Z_0 = |S_{21}|^2/2Z_0|V_1^+|^2 = |V_1^+|^2/4Z_0$, which is one-half (−3 dB) of the input power. ■

We now show how the $[S]$ matrix can be determined from the $[Z]$ (or $[Y]$) matrix and vice versa. First, we must assume that the characteristic impedances, Z_{0n}, of all ports are identical. (This restriction will be removed when we discuss generalized scattering parameters.) Then for convenience, we can set $Z_{0n} = 1$. From (4.24) the total voltage and current at the nth port can be written as

$$V_n = V_n^+ + V_n^-, \quad (4.4$$

$$I_n = I_n^+ - I_n^- = V_n^+ - V_n^-. \quad (4.4$$

Using the definition of $[Z]$ from (4.25) with (4.42) gives

$$[Z][I] = [Z][V^+] - [Z][V^-] = [V] = [V^+] + [V^-],$$

which can be rewritten as

$$([Z] + [U])[V^-] = ([Z] - [U])[V^+], \quad (4.4$$

where $[U]$ is the unit, or identity, matrix defined as

$$[U] = \begin{bmatrix} 1 & 0 & \cdots & 0 \\ 0 & 1 & & \vdots \\ \vdots & & \ddots & \\ 0 & & \cdots & 1 \end{bmatrix}.$$

Comparing (4.43) to (4.40) suggests that

$$[S] = ([Z] + [U])^{-1}([Z] - [U]), \quad (4.44)$$

giving the scattering matrix in terms of the impedance matrix. Note that for a one-port network (4.44) reduces to

$$S_{11} = \frac{z_{11} - 1}{z_{11} + 1},$$

in agreement with the result for the reflection coefficient seen looking into a load with a normalized input impedance of z_{11}.

To find $[Z]$ in terms of $[S]$, rewrite (4.44) as $[Z][S] + [U][S] = [Z] - [U]$, and solve for $[Z]$ to give

$$[Z] = ([U] + [S])([U] - [S])^{-1}. \quad (4.45)$$

Reciprocal Networks and Lossless Networks

As we discussed in Section 4.2, the impedance and admittance matrices are symmetric for reciprocal networks, and purely imaginary for lossless networks. Similarly, the scattering matrices for these types of networks have special properties. We will show that the $[S]$ matrix for a reciprocal network is symmetric, and that the $[S]$ matrix for a lossless network is unitary.

By adding (4.42a) and (4.42b) we obtain

$$V_n^+ = \frac{1}{2}(V_n + I_n),$$

or

$$[V^+] = \frac{1}{2}([Z] + [U])[I]. \quad (4.46a)$$

By subtracting (4.42a) and (4.42b) we obtain

$$V_n^- = \frac{1}{2}(V_n - I_n),$$

or

$$[V^-] = \frac{1}{2}([Z] - [U])[I]. \quad (4.46b)$$

Eliminating $[I]$ from (4.46a) and (4.46b) gives

$$[V^-] = ([Z] - [U])([Z] + [U])^{-1}[V^+],$$

so that

$$[S] = ([Z] - [U])([Z] + [U])^{-1}. \quad (4.47)$$

Taking the transpose of (4.47) gives

$$[S]^t = \left\{([Z] + [U])^{-1}\right\}^t([Z] - [U])^t.$$

Now $[U]$ is diagonal, so $[U]^t = [U]$; and if the network is reciprocal, $[Z]$ is symmetric so that $[Z]^t = [Z]$. The above then reduces to

$$[S]^t = ([Z] + [U])^{-1}([Z] - [U]),$$

which is equivalent to (4.44). We have thus shown that

$$[S] = [S]^t,$$

for reciprocal networks.

If the network is lossless, then no real power can be delivered to the network. Thus, if the characteristic impedances of all the ports are identical and assumed to be unity, the average power delivered to the network is

$$P_{av} = \frac{1}{2}\mathrm{Re}\{[V]^t[I]^*\} = \frac{1}{2}\mathrm{Re}\{([V^+]^t + [V^-]^t)([V^+]^* - [V^-]^*)\}$$

$$= \frac{1}{2}\mathrm{Re}\{[V^+]^t[V^+]^* - [V^+]^t[V^-]^* + [V^-]^t[V^+]^* - [V^-]^t[V^-]^*\}$$

$$= \frac{1}{2}[V^+]^t[V^+]^* - \frac{1}{2}[V^-]^t[V^-]^* = 0, \quad (4$$

since the terms $-[V^+]^t[V^-]^* + [V^-]^t[V^+]^*$ are of the form $A - A^*$, and so are purely imaginary. Of the remaining terms in (4.49), $(1/2)[V^+]^t[V^+]^*$ represents the total incident power, while $(1/2)[V^-]^t[V^-]^*$ represents the total reflected power. So for a lossless junction, we have the intuitive result that the incident and reflected powers are equal:

$$[V^+]^t[V^+]^* = [V^-]^t[V^-]^*. \quad (4$$

Using $[V^-] = [S][V^+]$ in (4.50) gives

$$[V^+]^t[V^+]^* = [V^+]^t[S]^t[S]^*[V^+]^*,$$

so that, for nonzero $[V^+]$,

$$[S]^t[S]^* = [U],$$

or

$$[S]^* = \{[S]^t\}^{-1}. \quad (4$$

A matrix that satisfies the condition of (4.51) is called a *unitary matrix*.

The matrix equation of (4.51) can be written in summation form as

$$\sum_{k=1}^{N} S_{ki}S_{kj}^* = \delta_{ij}, \quad \text{for all } i, j, \quad (4$$

where $\delta_{ij} = 1$ if $i = j$ and $\delta_{ij} = 0$ if $i \neq j$ is the Kronecker delta symbol. Thus, if $i = j$, (4.52) reduces to

$$\sum_{k=1}^{N} S_{ki}S_{ki}^* = 1, \quad (4.5$$

while if $i \neq j$ (4.52) reduces to

$$\sum_{k=1}^{N} S_{ki}S_{kj}^* = 0, \quad \text{for } i \neq j. \quad (4.5$$

In words, (4.53a) states that the dot product of any column of $[S]$ with the conjugate of that column gives unity, while (4.53b) states that the dot product of any column with the conjugate of a different column gives zero (orthogonal). If the network is reciprocal, then $[S]$ is symmetric, and the same statements can be made about the rows of the scattering matrix.

EXAMPLE 4.5 APPLICATION OF SCATTERING PARAMETERS

A two-port network is known to have the following scattering matrix:

$$[S] = \begin{bmatrix} 0.15\angle 0° & 0.85\angle -45° \\ 0.85\angle 45° & 0.2\angle 0° \end{bmatrix}$$

Determine if the network is reciprocal, and lossless. If port two is terminated with a matched load, what is the return loss seen at port 1? If port two is terminated with a short circuit, what is the return loss seen at port 1?

Solution

Since $[S]$ is not symmetric, the network is not reciprocal. To be lossless, the S parameters must satisfy (4.53). Taking the first column ($i = 1$ in (4.53a)) gives

$$|S_{11}|^2 + |S_{21}|^2 = (0.15)^2 + (0.85)^2 = 0.745 \neq 1,$$

so the network is not lossless.

When port 2 is terminated with a matched load, the reflection coefficient seen at port 1 is $\Gamma = S_{11} = 0.15$. So the return loss is

$$RL = -20\log|\Gamma| = -20\log(0.15) = 16.5 \text{ dB}.$$

When port 2 is terminated with a short circuit, the reflection coefficient seen at port 1 can be found as follows. From the definition of the scattering matrix and the fact that $V_2^+ = -V_2^-$ (for a short circuit at port 2), we can write

$$V_1^- = S_{11}V_1^+ + S_{12}V_2^+ = S_{11}V_1^+ - S_{12}V_2^-,$$

$$V_2^- = S_{21}V_1^+ + S_{22}V_2^+ = S_{21}V_1^+ - S_{22}V_2^-.$$

The second equation gives

$$V_2^- = \frac{S_{21}}{1 + S_{22}}V_1^+.$$

Dividing the first equation by V_1^+ and using the above result gives the reflection coefficient seen at port 1 as

$$\Gamma = \frac{V_1^-}{V_1^+} = S_{11} - S_{12}\frac{V_2^-}{V_1^+} = S_{11} - \frac{S_{12}S_{21}}{1 + S_{22}}$$

$$= 0.15 - \frac{(0.85\angle -45°)(0.85\angle 45°)}{1 + 0.2} = -0.452.$$

So the return loss is $RL = -20\log|\Gamma| = -20\log(0.452) = 6.9$ dB. ∎

An important point to understand about S parameters is that the reflection coefficient looking into port n is not equal to S_{nn}, unless all other ports are matched (this is illustrated in the above example). Similarly, the transmission coefficient from port m to port n is not equal to S_{nm}, unless all other ports are matched. The S parameters of a network are properties only of the network itself (assuming the network is linear), and are defined under the condition

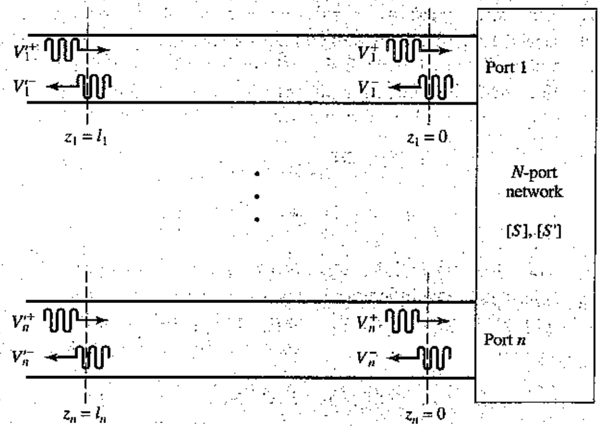

FIGURE 4.9 Shifting reference planes for an N-port network.

that all ports are matched. Changing the terminations or excitations of a network does not change its S parameters, but may change the reflection coefficient seen at a given port, or the transmission coefficient between two ports.

A Shift in Reference Planes

Because the S parameters relate amplitudes (magnitude and phase) of traveling waves incident on and reflected from a microwave network, phase reference planes must be specified for each port of the network. We now show how the S parameters are transformed when the reference planes are moved from their original locations.

Consider the N-port microwave network shown in Figure 4.9, where the original terminal planes are assumed to be located at $z_n = 0$ for the nth port, and where z_n is an arbitrary coordinate measured along the transmission line feeding the nth port. The scattering matrix for the network with this set of terminal planes is denoted by $[S]$. Now consider a new set of reference planes defined at $z_n = \ell_n$, for the nth port, and let the new scattering matrix be denoted as $[S']$. Then in terms of the incident and reflected port voltages we have that

$$[V^-] = [S][V^+], \tag{4.54a}$$

$$[V'^-] = [S'][V'^+], \tag{4.54b}$$

where the unprimed quantities are referenced to the original terminal planes at $z_n = 0$, and the primed quantities are referenced to the new terminal planes at $z_n = \ell_n$.

Now from the theory of traveling waves on lossless transmission lines we can relate the new wave amplitudes to the original ones as

$$V_n'^+ = V_n^+ e^{j\theta_n}, \tag{4.55a}$$

$$V_n'^- = V_n^- e^{-j\theta_n}, \tag{4.55b}$$

where $\theta_n = \beta_n \ell_n$ is the electrical length of the outward shift of the reference plane of port n.

Writing (4.55) in matrix form and substituting into (4.54a) gives

$$\begin{bmatrix} e^{j\theta_1} & & & 0 \\ & e^{j\theta_2} & & \\ & & \ddots & \\ 0 & & & e^{j\theta_N} \end{bmatrix} [V'^-] = [S] \begin{bmatrix} e^{-j\theta_1} & & & 0 \\ & e^{-j\theta_2} & & \\ & & \ddots & \\ 0 & & & e^{-j\theta_N} \end{bmatrix} [V'^+].$$

Multiplying by the inverse of the first matrix on the left gives

$$[V'^-] = \begin{bmatrix} e^{-j\theta_1} & & & 0 \\ & e^{-j\theta_2} & & \\ & & \ddots & \\ 0 & & & e^{-j\theta_N} \end{bmatrix} [S] \begin{bmatrix} e^{-j\theta_1} & & & 0 \\ & e^{-j\theta_2} & & \\ & & \ddots & \\ 0 & & & e^{-j\theta_N} \end{bmatrix} [V'^+].$$

Comparing with (4.54b) shows that

$$[S'] = \begin{bmatrix} e^{-j\theta_1} & & & 0 \\ & e^{-j\theta_2} & & \\ & & \ddots & \\ 0 & & & e^{-j\theta_N} \end{bmatrix} [S] \begin{bmatrix} e^{-j\theta_1} & & & 0 \\ & e^{-j\theta_2} & & \\ & & \ddots & \\ 0 & & & e^{-j\theta_N} \end{bmatrix}, \tag{4.56}$$

which is the desired result. Note that $S'_{nn} = e^{-2j\theta_n} S_{nn}$, meaning that the phase of S_{nn} is shifted by twice the electrical length of the shift in terminal plane n, because the wave travels twice over this length upon incidence and reflection.

Generalized Scattering Parameters

So far we have considered the scattering parameters for networks with the same characteristic impedance for all ports. This is the case in many practical situations, where the characteristic impedance is often 50 Ω. In other cases, however, the characteristic impedances of a multiport network may be different, which requires a generalization of the scattering parameters as defined up to this point.

Consider the N-port network shown in Figure 4.10, where Z_{0n} is the (real) characteristic impedance of the nth port, and V_n^+ and V_n^-, respectively, represent the incident and reflected voltage waves at port n. In order to obtain physically meaningful power relations in terms

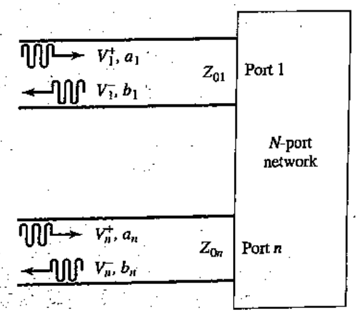

FIGURE 4.10 An N-port network with different characteristic impedances.

of wave amplitudes, we must define a new set of wave amplitudes as

$$a_n = V_n^+/\sqrt{Z_{0n}}, \quad (4.57a)$$

$$b_n = V_n^-/\sqrt{Z_{0n}}, \quad (4.57b)$$

where a_n represents an incident wave at the nth port, and b_n represents a reflected wave from that port [1], [5]. Then from (4.42a,b) we have that

$$V_n = V_n^+ + V_n^- = \sqrt{Z_{0n}}(a_n + b_n), \quad (4.58a)$$

$$I_n = \frac{1}{Z_{0n}}(V_n^+ - V_n^-) = \frac{1}{\sqrt{Z_{0n}}}(a_n - b_n). \quad (4.58b)$$

Now the average power delivered to the nth port is

$$P_n = \frac{1}{2}\text{Re}\{V_n I_n^*\} = \frac{1}{2}\text{Re}\{|a_n|^2 - |b_n|^2 + (b_n a_n^* - b_n^* a_n)\} = \frac{1}{2}|a_n|^2 - \frac{1}{2}|b_n|^2, \quad (4.59)$$

since the quantity $(b_n a_n^* - b_n^* a_n)$ is purely imaginary. This is a physically satisfying result, since it says that the average power delivered through port n is equal to the power in the incident wave minus the power in the reflected wave. If expressed in terms of V_n^+ and V_n^-, the corresponding result would be dependent on the characteristic impedance of the nth port.

A generalized scattering matrix can then be used to relate the incident and reflected waves defined in (4.57):

$$[b] = [S][a], \quad (4.60)$$

where the i, jth element of the scattering matrix is given by

$$S_{ij} = \left.\frac{b_i}{a_j}\right|_{a_k=0 \text{ for } k\neq j}, \quad (4.61)$$

and is analogous to the result of (4.41) for networks with identical characteristic impedance at all ports. Using (4.57) in (4.61) gives

$$S_{ij} = \left.\frac{V_i^-\sqrt{Z_{0j}}}{V_j^+\sqrt{Z_{0i}}}\right|_{V_k^+=0 \text{ for } k\neq j}, \quad (4.62)$$

which shows how the S parameters of a network with equal characteristic impedance $(V_i^-/V_j^+$ with $V_k^+ = 0$ for $k \neq j)$ can be converted to a network connected to transmission lines with unequal characteristic impedances.

POINT OF INTEREST: The Vector Network Analyzer

The S parameters of passive and active networks can be measured with a vector network analyzer, which is a two- (or four-) channel microwave receiver designed to process the magnitude and phase of the transmitted and reflected waves from the network. A simplified block diagram of a network analyzer similar to the HP8510 system is shown below. In operation, the RF source is usually set to sweep over a specified bandwidth. A four-port reflectometer samples the incident, reflected, and transmitted RF waves; a switch allows the network to be driven from either port 1 or port 2. Four dual-conversion channels convert these signals to 100 kHz IF frequencies, which are then detected and converted to digital form. A powerful internal computer is used to calculate

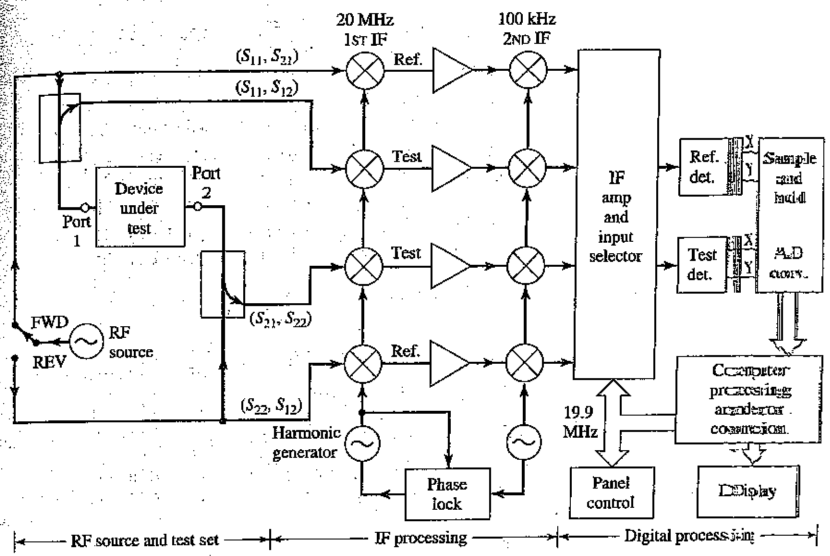

and display the magnitude and phase of the S parameters, or other quantities that can be derived from the S parameters, such as SWR, return loss, group delay, impedance, etc. An important feature of this network analyzer is the substantial improvement in accuracy made possible with error correcting software. Errors caused by directional coupler mismatch, imperfect directivity, loss, and variations in the frequency response of the analyzer system are accounted for by using a twelve-term error model and a calibration procedure. Another useful feature is the capability to determine the time domain response of the network by calculating the inverse Fourier transform of the frequency domain data.

4.4 THE TRANSMISSION (ABCD) MATRIX

The Z, Y, and S parameter representations can be used to characterize a microwave network with an arbitrary number of ports, but in practice many microwave networks consist of a cascade connection of two or more two-port networks. In this case it is convenient to define a 2×2 transmission, or $ABCD$ matrix, for each two-port network. We will then see that the $ABCD$ matrix of the cascade connection of two or more two-port networks can be easily found by multiplying the $ABCD$ matrices of the individual two-ports.

The $ABCD$ matrix is defined for a two-port network in terms of the total voltages and currents as shown in Figure 4.11a and the following:

$$V_1 = AV_2 + BI_2,$$
$$I_1 = CV_2 + DI_2,$$

or in matrix form as

$$\begin{bmatrix} V_1 \\ I_1 \end{bmatrix} = \begin{bmatrix} A & B \\ C & D \end{bmatrix}\begin{bmatrix} V_2 \\ I_2 \end{bmatrix}. \quad (4.63)$$

It is important to note from Figure 4.11a that a change in the sign convention of I_2 has been made from our previous definitions, which had I_2 as the current flowing into port 2.

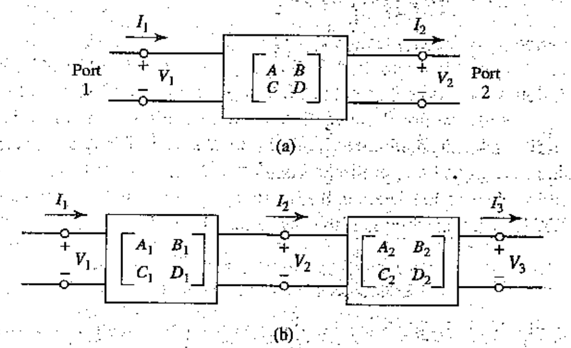

FIGURE 4.11 (a) A two-port network; (b) a cascade connection of two-port networks.

The convention that I_2 flows *out* of port 2 will be used when dealing with *ABCD* matrices so that in a cascade network I_2 will be the same current that flows into the adjacent network, as shown in Figure 4.11b. Then the left-hand side of (4.63) represents the voltage and current at port 1 of the network, while the column on the right-hand side of (4.63) represents the voltage and current at port 2.

In the cascade connection of two two-port networks shown in Figure 4.11b, we have that

$$\begin{bmatrix} V_1 \\ I_1 \end{bmatrix} = \begin{bmatrix} A_1 & B_1 \\ C_1 & D_1 \end{bmatrix} \begin{bmatrix} V_2 \\ I_2 \end{bmatrix}, \tag{4.64a}$$

$$\begin{bmatrix} V_2 \\ I_2 \end{bmatrix} = \begin{bmatrix} A_2 & B_2 \\ C_2 & D_2 \end{bmatrix} \begin{bmatrix} V_3 \\ I_3 \end{bmatrix}. \tag{4.64b}$$

Substituting (4.64b) into (4.64a) gives

$$\begin{bmatrix} V_1 \\ I_1 \end{bmatrix} = \begin{bmatrix} A_1 & B_1 \\ C_1 & C_1 \end{bmatrix} \begin{bmatrix} A_2 & B_2 \\ C_2 & D_2 \end{bmatrix} \begin{bmatrix} V_3 \\ I_3 \end{bmatrix}, \tag{4.65}$$

which shows that the *ABCD* matrix of the cascade connection of the two networks is equal to the product of the *ABCD* matrices representing the individual two-ports. Note that the order of multiplication of the matrix must be the same as the order in which the networks are arranged, since matrix multiplication is not, in general, commutative.

The usefulness of the *ABCD* matrix representation lies in the fact that a library of *ABCD* matrices for elementary two-port networks can be built up, and applied in building-block fashion to more complicated microwave networks that consist of cascades of these simpler two-ports. Table 4.1 lists a number of useful two-port networks and their *ABCD* matrices.

EXAMPLE 4.6 EVALUATION OF *ABCD* PARAMETERS

Find the *ABCD* parameters of a two-port network consisting of a series impedance Z between ports 1 and 2 (the first entry in Table 4.1).

Solution

From the defining relations of (4.63), we have that

$$A = \left.\frac{V_1}{V_2}\right|_{I_2=0},$$

which indicates that A is found by applying a voltage V_1 at port 1, and measuring

TABLE 4.1 The *ABCD* Parameters of Some Useful Two-Port Circuits

Circuit	*ABCD* Parameters	
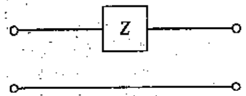	$A = 1$ $C = 0$	$B = Z$ $D = 1$
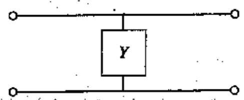	$A = 1$ $C = Y$	$B = 0$ $D = 1$
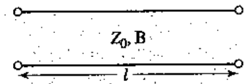	$A = \cos\beta\ell$ $C = jY_0 \sin\beta\ell$	$B = jZ_0 \sin\beta\ell$ $D = \cos\beta\ell$
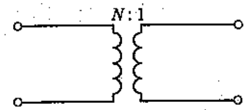	$A = N$ $C = 0$	$B = 0$ $D = \frac{1}{N}$
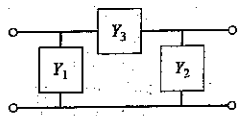	$A = 1 + \frac{Y_2}{Y_3}$ $C = Y_1 + Y_2 + \frac{Y_1 Y_2}{Y_3}$	$B = \frac{1}{Y_3}$ $D = 1 + \frac{Y_1}{Y_3}$
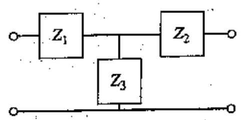	$A = 1 + \frac{Z_1}{Z_3}$ $C = \frac{1}{Z_3}$	$B = Z_1 + Z_2 + \frac{Z_1 Z_2}{Z_3}$ $D = 1 + \frac{Z_2}{Z_3}$

the open-circuit voltage V_2 at port 2. Thus, $A = 1$. Similarly,

$$B = \left.\frac{V_1}{I_2}\right|_{V_2=0} = \frac{V_1}{V_1/Z} = Z,$$

$$C = \left.\frac{I_1}{V_2}\right|_{I_2=0} = 0,$$

$$D = \left.\frac{I_1}{I_2}\right|_{V_2=0} = \frac{I_1}{I_1} = 1.$$

Relation to Impedance Matrix

Knowing the Z parameters of a network, one can determine the *ABCD* parameters. Thus, from the definition of the *ABCD* parameters in (4.63), and from the defining relations for the Z parameters of (4.25) for a two-port network with I_2 to be consistent with the sign convention used with *ABCD* parameters,

$$V_1 = I_1 Z_{11} - I_2 Z_{12}, \tag{4.66a}$$

$$V_2 = I_1 Z_{21} - I_2 Z_{22}, \tag{4.66b}$$

we have that

$$A = \left.\frac{V_1}{V_2}\right|_{I_2=0} = \frac{I_1 Z_{11}}{I_1 Z_{21}} = Z_{11}/Z_{21}, \tag{4.67a}$$

$$B = \left.\frac{V_1}{I_2}\right|_{V_2=0} = \left.\frac{I_1 Z_{11} - I_2 Z_{12}}{I_2}\right|_{V_2=0} = Z_{11}\left.\frac{I_1}{I_2}\right|_{V_2=0} - Z_{12}$$

$$= Z_{11}\frac{I_1 Z_{22}}{I_1 Z_{21}} - Z_{12} = \frac{Z_{11}Z_{22} - Z_{12}Z_{21}}{Z_{21}}, \tag{4.67b}$$

$$C = \left.\frac{I_1}{V_2}\right|_{I_2=0} = \frac{I_1}{I_1 Z_{21}} = 1/Z_{21}, \tag{4.67c}$$

$$D = \left.\frac{I_1}{I_2}\right|_{V_2=0} = \frac{I_2 Z_{22}/Z_{21}}{I_2} = Z_{22}/Z_{21}. \tag{4.67d}$$

If the network is reciprocal, then $Z_{12} = Z_{21}$ and (4.67) can be used to show that $AD - BC = 1$.

Equivalent Circuits for Two-Port Networks

The special case of a two-port microwave network occurs so frequently in practice that it deserves further attention. Here we will discuss the use of equivalent circuits to represent an arbitrary two-port network. Useful conversions for two-port network parameters are given in Table 4.2.

Figure 4.12a shows a transition between a coaxial line and a microstrip line, and serves as an example of a two-port network. Terminal planes can be defined at arbitrary points on the two transmission lines; a convenient choice might be as shown in the figure. But because of the physical discontinuity in the transition from a coaxial line to a microstrip line, electric and/or magnetic energy can be stored in the vicinity of the junction, leading to reactive effects. Characterization of such effects can be obtained by measurement or by theoretical analysis (although such an analysis may be quite complicated), and represented by the two-port "black box" shown in Figure 4.12b. The properties of the transition can then be expressed in terms of the network parameters (Z, Y, S, or $ABCD$) of the two-port network. This type of treatment can be applied to a variety of two-port junctions, such as transitions from one type of transmission line to another, transmission line discontinuities such as step changes in width, or bends, etc. When modeling a microwave junction in this way, it is often useful to replace the two-port "black box" with an equivalent circuit containing a few idealized components, as shown in Figure 4.12c. (This is particularly useful if the component values can be related to some physical features of the actual junction.) There is an unlimited number of ways in which such equivalent circuits can be defined; we will discuss some of the most common and useful types below.

As we have seen from the previous sections, an arbitrary two-port network can be described in terms of impedance parameters as

$$V_1 = Z_{11}I_1 + Z_{12}I_2,$$
$$V_2 = Z_{21}I_1 + Z_{22}I_2, \tag{4.68a}$$

or in terms of admittance parameters as

$$I_1 = Y_{11}V_1 + Y_{12}V_2,$$
$$I_2 = Y_{21}V_1 + Y_{22}V_2. \tag{4.68b}$$

TABLE 4.2 Conversions Between Two-Port Network Parameters

	S	Z	Y	$ABCD$
S_{11}	S_{11}	$\frac{(Z_{11}-Z_0)(Z_{22}+Z_0)-Z_{12}Z_{21}}{\Delta Z}$	$\frac{(Y_0-Y_{11})(Y_0+Y_{22})+Y_{12}Y_{21}}{\Delta Y}$	$\frac{A+B/Z_0-CZ_0-D}{A+B/Z_0+CZ_0+D}$
S_{12}	S_{12}	$\frac{2Z_{12}Z_0}{\Delta Z}$	$\frac{-2Y_{12}Y_0}{\Delta Y}$	$\frac{2(AD-BC)}{A+B/Z_0+CZ_0+D}$
S_{21}	S_{21}	$\frac{2Z_{21}Z_0}{\Delta Z}$	$\frac{-2Y_{21}Y_0}{\Delta Y}$	$\frac{2}{A+B/Z_0+CZ_0+D}$
S_{22}	S_{22}	$\frac{(Z_{11}+Z_0)(Z_{22}-Z_0)-Z_{12}Z_{21}}{\Delta Z}$	$\frac{(Y_0+Y_{11})(Y_0-Y_{22})+Y_{12}Y_{21}}{\Delta Y}$	$\frac{-A+B/Z_0-CZ_0+D}{A+B/Z_0+CZ_0+D}$
Z_{11}	$Z_0\frac{(1+S_{11})(1-S_{22})+S_{12}S_{21}}{(1-S_{11})(1-S_{22})-S_{12}S_{21}}$	Z_{11}	$\frac{Y_{22}}{\lvert Y\rvert}$	$\frac{A}{C}$
Z_{12}	$Z_0\frac{2S_{12}}{(1-S_{11})(1-S_{22})-S_{12}S_{21}}$	Z_{12}	$\frac{-Y_{12}}{\lvert Y\rvert}$	$\frac{AD-BC}{C}$
Z_{21}	$Z_0\frac{2S_{21}}{(1-S_{11})(1-S_{22})-S_{12}S_{21}}$	Z_{21}	$\frac{-Y_{21}}{\lvert Y\rvert}$	$\frac{1}{C}$
Z_{22}	$Z_0\frac{(1-S_{11})(1+S_{22})+S_{12}S_{21}}{(1-S_{11})(1-S_{22})-S_{12}S_{21}}$	Z_{22}	$\frac{Y_{11}}{\lvert Y\rvert}$	$\frac{D}{C}$
Y_{11}	$Y_0\frac{(1-S_{11})(1+S_{22})+S_{12}S_{21}}{(1+S_{11})(1+S_{22})-S_{12}S_{21}}$	$\frac{Z_{22}}{\lvert Z\rvert}$	Y_{11}	$\frac{D}{B}$
Y_{12}	$Y_0\frac{-2S_{12}}{(1+S_{11})(1+S_{22})-S_{12}S_{21}}$	$\frac{-Z_{12}}{\lvert Z\rvert}$	Y_{12}	$\frac{BC-AD}{B}$
Y_{21}	$Y_0\frac{-2S_{21}}{(1+S_{11})(1+S_{22})-S_{12}S_{21}}$	$\frac{-Z_{21}}{\lvert Z\rvert}$	Y_{21}	$\frac{-1}{B}$
Y_{22}	$Y_0\frac{(1+S_{11})(1-S_{22})+S_{12}S_{21}}{(1+S_{11})(1+S_{22})-S_{12}S_{21}}$	$\frac{Z_{11}}{\lvert Z\rvert}$	Y_{22}	$\frac{A}{B}$
A	$\frac{(1+S_{11})(1-S_{22})+S_{12}S_{21}}{2S_{21}}$	$\frac{Z_{11}}{Z_{21}}$	$\frac{-Y_{22}}{Y_{21}}$	A
B	$Z_0\frac{(1+S_{11})(1+S_{22})-S_{12}S_{21}}{2S_{21}}$	$\frac{\lvert Z\rvert}{Z_{21}}$	$\frac{-1}{Y_{21}}$	B
C	$\frac{1}{Z_0}\frac{(1-S_{11})(1-S_{22})-S_{12}S_{21}}{2S_{21}}$	$\frac{1}{Z_{21}}$	$\frac{-\lvert Y\rvert}{Y_{21}}$	C
D	$\frac{(1-S_{11})(1+S_{22})+S_{12}S_{21}}{2S_{21}}$	$\frac{Z_{22}}{Z_{21}}$	$\frac{-Y_{11}}{Y_{21}}$	D

$\lvert Z\rvert = Z_{11}Z_{22} - Z_{12}Z_{21}$; $\lvert Y\rvert = Y_{11}Y_{22} - Y_{12}Y_{21}$; $\Delta Y = (Y_{11}+Y_0)(Y_{22}+Y_0) - Y_{12}Y_{21}$; $\Delta Z = (Z_{11}+Z_0)(Z_{22}+Z_0) - Z_{12}Z_{21}$; $Y_0 = 1/Z_0$

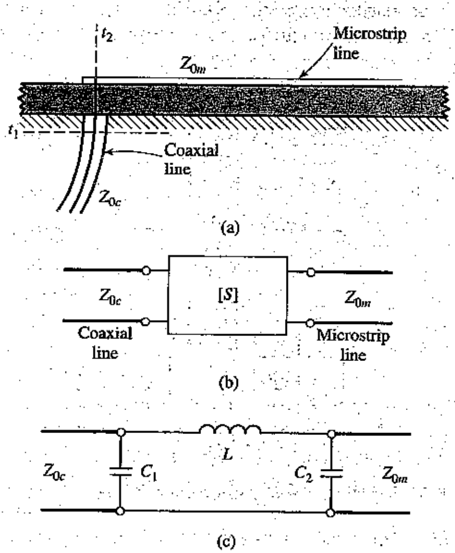

FIGURE 4.12 A coax-to-microstrip transition and equivalent circuit representations. (a) Geometry of the transition. (b) Representation of the transition by a "black box." (c) A possible equivalent circuit for the transition [6].

If the network is reciprocal, then $Z_{12} = Z_{21}$ and $Y_{12} = Y_{21}$. These representations lead naturally to the T and π equivalent circuits shown in Figure 4.13a and 4.13b. The relations in Table 4.2 can be used to relate the component values to other network parameters.

Other equivalent circuits can also be used to represent a two-port network. If the network is reciprocal, there are six degrees of freedom (the real and imaginary parts of three matrix elements), so the equivalent circuit should have six independent parameters. A nonreciprocal network cannot be represented by a passive equivalent circuit using reciprocal elements.

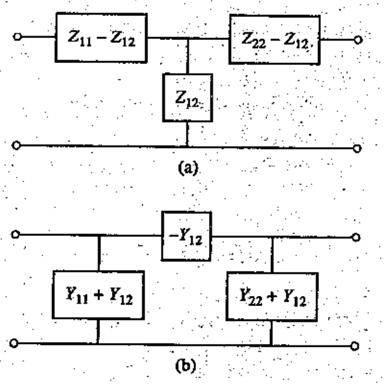

FIGURE 4.13 Equivalent circuits for a reciprocal two-port network. (a) T equivalent. (b) π equivalent.

If the network is lossless, which is a good approximation for many practical two-port junctions, some simplifications can be made in the equivalent circuit. As was shown in Section 4.2, the impedance or admittance matrix elements are purely imaginary for a lossless network. This reduces the degrees of freedom for such a network to three, and implies that the T and π equivalent circuits of Figure 4.13 can be constructed from purely reactive elements.

4.5 SIGNAL FLOW GRAPHS

We have seen how transmitted and reflected waves can be represented by scattering parameters, and how the interconnection of sources, networks, and loads can be treated with various matrix representations. In this section we discuss the signal flow graph, which is an additional technique that is very useful for the analysis of microwave networks in terms of transmitted and reflected waves. We first discuss the features and the construction of the flow graph itself, and then present a technique for the reduction, or solution, of the flow graph.

The primary components of a signal flow graph are nodes and branches:

- Nodes: Each port, i, of a microwave network has two nodes, a_i and b_i. Node a_i is identified with a wave entering port i, while node b_i is identified with a wave reflected from port i. The voltage at a node is equal to the sum of all signals entering that node.
- Branches: A branch is a directed path between two nodes, representing signal flow from one node to another. Every branch has an associated S parameter or reflection coefficient.

At this point it is useful to consider the flow graph of an arbitrary two-port network, as shown in Figure 4.14. Figure 4.14a shows a two-port network with incident and reflected waves at each port, and Figure 4.14b shows the corresponding signal flow graph representation. The flow graph gives an intuitive graphical illustration of the network behavior.

For example, a wave of amplitude a_1 incident at port 1 is split, with part going through S_{11} and out port 1 as a reflected wave and part transmitted through S_{21} to node b_2. At node b_2, the wave goes out port 2; if a load with nonzero reflection coefficient is connected at port 2, this wave will be at least partly reflected and reenter the two-port network at node a_2. Part of the wave can be reflected back out port 2 via S_{22}, and part can be transmitted out port 1 through S_{12}.

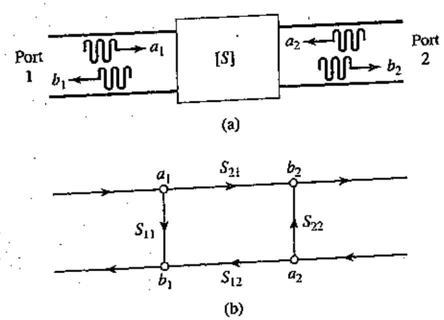

FIGURE 4.14 The signal flow graph representation of a two-port network. (a) Definition of incident and reflected waves. (b) Signal flow graph.

Chapter Eight

Microwave Filters

A microwave filter is a two-port network used to control the frequency response at a certain point in a microwave system by providing transmission at frequencies within the passband of the filter and attenuation in the stopband of the filter. Typical frequency responses include low-pass, high-pass, bandpass, and band-reject characteristics. Applications can be found in virtually any type of microwave communication, radar, or test and measurement system.

Microwave filter theory and practice began in the years preceding World War II, by pioneers such as Mason, Sykes, Darlington, Fano, Lawson, and Richards. The image parameter method of filter design was developed in the late 1930s and was useful for low-frequency filters in radio and telephony. In the early 1950s a group at Stanford Research Institute, consisting of G. Matthaei, L. Young, E. Jones, S. Cohn, and others, became very active in microwave filter and coupler development. A voluminous handbook on filters and couplers resulted from this work and remains a valuable reference [1]. Today, most microwave filter design is done with sophisticated computer-aided design (CAD) packages based on the insertion loss method. Because of continuing advancements in network synthesis with distributed elements, the use of low-temperature superconductors, and the incorporation of active devices in filter circuits, microwave filter design remains an active research area.

We begin our discussion of filter theory and design with the frequency characteristics of periodic structures, which consist of a transmission line or waveguide periodically loaded with reactive elements. These structures are of interest in themselves, because of the application to slow-wave components and traveling-wave amplifier design, and also because they exhibit basic passband-stopband responses that lead to the image parameter method of filter design.

Filters designed using the *image parameter method* consist of a cascade of simpler two-port filter sections to provide the desired cutoff frequencies and attenuation characteristics, but do not allow the specification of a frequency response over the complete operating range. Thus, although the procedure is relatively simple, the design of filters by the image parameter method often must be iterated many times to achieve the desired results.

A more modern procedure, called the *insertion loss method*, uses network synthesis techniques to design filters with a completely specified frequency response. The design is simplified by beginning with low-pass filter prototypes that are normalized in terms of impedance and

frequency. Transformations are then applied to convert the prototype designs to the desired frequency range and impedance level.

Both the image parameter and insertion loss method of filter design provide lumped-element circuits. For microwave applications such designs usually must be modified to use distributed elements consisting of transmission line sections. The Richard's transformation and the Kuroda identities provide this step. We will also discuss transmission line filters using stepped impedances and coupled lines; filters using coupled resonators will also be briefly described.

The subject of microwave filters is quite extensive, due to the importance of these components in practical systems and the wide variety of possible implementations. We give here a treatment of only the basic principles and some of the more common filter designs, and refer the reader to references such as [1], [2], [3], and [4] for further discussion.

8.1 PERIODIC STRUCTURES

An infinite transmission line or waveguide periodically loaded with reactive elements is referred to as a periodic structure. As shown in Figure 8.1, periodic structures can take various forms, depending on the transmission line media being used. Often the loading elements are formed as discontinuities in the line, but in any case they can be modeled as lumped reactances across a transmission line as shown in Figure 8.2. Periodic structures support slow-wave propagation (slower than the phase velocity of the unloaded line), and

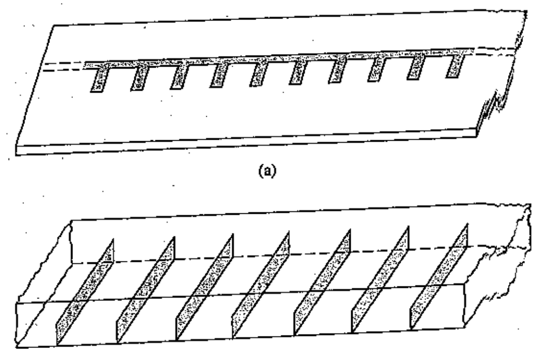

(a)

(b)

FIGURE 8.1 Examples of periodic structures. (a) Periodic stubs on a microstrip line. (b) Periodic diaphragms in a waveguide.

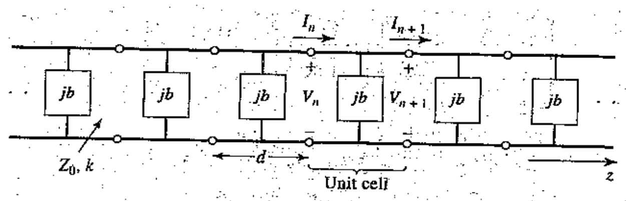

FIGURE 8.2 Equivalent circuit of a periodically loaded transmission line. The unloaded line has characteristic impedance Z_0 and propagation constant k.

have passband and stopband characteristics similar to those of filters; they find application in traveling-wave tubes, masers, phase shifters, and antennas.

Analysis of Infinite Periodic Structures

We begin by studying the propagation characteristics of the infinite loaded line shown in Figure 8.2. Each unit cell of this line consists of a length d of transmission line with a shunt susceptance across the midpoint of the line; the susceptance b is normalized to the characteristic impedance, Z_0. If we consider the infinite line as being composed of a cascade of identical two-port networks, we can relate the voltages and currents on either side of the nth unit cell using the $ABCD$ matrix:

$$\begin{bmatrix} V_n \\ I_n \end{bmatrix} = \begin{bmatrix} A & B \\ C & D \end{bmatrix} \begin{bmatrix} V_{n+1} \\ I_{n+1} \end{bmatrix}, \tag{8.1}$$

where A, B, C, and D are the matrix parameters for a cascade of a transmission line section of length $d/2$, a shunt susceptance b, and another transmission line section of length $d/2$. From Table 4.1 we then have, in normalized form,

$$\begin{bmatrix} A & B \\ C & D \end{bmatrix} = \begin{bmatrix} \cos\frac{\theta}{2} & j\sin\frac{\theta}{2} \\ j\sin\frac{\theta}{2} & \cos\frac{\theta}{2} \end{bmatrix} \begin{bmatrix} 1 & 0 \\ jb & 1 \end{bmatrix} \begin{bmatrix} \cos\frac{\theta}{2} & j\sin\frac{\theta}{2} \\ j\sin\frac{\theta}{2} & \cos\frac{\theta}{2} \end{bmatrix}$$

$$= \begin{bmatrix} \left(\cos\theta - \frac{b}{2}\sin\theta\right) & j\left(\sin\theta + \frac{b}{2}\cos\theta - \frac{b}{2}\right) \\ j\left(\sin\theta + \frac{b}{2}\cos\theta + \frac{b}{2}\right) & \left(\cos\theta - \frac{b}{2}\sin\theta\right) \end{bmatrix}, \tag{8.2}$$

where $\theta = kd$, and k is the propagation constant of the unloaded line. The reader can verify that $AD - BC = 1$, as required for reciprocal networks.

For a wave propagating in the $+z$ direction, we must have

$$V(z) = V(0)e^{-\gamma z}, \tag{8.3a}$$

$$I(z) = I(0)e^{-\gamma z}, \tag{8.3b}$$

for a phase reference at $z = 0$. Since the structure is infinitely long, the voltage and current at the nth terminals can differ from the voltage and current at the $n + 1$ terminals only by

the propagation factor, $e^{-\gamma d}$. Thus,

$$V_{n+1} = V_n e^{-\gamma d}, \tag{8.4a}$$

$$I_{n+1} = I_n e^{-\gamma d}. \tag{8.4b}$$

Using this result in (8.1) gives the following:

$$\begin{bmatrix} V_n \\ I_n \end{bmatrix} = \begin{bmatrix} A & B \\ C & D \end{bmatrix} \begin{bmatrix} V_{n+1} \\ I_{n+1} \end{bmatrix} = \begin{bmatrix} V_{n+1}e^{\gamma d} \\ I_{n+1}e^{\gamma d} \end{bmatrix},$$

or

$$\begin{bmatrix} A - e^{\gamma d} & B \\ C & D - e^{\gamma d} \end{bmatrix} \begin{bmatrix} V_{n+1} \\ I_{n+1} \end{bmatrix} = 0. \tag{8.5}$$

For a nontrivial solution, the determinant of the above matrix must vanish:

$$AD + e^{2\gamma d} - (A + D)e^{\gamma d} - BC = 0, \tag{8.6}$$

or, since $AD - BC = 1$,

$$1 + e^{2\gamma d} - (A + D)e^{\gamma d} = 0,$$

$$e^{-\gamma d} + e^{\gamma d} = A + D,$$

$$\cosh\gamma d = \frac{A + D}{2} = \cos\theta - \frac{b}{2}\sin\theta, \tag{8.7}$$

where (8.2) was used for the values of A and D. Now if $\gamma = \alpha + j\beta$, we have that

$$\cosh\gamma d = \cosh\alpha d\cos\beta d + j\sinh\alpha d\sin\beta d = \cos\theta - \frac{b}{2}\sin\theta. \tag{8.8}$$

Since the right-hand side of (8.8) is purely real, we must have either $\alpha = 0$ or $\beta = 0$.

Case 1: $\alpha = 0, \beta \neq 0$. This case corresponds to a nonattenuating, propagating wave on the periodic structure, and defines the passband of the structure. Then (8.8) reduces to

$$\cos\beta d = \cos\theta - \frac{b}{2}\sin\theta, \tag{8.9a}$$

which can be solved for β if the magnitude of the right-hand side is less than or equal to unity. Note that there are an infinite number of values of β that can satisfy (8.9a).

Case 2: $\alpha \neq 0, \beta = 0, \pi$. In this case the wave does not propagate, but is attenuated along the line; this defines the stopband of the structure. Because the line is lossless, power is not dissipated, but is reflected back to the input of the line. The magnitude of (8.8) reduces to

$$\cosh\alpha d = \left|\cos\theta - \frac{b}{2}\sin\theta\right| \geq 1, \tag{8.9b}$$

which has only one solution ($\alpha > 0$) for positively traveling waves; $\alpha < 0$ applies for negatively traveling waves. If $\cos\theta - (b/2)\sin\theta \leq -1$, (8.9b) is obtained from (8.8) by letting $\beta = \pi$; then all the lumped loads on the line are $\lambda/2$ apart, yielding an input impedance the same as if $\beta = 0$.

Thus, depending on the frequency and normalized susceptance values, the periodically loaded line will exhibit either passbands or stopbands, and so can be considered as a type of filter. It is important to note that the voltage and current waves defined in (8.3) and (8.4) are meaningful only when measured at the terminals of the unit cells, and do not apply to voltages and currents that may exist at points within a unit cell. These waves are similar to the elastic waves (*Bloch waves*) that propagate through periodic crystal lattices.

Besides the propagation constant of the waves on the periodically loaded line, we will also be interested in the characteristic impedance for these waves. We can define a characteristic impedance at the unit cell terminals as

$$Z_B = Z_0 \frac{V_{n+1}}{I_{n+1}}, \tag{8.10}$$

since V_{n+1} and I_{n+1} in the above derivation were normalized quantities. This impedance is also referred to as the *Bloch* impedance. From (8.5) we have that

$$(A - e^{\gamma d})V_{n+1} + BI_{n+1} = 0,$$

so (8.10) yields

$$Z_B = \frac{-BZ_0}{A - e^{\gamma d}}.$$

From (8.6) we can solve for $e^{\gamma d}$ in terms of A and D as follows:

$$e^{\gamma d} = \frac{(A + D) \pm \sqrt{(A + D)^2 - 4}}{2}.$$

Then the Bloch impedance has two solutions given by

$$Z_B^{\pm} = \frac{-2BZ_0}{2A - A - D \mp \sqrt{(A + D)^2 - 4}}. \tag{8.11}$$

For symmetrical unit cells (as assumed in Figure 8.2) we will always have $A = D$. In this case (8.11) reduces to

$$Z_B^{\pm} = \frac{\pm BZ_0}{\sqrt{A^2 - 1}}. \tag{8.12}$$

The $\pm$ solutions correspond to the characteristic impedance for positively and negatively traveling waves, respectively. For symmetrical networks these impedances are the same except for the sign; the characteristic impedance for a negatively traveling wave turns out to be negative because we have defined I_n in Figure 8.2 as always being in the positive direction.

From (8.2) we see that B is always purely imaginary. If $\alpha = 0$, $\beta \neq 0$ (passband), then (8.7) shows that $\cosh \gamma d = A \leq 1$ (for symmetrical networks) and (8.12) shows that Z_B will be real. If $\alpha \neq 0$, $\beta = 0$ (stopband), then (8.7) shows that $\cosh \gamma d = A \geq 1$, and (8.12) shows that Z_B is imaginary. This situation is similar to that for the wave impedance of a waveguide, which is real for propagating modes and imaginary for cutoff, or evanescent, modes.

Terminated Periodic Structures

Next consider a truncated periodic structure, terminated in a load impedance Z_L, as shown in Figure 8.3. At the terminals of an arbitrary unit cell, the incident and reflected voltages and currents can be written as (assuming operation in the passband)

$$V_n = V_0^+ e^{-j\beta nd} + V_0^- e^{j\beta nd}, \tag{8.13a}$$

$$I_n = I_0^+ e^{-j\beta nd} + I_0^- e^{j\beta nd} = \frac{V_0^+}{Z_B^+} e^{-j\beta nd} + \frac{V_0^-}{Z_B^-} e^{j\beta nd}, \tag{8.13b}$$

where we have replaced γz in (8.3) with $j\beta nd$, since we are interested only in terminal quantities.

Now define the following incident and reflected voltages at the nth unit cell:

$$V_n^+ = V_0^+ e^{-j\beta nd}, \tag{8.14a}$$

$$V_n^- = V_0^- e^{j\beta nd}. \tag{8.14b}$$

Then (8.13) can be written as

$$V_n = V_n^+ + V_n^-, \tag{8.15a}$$

$$I_n = \frac{V_n^+}{Z_B^+} + \frac{V_n^-}{Z_B^-}. \tag{8.15b}$$

At the load, where $n = N$, we have

$$V_N = V_N^+ + V_N^- = Z_L I_N = Z_L \left(\frac{V_N^+}{Z_B^+} + \frac{V_N^-}{Z_B^-} \right), \tag{8.16}$$

so the reflection coefficient at the load can be found as

$$\Gamma = \frac{V_N^-}{V_N^+} = -\frac{Z_L/Z_B^+ - 1}{Z_L/Z_B^- - 1}. \tag{8.17}$$

If the unit cell network is symmetrical ($A = D$), then $Z_B^+ = -Z_B^- = Z_B$, which reduces (8.17) to the familiar result that

$$\Gamma = \frac{Z_L - Z_B}{Z_L + Z_B}. \tag{8.18}$$

So to avoid reflections on the terminated periodic structure, we must have $Z_L = Z_B$, which is real for a lossless structure operating in a passband. If necessary, a quarter-wave transformer can be used between the periodically loaded line and the load.

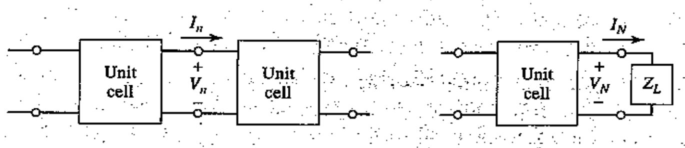

FIGURE 8.3 A periodic structure terminated in a normalized load impedance Z_L.

FIGURE 8.5 A capacitively loaded line.

k-β Diagrams and Wave Velocities

When studying the passband and stopband characteristics of a periodic structure, it is useful to plot the propagation constant, β, versus the propagation constant of the unloaded line, k (or ω). Such a graph is called a *k-β diagram*, or *Brillouin* diagram (after L. Brillouin, a physicist who studied wave propagation in periodic crystal structures).

The k-β diagram can be plotted from (8.9a), which is the dispersion relation for a general periodic structure. In fact, a k-β diagram can be used to study the dispersion characteristics of many types of microwave components and transmission lines. For instance, consider the dispersion relation for a waveguide mode:

$$\beta = \sqrt{k^2 - k_c^2},$$

or

$$k = \sqrt{\beta^2 + k_c^2}, \tag{8.19}$$

FIGURE 8.6 k-β diagram for Example 8.1.

structure. To evaluate the Bloch impedance, we use (8.2) and (8.12):

$$\frac{b}{2} = \frac{\omega C_0 Z_0}{2} = 1.256,$$

$$\theta = k_0 d = 36°,$$

$$A = \cos\theta - \frac{b}{2}\sin\theta = 0.0707,$$

$$B = j\left(\sin\theta + \frac{b}{2}\cos\theta - \frac{b}{2}\right) = j0.3479.$$

Then,

$$Z_B = \frac{BZ_0}{\sqrt{A^2 - 1}} = \frac{(j0.3479)(50)}{j\sqrt{1 - (0.0707)^2}} = 17.4\ \Omega.$$

■

8.2 FILTER DESIGN BY THE IMAGE PARAMETER METHOD

The image parameter method of filter design involves the specification of passband and stopband characteristics for a cascade of two-port networks, and so is similar in concept to the periodic structures that were studied in Section 8.1. The method is relatively simple but has the disadvantage that an arbitrary frequency response cannot be incorporated into the design. This is in contrast to the insertion loss method, which is the subject of the following section. Nevertheless, the image parameter method is useful for simple filters and provides a link between infinite periodic structures and practical filter design. The image parameter method also finds application in solid-state traveling-wave amplifier design.

Image Impedances and Transfer Functions for Two-Port Networks

We begin with definitions of the image impedances and voltage transfer function for an arbitrary reciprocal two-port network; these results are required for the analysis and design of filters by the image parameter method.

Consider the arbitrary two-port network shown in Figure 8.7, where the network is specified by its $ABCD$ parameters. Note that the reference direction for the current at port 2 has been chosen according to the convention for $ABCD$ parameters. The image impedances, Z_{i1} and Z_{i2}, are defined for this network as follows:

Z_{i1} = input impedance at port 1 when port 2 is terminated with Z_{i2},

Z_{i2} = input impedance at port 2 when port 1 is terminated with Z_{i1}.

Thus both ports are matched when terminated in their image impedances. We will now derive expressions for the image impedances in terms of the $ABCD$ parameters of a network.

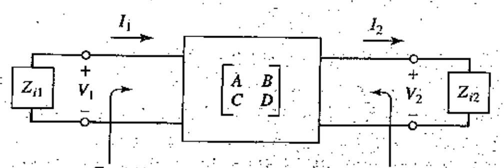

FIGURE 8.7 A two-port network terminated in its image impedances.

The port voltages and currents are related as

$$V_1 = AV_2 + BI_2, \tag{8.22a}$$

$$I_1 = CV_2 + DI_2. \tag{8.22b}$$

The input impedance at port 1, with port 2 terminated in Z_{i2}, is

$$Z_{in1} = \frac{V_1}{I_1} = \frac{AV_2 + BI_2}{CV_2 + DI_2} = \frac{AZ_{i2} + B}{CZ_{i2} + D}, \tag{8.23}$$

since $V_2 = Z_{i2} I_2$.

Now solve (8.22) for V_2, I_2 by inverting the $ABCD$ matrix. Since $AD - BC = 1$ for a reciprocal network, we obtain

$$V_2 = DV_1 - BI_1, \tag{8.24a}$$

$$I_2 = -CV_1 + AI_1. \tag{8.24b}$$

Then the input impedance at port 2, with port 1 terminated in Z_{i1}, can be found as

$$Z_{in2} = \frac{-V_2}{I_2} = -\frac{DV_1 - BI_1}{-CV_1 + AI_1} = \frac{DZ_{i1} + B}{CZ_{i1} + A}, \tag{8.25}$$

since $V_1 = -Z_{i1} I_1$ (circuit of Figure 8.7).

We desire that $Z_{in1} = Z_{i1}$ and $Z_{in2} = Z_{i2}$, so (8.23) and (8.25) give two equations for the image impedances:

$$Z_{i1}(CZ_{i2} + D) = AZ_{i2} + B, \tag{8.26a}$$

$$Z_{i1}D - B = Z_{i2}(A - CZ_{i1}). \tag{8.26b}$$

Solving for Z_{i1} and Z_{i2} gives

$$Z_{i1} = \sqrt{\frac{AB}{CD}}, \tag{8.27a}$$

$$Z_{i2} = \sqrt{\frac{BD}{AC}}, \tag{8.27b}$$

with $Z_{i2} = DZ_{i1}/A$. If the network is symmetric, then $A = D$ and $Z_{i1} = Z_{i2}$ as expected.

Now consider the voltage transfer function for a two-port network terminated in its image impedances. With reference to Figure 8.8 and (8.24a), the output voltage at port 2 can be expressed as

$$V_2 = DV_1 - BI_1 = \left(D - \frac{B}{Z_{i1}}\right)V_1. \tag{8.28}$$

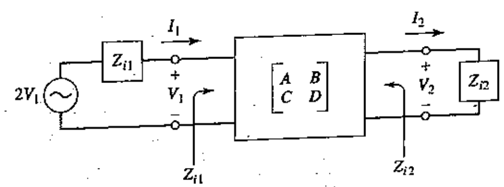

FIGURE 8.8 A two-port network terminated in its image impedances and driven with a voltage generator.